Enhancing the correlative ecological niche modeling framework to incorporate the temporal dimension of species' distributions

By

Kate Ingenloff
M.A., University of Kansas, 2013
B.Sc., Texas A&M University, 2005

Submitted to the graduate degree program in Ecology & Evolutionary Biology and the Graduate Faculty of the University of Kansas in partial fulfillment of the requirements for the degree of Doctor of Philosophy.

_____

Chair: A. Townsend Peterson

_____

Sharon Billings

_____

Paulyn Cartwright

_____

Robert Moyle

_____

Leigh Stearns

Date Defended: 22 July 2020

The dissertation committee for Kate Ingenloff certifies that this is the approved
version of the following dissertation:

Enhancing the correlative ecological niche modeling framework to incorporate the temporal dimension of species' distributions

_____

Chair: A. Townsend Peterson

Date Approved: 22 July 2020

ABSTRACT

Anthropogenic climate change is impacting biodiversity at all scales. Detailed spatio-temporal information about geographic distributions of species will be critical to mitigating the ramifications of these impacts. The field of distributional ecology seeks to define and explain spatial and temporal variation in species' distributions. Correlative ecological niche modelling (e.g., ecological niche modeling, species distributional modeling), which aims to characterize species' ecological niches in environmental space, is a popular tool used to address questions regarding species' distributions in geographic space. These approaches are powerful, capable of rendering conservation planning more understandable and accessible to diverse stakeholders; as such, they are increasingly incorporated into natural resources management and conservation planning. The traditional modelling framework uses primary biodiversity data in a time-averaged approach wherein covariate data for a relevant time period are averaged and treated as static to estimate a species' niche in environmental space and project that the estimation onto the geographic landscape. However, these methods impose limitations on model output quality for highly mobile, behaviorally complex, and more ephemeral species. Improved methods can enhance understanding of macroscale factors driving distributional dynamics of these species to provide crucial information that will fill important knowledge gaps necessary to project and explore future distributional potential.

Here, I present a suite of studies aimed at optimizing the current correlative niche modeling frameworks to enhance performance for highly mobile species, emphasizing improvements using open source data and platforms. Focusing on pelagic seabirds, which often behave as generalists at the species level yet exhibit high degrees of intra-specific variation in behavior, my dissertation consists of three distinct components. Chapter 1 establishes a baseline of model performance under

a seasonal, time-averaged modeling approach for the Wandering Albatross (*Diomedea exulans*). Chapter 2 introduces modifications to the data preparation process so as to incorporate the temporal dimension into the traditional niche modeling framework, using the Wood Thrush (*Hylocichla mustelina*) as a case study. Finally, Chapter 3 applies the improved data preparation workflow introduced in Chapter 2 to the study species for which baseline models were developed in Chapter 1—*Diomedea exulans*. Improved correlative niche models will be able to inform species-level management and policy development more effectively for highly mobile and/or migratory species, as well as disease vectors of public health interest.

ACKNOWLEDGEMENTS

The seemingly miraculous completion of this dissertation would not have been possible without the assistance of a great many people (only a small portion of which are highlighted below), one fuzzy quadruped, and obscene amounts of coffee and smoked meat. First and foremost, I am exceedingly grateful for the mentorship of my adviser, friend, and colleague, **Dr. A. Townsend Peterson**. I would never have stuck it out through this slog post-comps, nor would I be the well-rounded scientist I am today, without his support and guidance. I am also incredibly grateful for my four research advisory committee members—**Drs. Sharon Billings**, **Paulyn Cartwright**, **Rob Moyle**, and **Leigh Stearns**—who were instrumental in keeping me on track when I would have gladly continued volunteering for non-dissertation related side quests until we all simply forgot that I had my own research to finish. The broader lab group, including both the **Peterson and Soberón labs**, and the **KU Ecological Niche Modeling Group**, provided insightful conversations yielding critical research inspiration, morale boosts, and a level of comradery I'm concerned may never be rivalled in future lab settings. I'm particularly appreciative for the colorful and often irreverent humor of **Lindsay Campbell**, **Chris Hensz**, **Racheal Bible**, and **Ali Khalighifar**. Without the expert guidance of **Aagje Ashe** and **Jamie Keeler**, I would have been doomed to die a slow, painful death in the bureaucratic labyrinth that is graduate school. Thank you both for not retiring or moving on to greener pastures before I finally escaped. And, finally, I would be remiss if I did not express my gratitude for the passive aggressive support of my academic and professional pursuits by the late **Dr. Tom Taylor**.

Naturally, I also owe a very special thank you to family and friends, without whom I undoubtedly would have said 'fuck it' and moved back into a hut in some remote village in sub-Saharan Africa. In particular, my CT and PhD spouses, **Juli and Jason Emry**, provided

unwavering support, strategically-timed tough love, booze, and sustenance, and additional sets of eyes to assist with last-minute manuscript and proposal edits. ⚓ **Gabe Dalton** provided solid support for well over a decade, keeping me grounded and excited about my research when the slog of setbacks took their toll. ⚓ I am eternally thankful for **Amy Miller** who, for some crazy reason, willingly took in a stray graduate student during their final year of study. ⚓ My Liberty Hall family was instrumental in keeping me grounded even as I progressed further into the bowels of the academy. ⚓ And, my dog, **Bida "The Fuzz" Ingenloff**, successfully forced me to develop some semblance of work-life balance, provided much needed stress relief, and ensured that I never truly self-isolated; the danger noodles, **T** and **Z**, were the quietest roommates ever.

Finally, I'm grateful for **Teva Phamaceutical**'s consistent production of their D-Amphetamine Salt Combo 20mg. Without you, the debris trail of partially completed projects that have fallen victim to my ADHD would be much greater than it already is and undoubtedly include this dissertation.

This dissertation is dedicated to my parents,

Rick and Paula Ingenloff,

who have always championed me even as I embarked upon paths

that appeared to have no actual destination,

or indeed, any obvious purpose at all.

I am indeed the undisputed winner of the parental lottery.

My love and thanks to you both.

TABLE OF CONTENTS

INTRODUCTION

Anthropogenic climate change will affect global biodiversity at all scales, from individual organisms to entire ecosystems. Indeed, as climatic variables are primary drivers of species' geographic distributions (Guisan & Zimmermann 2000; Pearson & Dawson 2003), the impacts of climate change on biodiversity are already well-documented (Peñuelas *et al.* 2013; Pecl *et al.* 2017), including species' range shifts (Hughes 2000; Parmesan & Yohe 2003; Bellard *et al.* 2012), alteration of migration timing and routes (Lemoine & Böhning-Gaese 2003; Robinson *et al.* 2009; Møller. *et al.* 2010; Knudsen *et al.* 2011), changes in phenology (Hughes 2000; Root *et al.* 2003; Edwards & Richardson 2004; Thackeray *et al.* 2010; Bellard *et al.* 2012; Cook *et al.* 2012), and accelerated rates of extinction (Thomas *et al.* 2004). The ability to develop dynamic and adaptive management strategies will be critical to managing and protecting our biological diversity in the wake of such rapid global change.

The field of distributional ecology aims to understand the drivers of species' distributions across environmental and geographic landscapes through time. Correlative niche modelling, termed species distribution modelling (SDM) or ecological niche modelling (ENM), are at the heart of these distributional analyses. These methods characterize a species' ecological niche in environmental space, which can be used to address questions regarding potential distributions on the geographic landscape (Peterson 2006). These models correlate primary species occurrence data with select climatic and environmental covariates relevant to the species in question. Although simplistic compared to mechanistic models (Peterson, Papeş & Soberón 2015), correlative models can incorporate relevant ecological information via geographic comparisons, and can reveal how these parameters are linked (Barve *et al.* 2014). Their explicit linkage of geographic and environmental spaces can help render conservation planning more understandable and accessible

to a variety of stakeholders (Grecian *et al.* 2012). As such, they are liberally incorporated in a broad range of applications including assessment of species' future distributional, and invasive, potential under global climate change scenarios (Pacifici *et al.* 2015; Searcy & Shaffer 2016) for application in biodiversity conservation planning (Rodríguez *et al.* 2007; Franklin 2013; Eaton *et al.* 2018) and improving understanding of vectors of zoonotic disease (Peterson 2006; Peterson 2014), and investigating more broad-scale phylogeographic questions (Alvarado-Serrano & Knowles 2014).

As with all models, correlative approaches are limited by the quality and treatment of input data (Heikkinen, Marmion & Luoto 2012). In distributional ecology contexts, the traditional niche modeling framework uses primary species point-observation data in a time-averaged model calibration and testing approach wherein environmental (explanatory) covariates are averaged and treated as static across a relevant period of time (the researcher-designated study period). Although time-averaged modeling has proven quite valuable for exploring the distributional ecology of populations and species that are relatively static, the traditional niche modeling framework has had limited success estimating distributions of species that do not have fixed distributions such as ephemeral insect disease vectors (Peterson *et al.* 2005; Brandão-Filho *et al.* 2011) and highly mobile species such as pelagic seabirds at macroscales.

Seabirds are broadly recognized as ecological indicators of marine health (Piatt *et al.* 2007; Grecian *et al.* 2012; McGowan *et al.* 2013; Tancell *et al.* 2013), and yet while they comprise only ~3.5% of all bird species they are among the most threatened groups globally with approximately one third of the 359 seabird species listed as threatened and nearly half of all breeding populations in decline (Croxall *et al.* 2012; Lewison *et al.* 2012; Dias *et al.* 2019). Survival of these species relies on maintained health, and dynamic management, of marine ecosystems; but, seabird data

tends to be incomplete at the species level. Pelagic seabirds are particularly difficult to study comprehensively in terms of ecology and distribution. Many are classified as ecological generalists overall, yet maintain individual- or group-level specializations (Ceia *et al.* 2012; Grecian *et al.* 2012). Further, they have a complex behavioral biology, exhibiting distinct behavior states (e.g., foraging, resting) spatiotemporally and within classes (age, sex, natal colony, breeding status; Phillips *et al.* 2005; Ceia *et al.* 2012). In view of their complex behavioral biology, high individual variability, complex habitat partitioning and movement strategies, and colonial nesting habits, available occurrence data are often limited to individual populations within a species (Weimerskirch, Åkesson & Pinaud 2006) and biased towards breeding or fledging individuals (Phillips *et al.* 2005; Weimerskirch, Åkesson & Pinaud 2006; Ceia *et al.* 2012; Grecian *et al.* 2012; Catry *et al.* 2013). This bias has left major gaps in knowledge of at-sea distributions of non-breeding taxa, which must be filled to facilitate development of dynamic conservation planning and prioritization of pelagic marine habitats (Weimerskirch *et al.* 2003; Taylor *et al.* 2011; Grecian *et al.* 2012; Lascelles *et al.* 2012).

Correlative niche modeling offers a method by which the complexities of the distributional dynamics of pelagic seabirds can be explored at the species level. Researchers have used these methods to address specific aspects of seabird distributional ecology such as habitat suitability (Ceia *et al.* 2012; Oppel *et al.* 2012; Catry *et al.* 2013; Louzao *et al.* 2013; McGowan *et al.* 2013; Scales *et al.* 2016), identification of hotspots in the present (Grecian *et al.* 2012) and past (Louzao *et al.* 2013), and selection of potential conservation sites (Tancell *et al.* 2013). Nearly all of these applications, however, utilize correlative niche modeling methods in a movement ecology context, utilizing tracking data from individuals within specific populations rather than for the species as a whole. Incorporation of the temporal dimension in movement ecology studies assessing the

movements of individuals within a population is standard protocol (Dodge *et al.* 2013), however this is not yet standardized in the species level analyses of distributional ecology.

Here, I present a suite of correlational niche modeling studies, the sum of which build upon the traditional modeling framework to incorporate the temporal dimension and produce dynamic niche predictions with an eye towards improving their utility for highly mobile species such as pelagic seabirds. The first chapter works within the typical distributional ecology framework to establish a baseline of model performance for three algorithms in a seasonal, time-averaged approach. In addition to providing a baseline of model performance, the analysis provides direction for methodological improvements focusing on input data preparation using the nomadic Wandering Albatross (*Diomedea exulans* Linnaeus, 1758). The second chapter introduces a series of modifications to the data preparation process of the canonical correlative niche modeling framework to incorporate the temporal dimension. The analysis serves as a proof-of-concept of the modified framework, providing a side-by-side comparison of model predictions produced through the implementation of traditional time-averaged niche modeling and the modified temporally-explicit modeling approach. For this I use the Wood Thrush (*Hylocichla mustelina*, Gmelin 1789), a seasonal migrant for which distributional knowledge is functionally complete and open-access point observation data are abundant, a critical consideration for use in developing and testing methodological improvements. Finally, the third chapter explores the utility of the modified, temporally-explicit modeling framework with the less predictable nomadic species *D. exulans*. Each chapter addresses a distinct facet of stepwise model development—baseline, proof-of-concept, application—to improve the predictive capacity of current correlative modeling methodologies for highly mobile species, thereby increasing the overall utility of these methods for applied outcomes. All three chapters were developed using strictly open access data and

programs, and relevant scripts made openly available, to ensure equitable access to all practitioners.

CHAPTER 1. Biologically-informed ecological niche models for highly mobile species: Non-

breeding Wandering Albatross (*Diomedea exulans*) distributions in the southern

oceans

ABSTRACT

Background: Although pelagic seabirds are broadly recognized as indicators of the health of marine systems, numerous gaps exist in knowledge of their at-sea distributions at the species level. These gaps have profound negative impacts on the robustness of marine conservation policies. Correlative modelling techniques have provided some information, but few studies have explored model development for non-breeding pelagic seabirds. Here, I present a first phase in developing robust niche models for highly mobile species as a baseline for further development.

Methodology: Using observational data from a 12-year time period, 217 unique model parameterizations across three correlative modeling algorithms (boosted regression trees, Maxent, and minimum volume ellipsoids) were tested in a time-averaged approach for their ability to recreate the at-sea distribution of non-breeding Wandering Albatrosses (*Diomedea exulans*) to provide a baseline for further development.

Principle Findings/Results: Overall, minimum volume ellipsoids outperformed both boosted regression trees and Maxent. However, while the latter two algorithms generally overfit the data, minimum volume ellipsoids tended to underfit the data.

Conclusions: The results of this exercise suggest a necessary evolution in how correlative modeling for highly mobile species like pelagic seabirds should be approached. These insights are crucial for understanding seabird-environment interactions at macroscales, which can facilitate ability to address population declines and inform effective marine conservation policy in the wake of rapid global change.

KEY WORDS

Boosted regression trees; digital accessible knowledge; distribution modeling; Maxent; minimum

volume ellipsoids; pelagic seabird distribution

INTRODUCTION

Impacts of global change are increasingly evident, and long-term changes in marine systems are likely to be quite profound (Doney et al. 2012). In spite of these changes, spatial planning and conservation implementation in marine systems are lagging compared to terrestrial regimes (Croxall et al. 2012; Game et al. 2009; Lewison et al. 2012). Of particular concern are pelagic zones, which currently lack adequate protection compared to other marine ecoregions. Seabirds and other marine predators can serve as proxies to help identify potential marine conservation sites (Lascelles et al. 2012; Piatt et al. 2007).

The strong spatio-temporal heterogeneity inherent in marine systems (Hyrenbach et al. 2000; Weimerskirch et al. 2005) is mirrored in the movements and behavior of pelagic seabird species tracking marine resources. Many pelagic seabird species appear to behave as generalists overall, while maintaining individual- or group-level specializations (Ceia et al. 2012). In view of their complex behavioral biology (Catry et al. 2013; Grecian et al. 2012), such as high individual variability (Phillips et al. 2005), complex habitat partitioning and movement strategies (Phillips et al. 2005; Weimerskirch et al. 2006), and colonial nesting habits, available data for many of these species are highly biased towards breeding individuals. This information bias has left gaps in knowledge about at-sea distributions of non-breeding individuals (Grecian et al. 2012; Lascelles et al. 2012; Taylor et al. 2011; Weimerskirch et al. 2003).

Correlative niche modelling approaches, termed species distribution modeling (SDM) or ecological niche modelling (ENM), have the potential to fill knowledge gaps regarding species' distributions (Lewison et al. 2012; Mateo et al. 2013; Rodríguez et al. 2007), aid in conservation planning (Peterson 2006; Rodríguez et al. 2007), assess conservation-human conflicts (Rodríguez et al. 2007), and provide insight into impacts of climate change on species' distributions (Peterson

2006). Ongoing conservation concerns regarding pelagic seabirds make them an important focus group in such studies. To date, however, nearly all applications of these approaches to pelagic seabirds have focused on individual populations rather than species as a whole, and few have explored algorithm function for seabirds outside the breeding season (Oppel et al. 2012; Ramos et al. 2015; Thiebot et al. 2011; Wakefield et al. 2011).

Wandering Albatrosses (*Diomedea exulans* Linnaeus, 1758) are biennial breeders (Milot et al. 2008; Prince et al. 1992) with multiple life stages (juvenile, immature, non-breeding adult, breeding adult) marked by distinct behaviors (Ceia et al. 2012; Phillips et al. 2005). Classified as Vulnerable (IUCN 2016), they are protected under the Agreement on the Conservation of Albatrosses and Petrels (ACAP) and are among the best-studied pelagic seabirds (ACAP 2009). Because occurrence data for this species are relatively rich, gaps in knowledge of their natural history are less drastic than in other pelagic species. This is a critical consideration for application to developing and testing methodological improvements. Studies have already noted impacts of global climate change on *D. exulans* and other pelagic marine species (Weimerskirch et al. 2003; Weimerskirch et al. 2012).

The aim of this study is to identify hemisphere-scale environmental associations of the geographic distribution of non-breeding *Diomedea exulans*, and work towards addressing the challenge of modeling these associations in highly mobile species. I present results of a first phase of correlational ecological niche modeling using traditional modeling techniques based on three algorithms and multiple parameterizations; I assessed each models' ability to anticipate seasonal environmental preferences of non-breeding *D. exulans*. This initial exploration focused on issues of algorithm selection and parameterization in time-averaged correlative modeling.

MATERIALS AND METHODS

Input Data. Models were calibrated using digitally accessible knowledge (DAK; Sousa-Baena et al. 2014) in the form of *Diomedea exulans* primary occurrence data and remotely-sensed environmental data for December 2000–November 2012. As temporal averaging of models may generalize spatial distributions and environmental associations (Peterson et al. 2005), the year was divided into thirds ('seasons') for this study (Table 1) based loosely on breeding biology, and designed to respond to possible shifts in foraging behavior by breeding adults: I = December–March (egg laying/incubation), G = April–July (brood guard/chick rearing), and P = August–November (fledging). The study area was restricted to -20˚S to -60˚S latitude, as this latitudinal range comfortably encompasses the generalized distributional extent of *D. exulans* (BirdLife International and NatureServe 2015a), reduces concern for significant gaps in environmental data coverage—particularly in seasonal, high-latitude regions—and constrains the extent to which implemented modeling algorithms must extrapolate.

Table 1. Delineation of seasons for time-averaged correlative models, associated breeding stage, and the number of *Diomedea exulans* occurrence data used in model calibration (Calibration), model calibration testing (Calibration testing), and testing after model transfer (Projection testing).

Seasons	Period	Breeding stage	*D. exulans* observation data			
			Calibration	Calibration testing	Projection testing	Total
I	December – March	egg laying/incubation	553	239	269	1061
G	April – July	brood guard/chick rearing	281	121	185	587
P	August – November	fledging	140	60	130	330

To characterize the sampling process that produced the data (Anderson 2003), observation- and specimen-based occurrence data for all members of the order Procellariiformes were obtained from the Global Biodiversity Information Facility (GBIF; accessed 5/26/2015,

doi:10.15468/dl.fquf8g; Appendix S1). *Diomedea exulans* observation data were separated from the greater dataset and divided by season (see above), cleaned of duplicates, gridded to the spatial resolution and extent of the environmental data, and rarefied to one point per pixel to reduce spatial bias (Kramer-Schadt et al. 2013; Phillips et al. 2009). As no information about sex or breeding status was associated with the occurrence data, distinguishing non-breeding from breeding individuals was impossible. However, because these analyses aimed to assess capacity for estimating non-breeding distributions, occurrence data south of 50˚S latitude were excluded from analyses (Weimerskirch et al. 2006; Weimerskirch et al. 1985). Of an initial 7903 *D. exulans* records, 1982 were available for use in modeling after cleaning; 136,947 records of the Order were used to characterize spatial sampling bias (see below).

Seven environmental layers were used to summarize the complex environmental landscape of the high-latitude marine systems under analysis. *Dynamic data* included four monthly variables of global MODIS Terra L3 SMI data at 4.6 km spatial resolution downloaded from the NASA OceanColor Web (Table S1.2; NASA 2014). Daytime and nighttime sea surface temperatures (SST) were used to average uneven heating/cooling of the ocean surface. Chlorophyll-*a* (Hyrenbach et al. 2007; Wakefield et al. 2009) and chromophoric dissolved organic matter (Coble 2007; Nelson & Siegel 2013; Urtizberea et al. 2013) were incorporated as proxies for ocean productivity. Imagery were converted from native HDF to ASCII grids, projected to WGS 84 using the Marine Geospatial Ecology Tools (MGET) ArcGIS toolbox (Roberts et al. 2010), and 'NoData' values in raster layers filled using a temporal filter followed by a spatial filter in R v 3.2.2 (R Development Core Team 2009). Next, environmental data layers were stacked by season, and the mean, maximum, minimum, and range of values were calculated for each variable. The resulting 16 time-averaged rasters were subjected to principle component analyses (PCA) to

reduce collinearity. The first five principle components (PCs) from each PCA per season were used in analyses; in all three seasons, the first PC explained ≥ 95% of variation (Table S1.3). *Geophysical (static) data* included bathymetry—ETOPO1 global relief data (Amante 2009)—and a derivative bathymetric slope layer. All seven environmental layers were standardized to 0.2083° resolution and projected in geographic coordinates (WGS 84). Additional information regarding input data is available in Appendix S1.

Figure 1. Model calibration regions for seasons I (December–March), P (August–November), and G (April–July). Base layers: ETOPO1 global relief data (Amante 2009) and Global Administrative Areas global shapefile (http://www.gadm.org).

Model Calibration. The biotic-abiotic-mobility (BAM) framework is a useful heuristic for developing strategies for model calibration (Soberón & Peterson 2005). The calibration region should match the mobility area (= the area that has been accessible to the species over relevant periods of time; Barve et al. 2011).
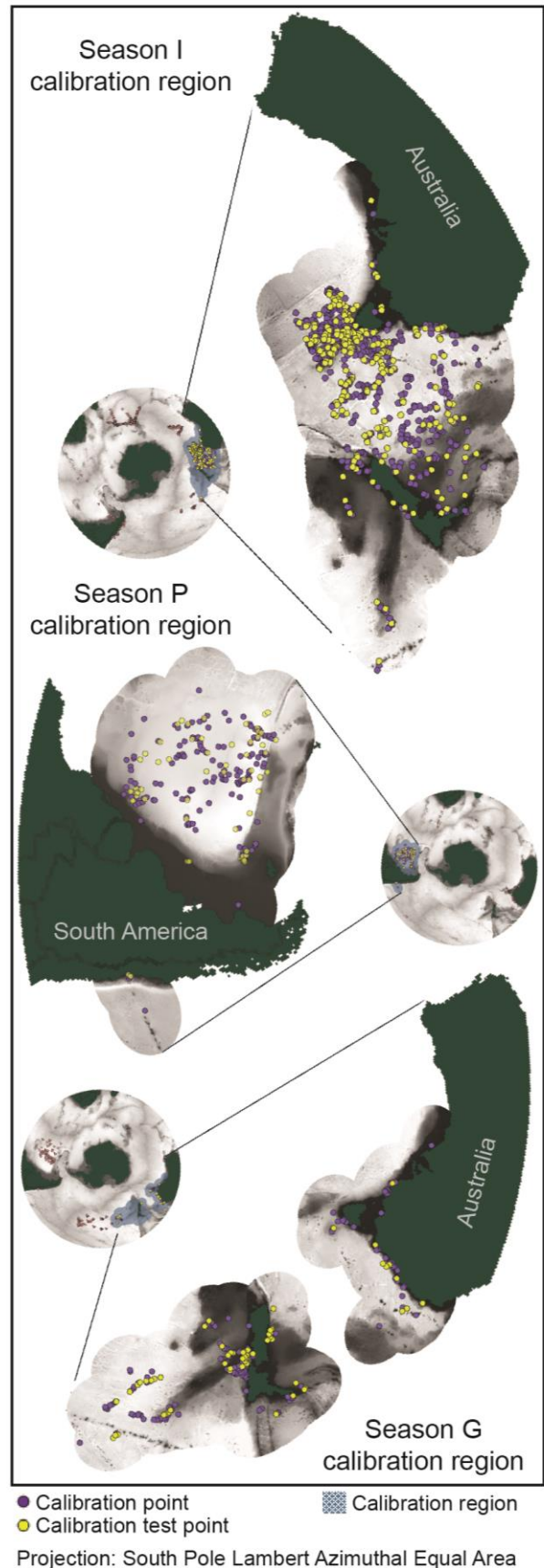
Mobility is not a major distributional constraint for *D. exulans* (Milot et al. 2008; Saupe et al. 2012; Soberón & Peterson 2005). As such, calibration regions were delineated as marine areas within a 500 km buffer around known occurrences in a particular season (Fig. 1; Barve et al. 2011; Saupe et al. 2012). To permit rigorous model evaluation, 30% of occurrence records were selected randomly and set aside for model evaluation. Models were calibrated using the remaining 70% of occurrence records.

A total of 217 model calibrations was tested for each of the three time-averaged seasons across three correlative niche modeling algorithms, yielding 651 models following the "no silver bullet" ideas of Qiao et al. (2015), in which many candidate approaches and algorithms are tested to identify the best-performing method for a particular situation. Two presence-only algorithms—Maxent (Phillips et al. 2006; Phillips et al. 2004) and minimum volume ellipsoids (MVE)—and one presence-absence algorithm—boosted regression trees (BRT; Elith et al. 2008)—were selected for testing.

Presence-only algorithms. Maxent version 3.3.3k (Phillips et al. 2006; Phillips et al. 2004) was calibrated under different settings for three parameters: prevalence, regularization multiplier, and bias layer. Initial sensitivity analyses using the jackknife procedure within Maxent identified an ideal combination of environmental variables for model calibration (bathymetry, PCs 1–4). All models were run using 100 bootstrapped replicates, 30% random test percentage, and 1000 maximum iterations; all other settings remained at 'default'.

Prevalence was tested over a range of 0.3–0.9 at intervals of 0.1. Prevalence has no impact on raw output scores in Maxent, but does affect the 'logistic' output (Elith et al. 2011; Merow et al. 2013); Elith et al. (2011) and Merow et al. (2013) provide in-depth discussion on the impact of prevalence on model performance. The regularization multiplier (RM) impacts model fit by

loosening or tightening the constraints of a model around the training data (Elith et al. 2011; Shcheglovitova & Anderson 2013). RM was tested at three levels: 1 (default), 1.5, and 2. Bias layers are incorporated into Maxent to account for sampling bias in the data and reflect relative sampling effort (Kramer-Schadt et al. 2013; Phillips et al. 2009). Two sets of bias layers derived from the procellarid occurrence data set aside during data cleaning and matching the grid system of the environmental grids were tested. Procellariiform observations per pixel were summed to produce the "raw" bias layer. To develop a more refined layer for comparison, the raw bias layer was subjected to a Log_2 transformation and kernel smoother to scale the value distribution more evenly (Table S1.4).

Minimum volume ellipsoids (MVEs) were calibrated for two sets of parameters: variable inclusion and threshold. MVEs calculate environmental distance using Mahalanobis distances based on a minimum volume ellipsoid drawn around the training (calibration) data. The simplicity of MVEs means few parameters. Six levels of variable inclusion (Runs; Table S1.5) and three thresholds (T; 0.9, 0.95, 0.99) were analyzed using R v 3.2.2 (R Development Core Team 2009). The threshold designates the central percentage of training data to be used in calculating the MVE, such that a higher threshold (e.g., 0.99) indicates greater confidence in the input data used for training compared to a lower threshold value (0.95 or 0.9). Scripts were modified from code provided by J. Soberón (*pers. comm.*), and are available in the Supplementary Materials (Appendix S3). As MVEs calculate relative environmental distance, model predictions were inverted and re-scaled (0–1) to render them comparable to the other algorithms.

Presence-absence algorithm. Boosted regression trees (BRTs) were calibrated under various settings of four parameters: pseudo-absence, tree complexity, learning rate, and bag fraction. Two levels of pseudo-absences (PA) were tested after Barbet-Massin et al. (2012; Table

S1.6): the first (PA–1) was set at 1500 randomly selected absences; the second (PA–2) was two times the total number of model calibration training points. Tree complexity (TC), which controls the maximum level of interactions permitted in model fitting, was tested over a range of 1–5, wherein TC = 1 indicates no variable interactions and TC = 5 permits interactions between ≤ 5 variables. Four learning rates (LR) were tested: 0.01, 0.005, 0.0025, and 0.001. Learning rate determines the relative contribution of each tree as the model grows, such that a slower learning rate tends to smooth effects of stochastic processes and reduces between-model variance. Bag fraction (BF) controls stochasticity by designating the random subset used for model calibration and testing; a smaller bag fraction is likely to lead to an increase in the chance of fitting of unusual variables. Four levels of BF were tested: 0.5, 0.6, 0.7, and 0.75. More in-depth explanations of BRTs are provided by Elith et al. (2008). Models were run to a minimum of 1000 trees using all seven environmental variables in R v 3.2.2 (R Development Core Team 2009) following scripts from Elith et al. (2008).

Model evaluation. Significance was evaluated for all model calibration and model transfer scenarios. In light of issues highlighted by Peterson et al. (2008) and Lobo et al. (2008), typical receiver operating characteristic (ROC) routines implemented within Maxent were not used. Instead, models were evaluated external to the Maxent package using the partial ROC (pROC) metric, for which the critical value is $AUC_{ratio} = 1.0$. pROC scores were calculated using the randomly selected 30% test data set aside prior to model calibration (see above), and occurrence data from the broader projection region to provide two levels of testing. pROC scores were calculated in R v 3.2.2 (R Development Core Team 2009) at an omission threshold of $E = 5\%$ over 2000 iterations using code provided by L. Osorio (*pers. comm.*). Significance was determined by

direct count of numbers of replicate analyses in which $\text{AUC}_{\text{ratio}} \leq 1$. Although AUC ratios are difficult to compare among very different calibration areas or modeling contexts, they can be used to assess within-algorithm, within-season performance (e.g., to evaluate the best performing model calibration for an individual algorithm).

Final model performance was assessed using two metrics to permit comparison of models across algorithms. The first metric was omission rate. Omission rates (percent of test data predicted as 'absent') were calculated using the *Diomedea exulans* observation data set aside and an 80% threshold (e.g., $E = 20\%$). As a second measure of performance, BirdLife International's important bird area (IBA) polygons for the Southern Hemisphere (BirdLife International and NatureServe 2016) were overlaid on the best model for each algorithm and season to evaluate visually the ability of each model to anticipate areas of known importance to *D. exulans*. A query of BirdLife International's marine e-atlas (BirdLife International and NatureServe 2015b) facilitated generation of a subset of 130 of the original 1275 polygons identified specifically as valuable to non-breeding *D. exulans* and classified as proposed or confirmed IBA areas. It is critical to note that these designations are based on limited data (e.g., a handful of tracking datasets) and do not necessarily encompass all areas of importance to non-breeding *D. exulans*. They do, however, provide a simple, qualitative view of model performance, thus their use in model evaluation here is considered secondary and supplemental to calculated omission rates.

RESULTS

Significance Testing. All 651 model calibration scenarios were significant ($p < 0.05$). In model transfer, only 52.7% (343 of 651) of models (across all combinations of algorithms, parameter settings, and environmental datasets) performed statistically significantly better than random. All 54 MVE models (18/season) were significant. Of the 480 BRT models (160/season), 36.3% (58) were significant in season I, 93.8% (150) in season G, and 11.9% (19) models in season P. And, of the 117 Maxent models (39/season), 94.9% (37) were significant in season G and 64.1% (25) in season P. None of the Maxent models transferred in season I were significant. Results from the top-performing model for season I are presented for comparison.
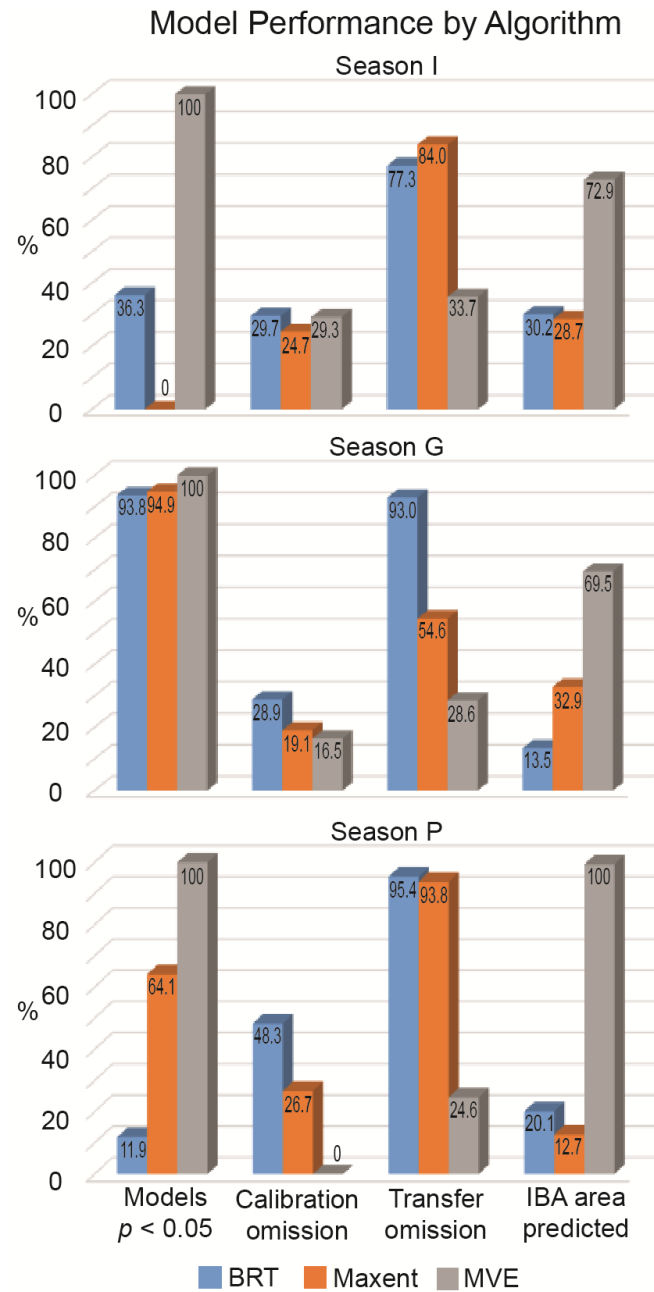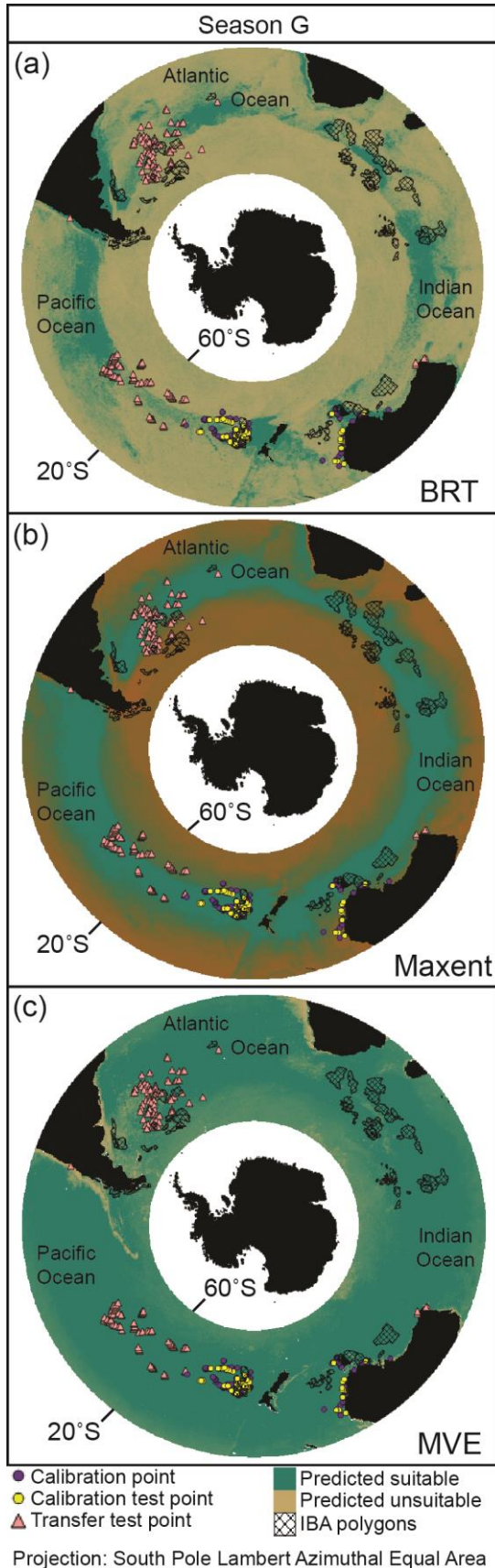

Figure 2. Model performance for best performing models by algorithm and season (I: December–March, G: April–July, and P: August–November): omission rates for model calibration and transfer, and percentage of total IBA area predicted.

Overall Model Performance. MVEs outperformed both Maxent and BRTs in all three seasons for both model evaluation metrics (Figure 2). MVEs thresholded at 0.9 and run = 3 (all

variables included except bathymetry and bathymetry slope) yielded the best models in seasons I (December–March) and G (August–November), and MVEs thresholded at 0.9 and run = 1 (all variables included) in season P (April–July). Model projections following an 80% threshold for the top models produced by each algorithm are presented in figures 3 (season G) and 4 (seasons I and P). To provide a more detailed view of model predictions relative to occurrence data and IBAs, three particularly well-sampled focus regions are shown: the waters surrounding New Zealand and Australia (Figs S2.1 – S2.3), the vicinity of the sub-Antarctic Islands off South America (Fig. S2.4), and the vicinity of the sub-Antarctic Islands near southern Africa (Fig. S2.5). The top five model projections for each algorithm are summarized by season in Table S2.1.

Model Calibration. In model calibration, MVE had the lowest omission rates in seasons G (16.5%) and P (0%). Maxent had the lowest omission rate in season I (24.7%).

Model Transfer. Though overall model performance declined in model transfer, MVE models maintained the lowest omission rates across all three seasons, with omission rate never exceeding 35% (Figure 2); its greatest drop in performance was in season P in which the omission rate jumped to 24.6% during model transfer. BRT and Maxent suffered the most drastic increases in omission. Omission rates for BRT and Maxent peaked at 95.4% and 93.8% respectively in season P. The greatest loss in performance occurred in season G for BRT where omission rose by 64.1% (from 28.9% in model calibration to 93.0% in model transfer), and in season P for Maxent where omission rates rose by 67.1% (from 26.7% in model calibration to 93.8% in model transfer). MVEs successfully predicted no less than 69.5% of IBA area in all three seasons (Figure 2). Maxent and BRT models, on the other hand, never predicted greater than 32.9% of IBA area.

Season G

(a) ... Atlantic Ocean ... Pacific Ocean ... 60°S ... 20°S ... Indian Ocean ... BRT

(b) ... Atlantic Ocean ... Pacific Ocean ... 60°S ... 20°S ... Indian Ocean ... Maxent

(c) ... Atlantic Ocean ... Pacific Ocean ... 60°S ... 20°S ... Indian Ocean ... MVE

● Calibration point
○ Calibration test point
△ Transfer test point

Predicted suitable
Predicted unsuitable
▨ IBA polygons

Projection: South Pole Lambert Azimuthal Equal Area

Parameterizing Algorithms. Boosted Regression Trees. In all, 46.7% (224) of the 480 BRT models (160/season) were significant in model transfer. PA, TC, and LR parameter selections all impacted evaluation statistics. BRT tended to overfit in model transfer (Figs 3a, 4a-b). Models parameterized for PA–2 and TC $\leq$ 2 performed best in seasons I and P, whereas models parameterized at PA–1 and TC $\geq$ 3 excelled in G (Table S2.1). Higher-performance was also associated with a faster LR (0.01) in I, a moderate LR (0.005–0.0025) in G, and a slower LR ($\leq$ 0.0025) in P.

Figure 3. Season G (August–November) model projections following an 80% threshold for the top models produced by (a) BRT (PA-2, tree complexity = 5, learning rate = 0.0025, bag fraction = 0.5), (b) Maxent (Log_2 bias layer, prevalence = 0.7, regularization multiplier = 2), and (c) MVE (threshold = 0.9, run = 3). Base layer: Global Administrative Areas global shapefile (http://www.gadm.org).
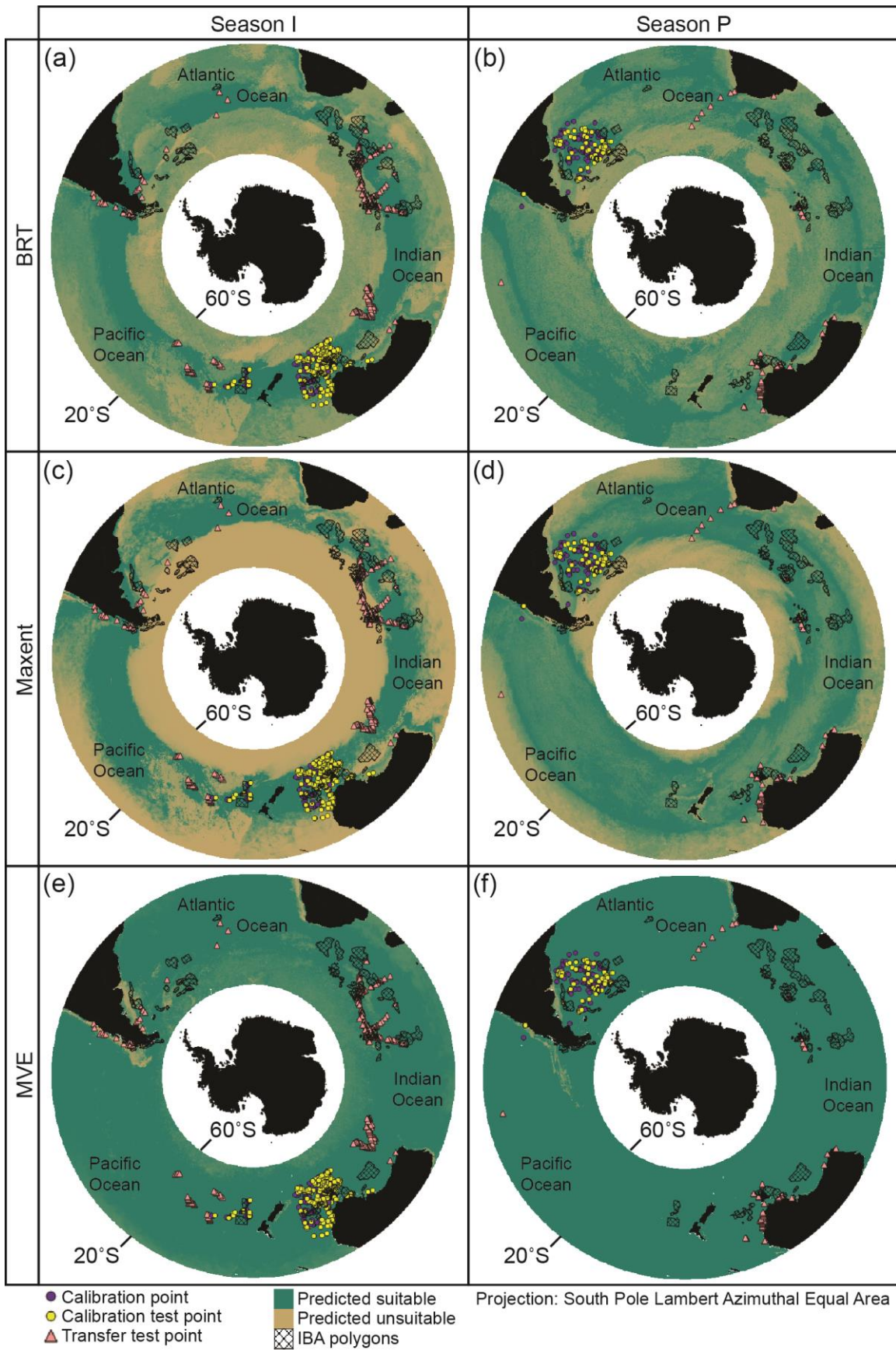
Figure 4. Season I (December–March) model projections following an 80% threshold for the top models produced by (a) BRT (PA-2, tree complexity = 1, learning rate = 0.01, bag fraction = 0.5), (c) Maxent (not significant; no bias layer, prevalence = 0.3, regularization multiplier = 2), and (e) MVE (threshold = 0.9, run = 3); and, season P (April–July) model projections following an 80% threshold for the top models produced by (b) BRT (PA-2, tree complexity = 1, learning rate = 0.05, bag fraction = 0.6), (d) Maxent (no bias layer, prevalence = 0.9, regularization multiplier = 1), and (f) MVE (threshold = 0.9, run = 1). Base layer: Global Administrative Areas global shapefile (http://www.gadm.org).

Maxent. In all, 53.0% (62) of 117 models (39/season) parameterized in Maxent were significant after model transfer. BRT tended to overfit in model transfer (Figs 3b, 4c-d). Bias and RM played the biggest role in model performance. The top models were calibrated with the Log_2 bias layer and RM ≥ 1.5 (G), and the raw bias layer (P; Table S2.1). None of the season I model projections were significant.

Minimum Volume Ellipsoids. All 54 models (18/season) calibrated using MVEs were statistically significant in model projection. MVE predictions were generally underfit (i.e., overly general) (Figs 3c, 4e-f). Top models incorporated more moderate numbers (2–4) of environmental variables (2 ≤ Run ≤ 4) for season G, and more variables (Run ≥ 2) in seasons I and P.

DISCUSSION

Correlative modeling offers a method by which the complexities of distributional dynamics of pelagic seabirds can be explored at the species level. Researchers have used these methods to address specific aspects of seabird distributional ecology such as habitat suitability (Catry et al. 2013; Ceia et al. 2012; Louzao et al. 2013; McGowan et al. 2013; Oppel et al. 2012; Scales et al. 2016), identification of hotspots in the present e and past (Louzao et al. 2013), selection of potential conservation areas, and potential climate change impacts (Krüger 2017). But, many of the more recent applications use ensemble modeling (Krüger 2017; Scales et al. 2016) or incorporate seabird

movement data (Clay 2016; Quillfeldt 2017) which, while increasing in quantity and availability, is nowhere near as prevalent or accessible as point observation data.

The purpose of this exercise was to develop a baseline of model performance across a suite of parameterizations with an eye towards a step-wise approach to improving correlative niche modeling techniques for pelagic and other highly mobile species. Although just under half of all models tested performed significantly better than random, predictive performance was adequate only for MVEs (low omission rates, high percentage of IBA areas predicted). Indeed, MVE models consistently indicated the greatest potential for capturing the complexity of *Diomedea exulans* distributional ecology with all calibrations significant in model calibration and model transfer. The best performing BRT and Maxent calibrations either had omission rates > 50% or predicted < 35% of the total area covered by BirdLife International's Marine IBAs (BirdLife International and NatureServe 2016) of known importance to *D. exulans*.

Though methods such as BRT and Maxent have a history of higher predictive performance (Elith et al. 2006; Phillips et al. 2009) the results presented here suggest that these more complex algorithms may not be ideal for summarizing the complexity of highly pelagic species. Parameterizations for both BRT and Maxent tended to overfit models: although Maxent exhibited a more moderate fit and higher predictive performance overall, Maxent models were still not necessarily 'good' at anticipating test occurrence data. Overall performance declined substantially during model transfer (i.e., extrapolation to the full study region) for both BRT and Maxent. Performance for the two complex algorithms was particularly poor in seasons I and P though Maxent improved slightly in season G. This less-than-stellar overall performance likely results from the combination of the spatial exclusion of data (i.e., method of determining breeding vs non-

breeding data), sampling bias within the observation data, and inability to discern breeding from non-breeding individuals (i.e., lack of biological information in the observation data).

My results highlight one of the major roadblocks for correlational niche-modeling methodologies: the loss of detail in signals because of over-generalization. Correlative modelling characterizes a species' use of environmental space to create a model that can then be used to address questions regarding the species' distribution in geographic space (Barve et al. 2011). Recent studies have shown that no single 'best' algorithm or parameter setting for SDM or ENM applications exists or is likely to exist (Merow et al. 2013; Qiao et al. 2015; Saupe et al. 2012; Shcheglovitova & Anderson 2013), and the results of this study are in close agreement. Therefore, algorithm selection and parameterization should be an iterative, hypothesis- or question-driven process. Myriad factors affect performance of correlational models, including the limitations of the specific algorithms, input data quality, appropriateness of selected explanatory (environmental) variables, spatial resolution (Bellier et al. 2010; Hyrenbach et al. 2007; Wakefield et al. 2009; Weimerskirch et al. 2005), and study region extent (Barbet-Massin et al. 2012; Barve et al. 2011; Hyrenbach et al. 2007). As a result of this complexity, a key point is that averaging environmental data across each of the three seasons limits the detail available in the modelling outputs (Peterson et al. 2005; Scales et al. 2016).

The most obvious limitation encountered in this preliminary study of model assessment for pelagic bird distributions is the quality of the occurrence data, lack of absence data (Elith et al. 2011), sampling bias inherent in opportunistically collected data (Elith et al. 2011; Grecian et al. 2012; Phillips et al. 2009; Weimerskirch et al. 2006), and lack of relevant additional biological information (i.e., sex, age, or breeding status; Grecian et al. 2012). These factors—lack of

biological information and bias—necessarily influence calibration region designation, ultimately impacting overall model performance.
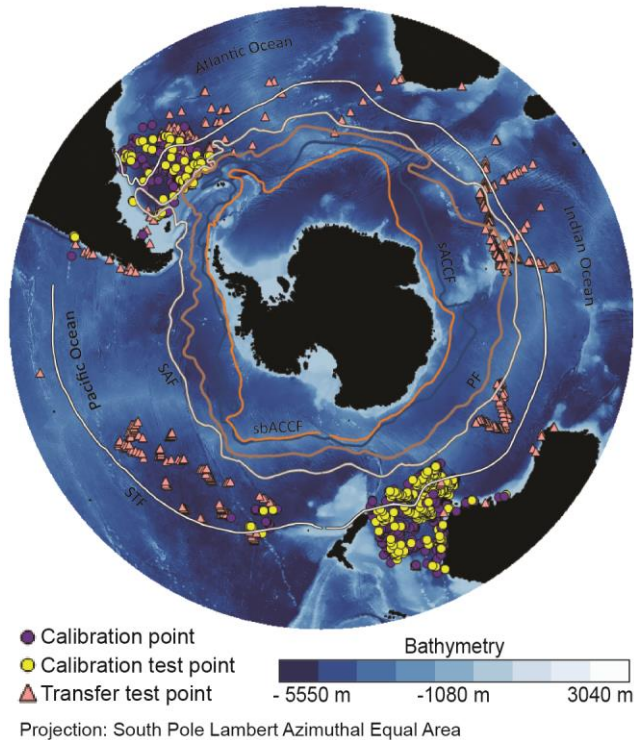

Figure 5. *Diomedea exulans* occurrence data overlaid with Southern Ocean front lines (STF – subtropical front; SAF – sub-Antarctic front; PF – polar front; sACCF – southern Antarctic Circumpolar Current; sbACCF – southern boundary Antarctic Circumpolar Current). Note the distinct spatial bias in observation data, particularly in the lack of data on the high seas.

Bias is a significant concern in assessing biodiversity patterns at macro-scales (Beck et al. 2014), and these biases are amplified when data are derived in bulk from portals such as GBIF (Beck et al. 2013; Beck et al. 2014; Graham et al. 2004; Yesson et al. 2007). *Diomedea exulans* point occurrence data used here are strongly biased towards the Argentine Basin, the Tasman Sea, south Pacific Ocean south of Tasmania, the Campbell Plateau and Chatham Rise around Australia and New Zealand, and areas directly adjacent to breeding colonies (Figure 5); occurrence data are minimal for the high seas in the South Pacific Ocean east of the Pacific Rise, east of the Atlantic Ridge in the South Atlantic Ocean, south of South Africa around Agulhas Basin and Plateau, and the Crozet Basin and the Southeast Indian Ridge in the Indian Ocean. This uneven sampling leads to gaps in documentation of the species' response to some environmental conditions, limiting model generality (Owens et al. 2013).

A final concern associated with DAK is taxonomic uncertainty (Graham et al. 2004). Great albatross taxonomy has undergone multiple revisions, only recently 'stabilizing' with four species in the *Diomedea exulans* complex (Burg & Croxall 2004; Chambers et al. 2009; Nunn et al. 1996; Rains et al. 2011). Morphological similarities between species and significant overlap of non-breeding individuals within the complex which make differentiation of species at-sea quite difficult (Onley & Scofield 2007). Lack of cohesive taxonomic resolution only further increases the potential for homogenization of species ecology, an important factor often not discussed which reduce the confidence and accuracy of correlative models.

Despite the intriguing result in which MVEs outperformed more complex algorithms, deriving ecological conclusions from low- or even moderate-performing models such as those that I have presented herein is premature. Rather, this study provides a baseline for development of better and more predictive models that will eventually be capable of accounting for the complex behaviors of such species. Further, it serves as a reminder that correlative niche modeling approaches are sensitive to a large suite of factors, and are impacted inherently by the study question itself. In light of the limitations of readily available seabird data (e.g., strong spatio-temporal biases, no information on sex and age of the individuals involved), development of such a baseline of algorithm behavior is necessary for successful for evaluating the efficacy of more complex data treatment strategies.

Improved correlative modeling approaches, building on the baseline presented herein, can significantly enhance understanding of macroscale factors driving distributional dynamics of species, including pelagic seabirds and other highly mobile species, and provide crucial information to fill important information gaps necessary to project and explore the future distributional potential (Catry et al. 2013; Louzao et al. 2011). These insights, in combination with

increasing knowledge of species' natural history and ecology, can inform conservation planners, and offer information vital to the research priorities identified by Lewison et al. (2012) including identification and mapping of movement corridors and foraging areas to understand impacts of global change on the distributions of pelagic seabirds and other highly mobile species.

CONFLICT OF INTEREST

The author declares that there is no conflict of interest.

REFERENCES

Anderson, R.P. (2003) Real vs. artefactual absences in species distributions: tests for *Oryzomys albigularis* (Rodentia:Muridae) in Venezuela. Journal of Biogeography, 30, 591–605.

Barbet-Massin, M., Jiguet, F., Albert, C.H. & Thuiller, W. (2012) Selecting pseudo-absences for species distribution models: how, where and how many? Methods in Ecology and Evolution, 3, 327–338.

Barve, N., Barve, V., Jiménez-Valverde, A., Lira-Noriega, A., Maher, S.P., Peterson, A.T., et al. (2011) The crucial role of the accessible area in ecological niche modeling and species distribution modeling. Ecological Modelling, 222, 1810–1819.

Beck, J., Ballesteros-Mejia, L., Nagel, P. & Kitching, I.J. (2013) Online solutions and the 'Wallacean shortfall': what does GBIF contribute to our knowledge of species' ranges? Diversity and Distributions, 19, 1043–1050.

Beck, J., Böller, M., Erhardt, A. & Schwanghart, W. (2014) Spatial bias in the GBIF database and its effect on modeling species' geographic distributions. Ecological Informatics, 19, 10–15.

Bellier, E.G., Certain, G., Planque, B., Monestiez, P. & Bretagnolle, V. (2010) Modelling habitat selection at multiple scales with multivariate geostatistics: an application to seabirds in open sea. Oikos, 119, 988–999.

Birdlife International and Natureserve (2015b) Marine IBA e-Atlas: http://maps.birdlife.org/marineIBAs/default.html.

Burg, T.M. & Croxall, J.P. (2004) Global population structure and taxonomy of the Wandering Albatross species complex. Molecular Ecology, 13, 2345–2355.

Catry, P., Lemos, R.T., Brickle, P., Phillips, R.A., Matias, R. & Granadeiro, J.P. (2013) Predicting the distribution of a threatened albatross: the importance of competition, fisheries and annual variability. Progress in Oceanography, 110, 1–10.

Ceia, F.R., Phillips, R.A., Ramos, J.A., Cherel, Y., Vieira, R.P., Richard, P., et al. (2012) Short- and long-term consistency in the foraging niche of Wandering Albatrosses. Marine Biology, 159, 1581–1591.

Chambers, G.K., Moeke, C., Steel, R. & Trueman, J.W. (2009) Phylogenetic analysis of the 24 named albatross taxa based on full mitochondrial cytochrome *b* DNA sequences. Notornis, 56, 82–94.

Clay, T.A., Manica, A., Ryan, P. G., Silk, J. R. D., Croxall, J. P., Ireland, L., Phillips, R. A. (2016) Proximate drivers of spatial segregation in non-breeding albatrosses. Scientific Reports, 6,

Coble, P.G. (2007) Marine optical biogeochemistry: The chemistry of ocean color. Chemical Reviews, 107, 402-418.

Croxall, J.P., Butchart, S.H.M., Lascelles, B., Stattersfield, A.J., Sullivan, B., Symes, A., et al. (2012) Seabird conservation status, threats and priority actions: a global assessment. Bird Conservation International, 22, 1–34.

Doney, S.C., Ruckelshaus, M., Duffy, J.E., Barry, J.P., Chan, F., English, C.A., et al. (2012) Climate change impacts on marine ecosystems. Annual Review of Marine Science, 4, 11-37.

Elith, J., Graham, C.H., Anderson, R.P., Dudík, M., Ferrier, S., Guisan, A., et al. (2006) Novel methods improve prediction of species' distributions from occurrence data. Ecography, 29, 129–151.

Elith, J., Leathwick, J.R. & Hastie, T. (2008) A working guide to boosted regression trees. Journal of Animal Ecology, 77, 802–813.

Elith, J., Phillips, S.J., Hastie, T., Dudík, M., Chee, Y.E. & Yates, C.J. (2011) A statistical explanation of MaxEnt for ecologists. Diversity and Distributions, 17, 43–57.

Game, E.T., Grantham, H.S., Hobday, A.J., Pressey, R.L., Lombard, A.T., Beckley, L.E., et al. (2009) Pelagic protected areas: the missing dimension in ocean conservation. Trends in Ecology & Evolution, 24, 360–369.

Graham, C.H., Ferrier, S., Huettman, F., Moritz, C. & Peterson, A.T. (2004) New developments in museum-based informatics and applications in biodiversity analysis. Trends in Ecology & Evolution, 19, 497–503.

Grecian, W.J., Witt, M.J., Attrill, M.J., Bearhop, S., Godley, B.J., Grémillet, D., et al. (2012) A novel projection technique to identify important at-sea areas for seabird conservation: an example using Northern Gannets breeding in the North East Atlantic. Biological Conservation, 156, 43–52.

Hyrenbach, K.D., Forney, K.A. & Dayton, P.K. (2000) Marine protected areas and ocean basin management. Aquatic Conservation—Marine and Freshwater Ecosystems, 10, 437–458.

Hyrenbach, K.D., Veit, R.R., Weimerskirch, H., Metzl, N. & Hunt, G.L. (2007) Community structure across a large-scale ocean productivity gradient: marine bird assemblages of the southern Indian Ocean. Deep-Sea Research Part I-Oceanographic Research Papers, 54, 1129–1145.

IUCN (2016) IUCN Red List of Threatened Species v2015-4: http://www.iucnredlist.org.

Kramer-Schadt, S., Niedballa, J., Pilgrim, J.D., Schroder, B., Lindenborn, J., Reinfelder, V., et al. (2013) The importance of correcting for sampling bias in MaxEnt species distribution models. Diversity and Distributions, 19, 1366–1379.

Krüger, L., Ramos, J.A., Xavier, J.C., Grémillet, D., González-Solís, J., Petry, M.V., Phillips, R.A., Wanless, R.M., Paiva, V.H. (2018) Projected distributions of Southern Ocean albatrosses, petrels and fisheries as a consequence of climatic change. Ecography, 41, 195–208.

Lascelles, B.G., Langham, G.M., Ronconi, R.A. & Reid, J.B. (2012) From hotspots to site protection: identifying Marine Protected Areas for seabirds around the globe. Biological Conservation, 156, 5–14.

Lewison, R., Oro, D., Godley, B., Underhill, L., Bearhop, S., Wilson, R.P., et al. (2012) Research priorities for seabirds: improving conservation and management in the 21st century. Endangered Species Research, 17, 93–121.

Lobo, J.M., Jiménez-Valverde, A. & Real, R. (2008) AUC: a misleading measure of the performance of predictive distribution models. Global Ecology and Biogeography, 17, 145–151.

Louzao, M., Aumont, O., Hothorn, T., Wiegand, T. & Weimerskirch, H. (2013) Foraging in a changing environment: habitat shifts of an oceanic predator over the last half century. Ecography, 36, 57–67.

Louzao, M., Pinaud, D., Péron, C., Delord, K., Wiegand, T. & Weimerskirch, H. (2011) Conserving pelagic habitats: seascape modelling of an oceanic top predator. Journal of Applied Ecology, 48, 121–132.

Mateo, R.G., De La Estrella, M., Felicísimo, Á.M., Munoz, J. & Guisan, A. (2013) A new spin on a compositionalist predictive modelling framework for conservation planning: a tropical case study in Ecuador. Biological Conservation, 160, 150–161.

Mcgowan, J., Hines, E., Elliott, M., Howar, J., Dransfield, A., Nur, N., et al. (2013) Using seabird habitat modeling to inform marine spatial planning in central California's National Marine Sanctuaries. PLoS One, 8, e71406.

Merow, C., Smith, M.J. & Silander, J.A. (2013) A practical guide to MaxEnt for modeling species' distributions: what it does, and why inputs and settings matter. Ecography, 36, 1058–1069.

Milot, E., Weimerskirch, H. & Bernatchez, L. (2008) The seabird paradox: dispersal, genetic structure and population dynamics in a highly mobile, but philopatric albatross species. Molecular Ecology, 17, 1658–1673.

Nelson, N.B. & Siegel, D.A. (2013) The global distribution and dynamics of chromophoric dissolved organic matter. Annual Review of Marine Science, 5, 447–476.

Nunn, G.B., Cooper, J., Jouventin, P., Robertson, C.J.R. & Robertson, G.G. (1996) Evolutionary relationships among extant albatrosses (Procellariiformes: Diomedeidae) established from complete cytochrome-B gene sequences. Auk, 113, 784–801.

Onley, D. & Scofield, P. (2007) Albatrosses, petrels, & shearwaters of the world. Princeton University Press, Princeton, New Jersey:

Oppel, S., Meirinho, A., Ramírez, I., Gardner, B., O'connell, A.F., Miller, P.I., et al. (2012) Comparison of five modelling techniques to predict the spatial distribution and abundance of seabirds. Biological Conservation, 156, 94–104.

Owens, H.L., Campbell, L.P., Dornak, L.L., Saupe, E.E., Barve, N., Soberon, J., et al. (2013) Constraints on interpretation of ecological niche models by limited environmental ranges on calibration areas. Ecological Modelling, 263, 10–18.

Peterson, A.T. (2006) Uses and requirements of ecological niche models and related distribution models. Biodiversity Informatics, 3, 59–72.

Peterson, A.T., Martínez-Campos, C., Nakazawa, Y. & Martínez-Meyer, E. (2005) Time-specific ecological niche modeling predicts spatial dynamics of vector insects and human dengue cases. Transactions of the Royal Society of Tropical Medicine and Hygiene, 99, 647–655.

Peterson, A.T., Papeş, M. & Soberón, J. (2008) Rethinking receiver operating characteristic analysis applications in ecological niche modeling. Ecological Modelling, 213, 63–72.

Phillips, R.A., Silk, J.R.D., Croxall, J.P., Afanasyev, V. & Bennett, V.J. (2005) Summer distribution and migration of nonbreeding albatrosses: individual consistencies and implications for conservation. Ecology, 86, 2386–2396.

Phillips, S.J., Anderson, R.P. & Schapire, R.E. (2006) Maximum entropy modeling of species geographic distributions. Ecological Modelling, 190, 231–259.

Phillips, S.J., Dudík, M., Elith, J., Graham, C.H., Lehmann, A., Leathwick, J., et al. (2009) Sample selection bias and presence-only distribution models: implications for background and pseudo-absence data. Ecological Applications, 19, 181–197.

Piatt, J.F., Sydeman, W.J. & Wiese, F. (2007) Introduction: a modern role for seabirds as indicators. Marine Ecology Progress Series, 352, 199–204.

Prince, P.A., Wood, A.G., Barton, T. & Croxall, J.P. (1992) Satellite tracking of Wandering Albatrosses (*Diomedea exulans*) in the South Atlantic. Antarctic Science, 4, 31–36.

Qiao, H.J., Soberón, J. & Peterson, A.T. (2015) No silver bullets in correlative ecological niche modelling: insights from testing among many potential algorithms for niche estimation. Methods in Ecology and Evolution, 6, 1126–1136.

Quillfeldt, P., Engler, J. O., Silk, J. R., Phillips, R. A. (2017) Influence of device accuracy and choice of algorithm for species distribution modelling of seabirds: a case study using black-browed albatrosses. Journal of Avian Biology, 48, 1549–1555.

R Development Core Team (2009) R: A language and environment for statistical computing. R Foundation for Statistical Computing: http://www.r-project.org.

Rains, D., Weimerskirch, H. & Burg, T.M. (2011) Piecing together the global population puzzle of Wandering Albatrosses: genetic analysis of the Amsterdam albatross *Diomedea amsterdamensis*. Journal of Avian Biology, 42, 69–79.

Ramos, R., Sanz, V., Militao, T., Bried, J., Neves, V.C., Biscoito, M., et al. (2015) Leapfrog migration and habitat preferences of a small oceanic seabird, Bulwer's petrel (*Bulweria bulwerii*). Journal of Biogeography, 42, 1651–1664.

Roberts, J.J., Best, B.D., Dunn, D.C. & Halpin, P.N. (2010) Marine Geospatial Ecology Tools: an integrated framework for eological geoprocessing with ArcGIS, Python, R, MATLAB, and C++. Environmental Modelling and Software, 25, 1197–1207.

Rodríguez , J.P., Brotons, L., Bustamante, J. & Seoane, J. (2007) The application of predictive modelling of species distribution to biodiversity conservation. Diversity and Distributions, 13, 243–251.

Saupe, E.E., Barve, V., Myers, C.E., Soberón, J., Barve, N., Hensz, C.M., et al. (2012) Variation in niche and distribution model performance: the need for a priori assessment of key causal factors. Ecological Modelling, 237, 11–22.

Scales, K.L., Miller, P.I., Ingram, S.N., Hazen, E.L., Bograd, S.J. & Phillips, R.A. (2016) Identifying predictable foraging habitats for a wide-ranging marine predator using ensemble ecological niche models. Diversity and Distributions, 22, 212–224.

Shcheglovitova, M. & Anderson, R.P. (2013) Estimating optimal complexity for ecological niche models: a jackknife approach for species with small sample sizes. Ecological Modelling, 269, 9–17.

Soberón, J. & Peterson, A.T. (2005) Interpretation of models of fundamental ecological niches and species' distributional areas. Biodiversity Informatics, 2, 1–10.

Sousa-Baena, M.S., Garcia, L.C. & Peterson, A.T. (2014) Completeness of digital accessible knowledge of the plants of Brazil and priorities for survey and inventory. Diversity and Distributions, 20, 369–381.

Thiebot, J.B., Lescroel, A., Pinaud, D., Trathan, P.N. & Bost, C.A. (2011) Larger foraging range but similar habitat selection in non-breeding versus breeding sub-Antarctic penguins. Antarctic Science, 23, 117–126.

Urtizberea, A., Dupont, N., Rosland, R. & Aksnes, D.L. (2013) Sensitivity of euphotic zone properties to CDOM variations in marine ecosystem models. Ecological Modelling, 256, 16–22.

Wakefield, E.D., Phillips, R.A. & Matthiopoulos, J. (2009) Quantifying habitat use and preferences of pelagic seabirds using individual movement data: a review. Marine Ecology Progress Series, 391, 165–182.

Wakefield, E.D., Phillips, R.A., Trathan, P.N., Arata, J., Gales, R., Huin, N., et al. (2011) Habitat preference, accessibility, and competition limit the global distribution of breeding Black-browed Albatrosses. Ecological Monographs, 81, 141–167.

Weimerskirch, H., Åkesson, S. & Pinaud, D. (2006) Postnatal dispersal of Wandering Albatrosses *Diomedea exulans*: implications for the conservation of the species. Journal of Avian Biology, 37, 23–28.

Weimerskirch, H., Gault, A. & Cherel, Y. (2005) Prey distribution and patchiness: factors in foraging success and efficiency of Wandering Albatrosses. Ecology, 86, 2611–2622.

Weimerskirch, H., Inchausti, P., Guinet, C. & Barbraud, C. (2003) Trends in bird and seal populations as indicators of a system shift in the Southern Ocean. Antarctic Science, 15, 249–256.

Weimerskirch, H., Jouventin, P., Mougin, J.L., Stahl, J.C. & Vanbeveren, M. (1985) Banding recoveries and the dispersal of seabirds breeding in French Austral and Antarctic Territories. Emu, 85, 22–33.

Weimerskirch, H., Louzao, M., De Grissac, S. & Delord, K. (2012) Changes in wind pattern alter albatross distribution and life-history traits. Science, 335, 211–214.

Yesson, C., Brewer, P.W., Sutton, T., Caithness, N., Pahwa, J.S., Burgess, M., et al. (2007) How global is the Global Biodiversity Information Facility? PLoS One, 2, e1124.

CHAPTER 2. Incorporating time into the traditional correlational distributional modeling framework: A proof-of-concept using the Wood Thrush (*Hylocichla mustelina*)

ABSTRACT

Background: Detailed spatio-temporal information about geographic distributions of species is critical for biodiversity analyses in conservation and planning. Traditional correlative modeling approaches use species observational data in model calibration and testing in a time-averaged framework. This method averages environmental values through time to yield a single environmental value for each site. Although valuable for exploring distributions of species at a broad level, this averaging is one of myriad factors impacting model quality and reliability.

Methods: We sought to optimize correlative niche model performance by incorporating time-specificity into the existing modeling framework. We modified the existing framework to account for temporal dynamics in species' distributions to produce more robust, temporally-explicit models. Using the Wood Thrush (*Hylostichla mustelina*) as our study species, we introduce a method of (1) deriving a temporally-explicit pseudo-absence dataset using kernel density estimates to replicate relative sampling of sites through time, and (2) incorporating temporally-explicit covariates in model calibration.

Results: By accounting for location, and month and year of primary data collection, the time-specific models successfully yielded dynamic predictions reflecting known distributional shifts in *Hylocichla mustelina*'s annual movement pattern.

Broader Impacts: The modified data preparation steps that we present incorporate temporal dimensions into traditional correlational modeling approaches improving predictive capacity and overall utility of these models for highly mobile, short-lived, or behaviorally complex species.

With the ability to estimate species' niches in greater detail, time-specific models will be able to address specific concerns of species-level management and policy development for highly mobile and/or migratory species, as well as disease vectors of public health interest.

INTRODUCTION

Understanding species' geographic distributions is critical for managing biodiversity. Correlative distributional modeling (a.k.a., species distributional modeling, ecological niche modeling) is a popular tool used for characterizing species' ecological niches in environmental space and projecting them into geographic dimensions (Peterson 2006). By relating primary biodiversity data to biologically relevant environmental covariates to provide spatially explicit predictions of climatic suitability, such models can inform about where survey data are limited or where knowledge gaps may impede development of more detailed models. These simple but powerful tools render geographic dimensions of biodiversity more understandable and accessible to diverse stakeholders and have been liberally incorporated into a broad range of research questions relevant to biodiversity and conservation (Rodríguez *et al.* 2007; Franklin 2013; Eaton *et al.* 2018), invasive species (Ingenloff *et al.* 2017), climate change (Beck 2013; Pacifici *et al.* 2015; Searcy & Shaffer 2016), phylogeography (Alvarado-Serrano & Knowles 2014), and human health (Peterson 2006; Rodríguez *et al.* 2007; Peterson 2014).

A notable limitation of current niche modeling methodologies is the temporal averaging of covariate data such that each unique geographic coordinate pair is assigned a single environmental value for the full study period. This averaging reduces predictive capacity for species that are highly mobile, behaviorally complex, or with a lifetime or life stages that are short with respect to the temporal span of environmental changes; although, using higher resolution weather data in place of long-term climate data has been shown to mitigate some of these impacts (Bateman, VanDerWal & Johnson 2012; Feldmeier *et al.* 2018). Traditional approaches use covariates that are averaged temporally, effectively treating covariates as static values for the breadth of the study period. The result is a single, static view of predicted suitability for the study species, which has

been the topic of discussion in light of species that switch among multiple niches between seasons (Martínez-Meyer, Peterson & Navarro-Sigüenza 2004). These approaches can result in over-generalization of estimates of ecological niches (Peterson *et al.* 2005; Barve *et al.* 2014; Ingenloff 2017), particularly for migratory or behaviorally complex organisms (Peterson *et al.* 2005; Ingenloff 2017). Modeling mobile species presents a particularly challenging situation because, to be meaningful, predictive models must capture both a seasonally dynamic landscape and associated species movements, which traditional methods are unable to account for (Elith, Kearney & Phillips 2010). In light of anthropogenic climate change and other human impacts, garnering an understanding of species' distributional dynamics through time, rather than a simple snapshot of overall potential geographic distribution, is critical.

Unlike the field of movement ecology where the pairing of covariate data contemporal to species observational data has been the standard for some time (Dodge *et al.* 2013), few correlative modeling studies in distributional ecology have incorporated time-specificity. Most studies applied a "seasonal" modeling approach—modeling of a single facet of a species' life history (e.g. breeding or wintering) using time-averaged approaches (Laube, Graham & Böhning-Gaese 2015; Skov *et al.* 2016; Soriano-Redondo *et al.* 2019). Fink *et al.* (2010) introduced spatiotemporal exploratory models (STEM) wherein an ensemble or mixture model is created from a suite of seasonally- or behaviorally-restricted distributional models to encompass the breadth of the study species' life history. Seasonal approaches, however, may be subject to reduced predictive capacity resulting from the need for user-designated subsetting of observational data and because it still involves considerable temporal averaging of environmental variation. Williams, Willemoes and Thorup (2017) explored a "full year" modeling framework that evaluated each month averaged across years to characterize accurately seasonal movements of cuckoos. Other researchers

overcame issues of over-generalization owing to time averaging with more unique approaches: e.g., Barve *et al.* (2014) combined detailed physiological measurements with temporally specific summaries of weather and climate to understand geographic distributions of Spanish moss. However, incorporation of mechanistic approaches within correlative modeling frameworks is constrained by an overwhelming lack of detailed physiological data for the vast majority of species (Peterson, Papeş & Soberón 2015). More recently, two studies incorporated time without excessive temporal-averaging or incorporation of mechanistic methods: Welch, Pressey and Reside (2018) produced monthly distributional models for seven shark species over 10-years, yielding a dynamic view of monthly projected distributions for the study period; and, Abrahms *et al.* (2019) used a multi-model ensemble approach to predict daily habitat suitability for blue whales. Still, explicit methodologies broadly accessible to the greater community of distributional ecology practitioners remain lacking.

Here, we introduce several modifications to the input data preparation process for traditional niche modeling frameworks that incorporate temporal dimensions and produce dynamic niche predictions. We use a well-sampled migratory species, the Wood Thrush (*Hylocichla mustelina* Gmelin, 1789), to demonstrate three modifications to the data preparation process: generation of a weighted time-specific pseudo-absence dataset, wherein covariate data are assigned to each occurrence corresponding to the place *and time* of collection, and spatiotemporal rarefication of presence and pseudo-absence data (Fig. 1). These modifications account for spatial and temporal survey bias in openly accessible primary occurrence data and alleviate the problem of over-generalization in niche characterization resulting from temporal averaging of covariates. We provide a comparison of this time-explicit method with the traditional time-averaged approach

and assess the ability of each to predict climatic suitability for the species across North and Central America.

MATERIALS AND METHODS

To maximize reproducibility, we obtained all data from open-access sources and ran all processes using the open-source statistical analysis program R v3.5.2 (R Development Core Team 2009). All supplementary information (doi.org/10.6084/m9.figshare.8160290.v2) and relevant R scripts (https://doi.org/10.6084/m9.figshare.8160227.v1) are freely available. Figure 1 illustrates the modified data preparation workflow described here relative to traditional time-averaged approaches (Supp. Fig. 1)
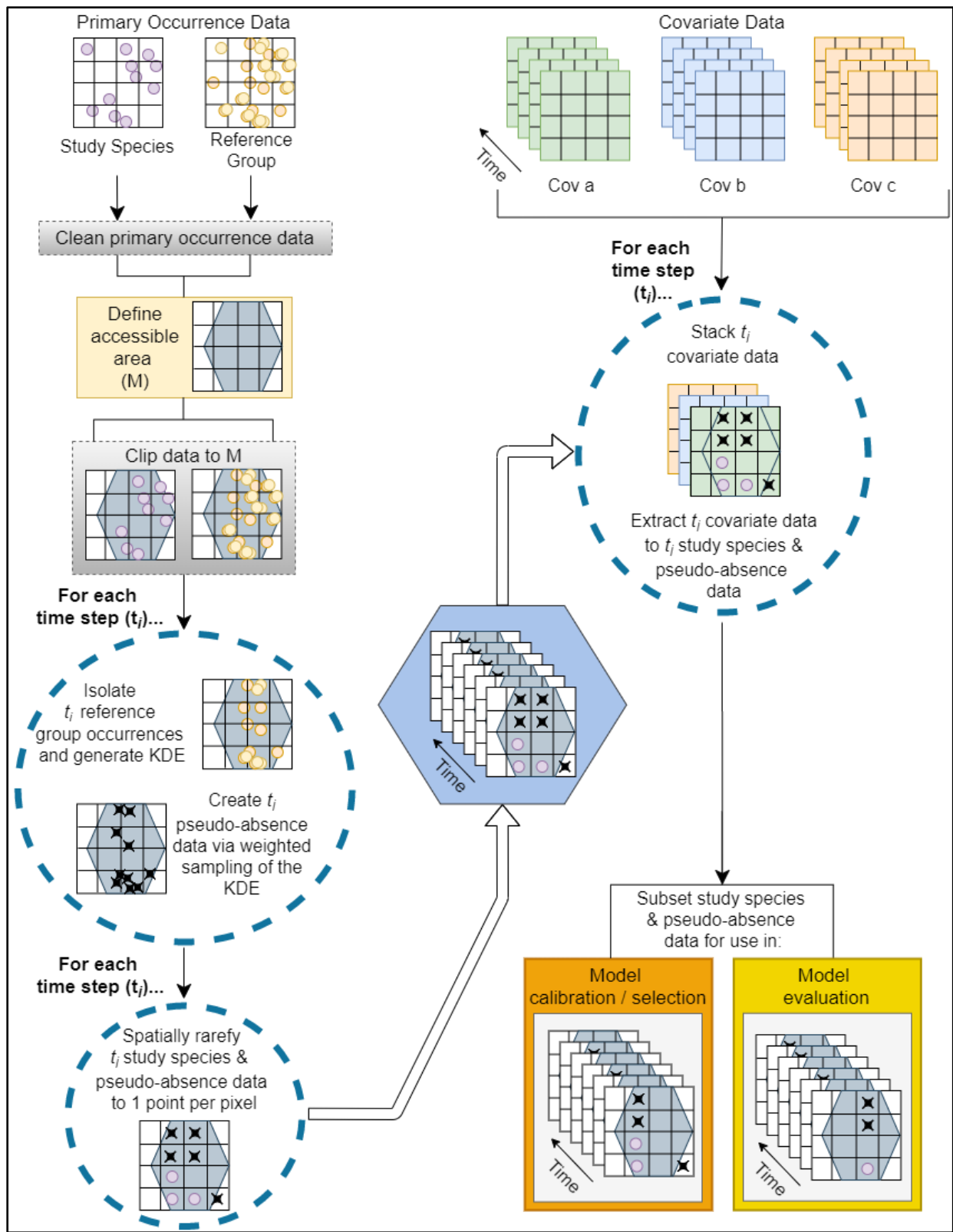
Figure 1. Modified input data preparation workflow for temporally-explicit correlative modeling. Blue dashed circles denote changes from the traditional methods.

Study Species.—We selected the long-distance migrant Wood thrush (*Hylocichla mustelina*) because distributional knowledge is effectively complete and data are abundant. Each year, *H. mustelina* travels between discrete breeding and wintering ranges. Breeding occurs during late spring and summer (mid-May into August) in the eastern United States and southeastern Canada in deciduous and mixed forests (Collar 2005; BirdLife International 2017). Early autumn, they begin a staggered migration from breeding to wintering grounds in southern Mexico and Central America, with more northerly populations migrating beginning in mid-August and more southerly populations delaying migration until late September and early October (Collar 2005; BirdLife International 2017). *H. mustelina* remains on the wintering grounds until late March–April. Vagrants have been recorded in the Caribbean, northern South America, western United States, and western Europe (Collar 2005).

Input Data

Occurrence data.—We downloaded two sets of primary occurrence data from the Global Biodiversity Information Facility (GBIF). The first was that of our study species, *Hylocichla mustelina* (GBIF 26 March 2018). The second, the reference group used to characterize the sampling process that produced the data (Anderson 2003), included the entire family Turdidae (GBIF 24-26 March 2018). We constrained both searches to records obtained via human observation between 1980–2018 with no known spatial issues for all of continental North and Central America. Initial data calls returned 532,633 *H. mustelina* records from 19 institutions and 4,848,853 Turdidae records from 47 institutions.

Data were subjected to a sequence of quality control checks including visual inspections to detect obvious outliers/inaccuracies (e.g., wrong hemisphere, long-distance vagrants), and removal

of records with imprecise (e.g., no decimal places) or missing geographic coordinates. Records collected after 2015 were removed owing to temporal limits of covariate data (see below). We delineated a model calibration region (accessible area for the species) based on the known natural history of *H. mustelina*, in which we identified the range of the core population including breeding and wintering locations, and a ~750 km buffer to account for their high-mobility, but excluding known areas of vagrancy (Supp Fig. 2; Barve *et al.* 2011). This reduced data available to 433,648 *H. mustelina* and 3,011,848 Turdidae records. We intended to run analyses using all data (1980–2015); however, generating the time-specific pseudo-absence dataset (see below) was so cumbersome computationally that we stopped analyses after March 2010. This reduced our data to 134,293 *H. mustelina* and 828,267 Turdidae records. We set aside 2014–2015 *H. mustelina* data (149,340 records) for use as an additional model evaluation dataset.

Pseudo-absence data.—Derivation of a pseudo-absence dataset from a reference group sampled in the same manner as the study species (Anderson 2003) is a common practice for correlative models requiring presence-absence data when true absence data are unavailable (Kramer-Schadt *et al.* 2013). Sampling bias, however, is a universal characteristic of primary biodiversity data (Kadmon, Farber & Danin 2004), and can be a significant problem in correlative modeling (Phillips *et al.* 2009; Anderson *et al.* 2016). While pseudo-absence data cannot correct for biases inherent in a presence dataset, they can assure that background data used in model calibration reflect sampling biases in presence data.

To incorporate time, we generated a "bias cloud": a time-specific pseudo-absence dataset reflective of sampling intensity through time for the duration of the study period (see dynamic pseudo-absence dataset in the Supplementary Information). To this end, we first divided the study period into discrete time steps; we chose an intermediate temporal resolution (monthly), but we

note that this could be applied to any temporal resolution for which the occurrence and covariate data both are available. For each time step, we subset reference group occurrence data (including the study species) sampled during that time step and generated a kernel density estimate (KDE) using the 'npudensbw' and 'npudens' functions in the 'np' package (Hayfield & Racine 2008). Kernel density bandwidth specifications were calculated using an Epanechonikov kernel, a least-squares cross-validation bandwidth selection method, and an adaptive-nearest neighbor continuous-variable as a balance between producing detailed KDEs and computational feasibility. We then applied a 95% threshold (excluding the lowest 5%) to the resulting KDE and took a weighted sample wherein the KDE value of each pixel functioned as the weight. The number of points extracted was proportional to the number of reference group observations in that time step relative to the overall dataset (see Supplementary Information for additional detail). The collective sampling from all time steps yielded a pseudo-absence dataset reflective of spatial and temporal sampling patterns within the reference group data.

Despite our intention of producing a pseudo-absence dataset through 2015, the process was halted at March 2010 as sampling through time increased drastically resulting in dramatically increased processing time for heavily sampled time steps (reaching nearly a week on a powerful lab desktop; Supp. Figs. 3 and 4). The pseudo-absence dataset for the amended study period (January 1980 – March 2010) totaled 241,958 pseudo-absences for the 363 time steps, approximately double the number of presence points. Although no *H. mustelina* observation data existed for 13 months during the study period (Supp. Table 1), the process produced pseudo-absence data for all time steps because reference group observations existed in all time steps—these mismatches between occurrence data and pseudo-absence data function in effect as absence information in model calibration.

Time-averaged and time-specific datasets.—To address sampling bias further, we rarefied *H. mustelina* data and pseudo-absences to a single point per pixel relative to the spatial resolution of the covariate data (Phillips *et al.* 2009; Kramer-Schadt *et al.* 2013). To create the time-averaged datasets, we spatially rarified the original data to a single point per pixel. For time-specific datasets, we rarified the original data spatially and temporally to one point per pixel per time step. The rarefication process reduced data to 34,004 (1980–2010) and 36,436 (2014–2015) *H. mustelina* records and 205,837 pseudo-absences for time-averaged analyses, and 76,119 (1980–2010) and 61,479 (2014–2015) *H. mustelina* records and 241,958 pseudo-absences for time-specific analyses. We ensured that temporal information (e.g., month and year) remained associated with all data for use in model evaluation.

Covariate data.—For simplicity, we used three monthly covariates from TerraClimate—precipitation, and minimum and maximum temperature—as these data cover a broad temporal range (1958–2015) available at monthly resolution (Abatzoglou *et al.* 2018). Data were cropped to the study region (Supp. Fig. 2) and left at their native 4.6 km resolution. Covariate data were available through 2015 only, limiting the overall study period to 1980–2015. We extracted covariate data to all rarefied time-specific occurrence and pseudo-absence records described above such that each point was associated with the climatic information specific to the place *and* point in time (month) of observation.

For time-averaged analyses, we derived a dataset of six summary layers that included mean and range for each of the three covariates for January 1980 – March 2010. Summary data were extracted to each occurrence and pseudo-absence record in the rarefied time-averaged datasets. We created a second set of summary covariates for 2014–2015 and extracted these data to the rarefied 2014–2015 time-averaged *H. mustelina* data.

After removing two records with no covariate values because they fell marginally on the climate data grid, we randomly divided each of the 1980–2010 datasets 50-50 for use in model calibration/selection and evaluation (Supp. Table 2). The 2014–2015 *H. mustelina* data were set aside for final model evaluation.

Correlational Niche Modeling

Following Qiao, Soberón and Peterson (2015), we explored a suite of model calibration scenarios for three commonly used presence-absence algorithms—generalized linear models (GLM), generalized additive models (GAM), and boosted regression trees (BRT)—to identify the parameterization yielding the best time-averaged and time-specific model for each algorithm. For each algorithm, we explored a suite of parameter settings, such that we generated large numbers of candidate models, and then selected a final model among them using criteria of predictive ability and simplicity.

Model calibration.—We calibrated GLMs with both main effects and pairwise interactions via an exhaustive search using the 'glmulti' function (Calcagno 2013). We used the 'gam' function (Wood 2011) to calibrate GAMs, assessing four smoothers (cubic splines, thin plate splines, P splines, and adaptive splines), two smoother basis dimensions (default, k = 25), two smoothing parameters (default, restricted maximum likelihood), and covariate interactions ranging from no interaction to full interactions. We visually assessed covariate responses for GLM and GAM calibrations using the 'response.plot2' function (Thuiller *et al.* 2016). Finally, we calibrated BRTs using the 'gbm.step' function (Hijmans *et al.* 2017), evaluating four levels of learning rate (default, 0.005, 0.0025, 0.001), two bag fraction levels (default, 0.6), and tree complexity from 0 up to three (time-specific) and four (time-averaged).

Model selection.—We used algorithm-appropriate metrics to select the best time-averaged and time-specific calibration (parameter settings) for each algorithm. We used the Akaike Information Criterion (AIC) for within-algorithm model selection of GLMs and GAMs (Warren & Seifert 2011). However, as AIC is inappropriate for tree-based algorithms, we used training and test data mean squares estimates (MSE) and test data omission rate for BRTs. MSE values were calculated using the 'MSE' function (Signorell *et al.* 2019). Potential discrepancies involved in comparing AIC to cross validation results were not a concern because we were not using these statistics for cross-algorithm comparisons.

Model transfer.—The six models selected (three time-averaged and three time-specific) were transferred across the study region for both study periods (1980–2010 and 2014–2015). Time-specific models were projected to each time step for both evaluation periods. Time-averaged models were projected to both sets of time-averaged covariate data. We thresholded model outputs to the minimum presence training value adjusted to permit 1% omission error ($E = 1\%$) to allow for some error in the data (Pearson *et al.* 2007). To allow comparisons with time-specific outputs, we plotted time-averaged test data for each time step onto static model outputs. The resulting monthly projections were then aggregated into image sequences in graphics interchange format (GIF) to produce dynamic visualizations of predicted climatic suitability through time using R packages 'magick' and 'gifski' (Ooms 2018a; Ooms 2018b).

Model evaluation.—We evaluated thresholded model projections using the temporally corresponding evaluation datasets. Specifically, we looked at model omission rates (how well test data were predicted by the model) and proportion of the study region predicted suitable. Because *H. mustelina* exhibits a predictable movement pattern between distinct breeding and wintering sites during the year, we also sought to assess model performance within these broader periods.

Thus, for assessment purposes only, we designated three "seasons" based on behavior: breeding (June–August), wintering (October–April), and migratory (May and September).

RESULTS

The model selection process yielded six models for evaluation: three time-averaged and three time-specific (details in Supplementary Information; Supp. Tables 3–4). Figure 2 provides a snapshot of time-specific model results for all three algorithms; time-averaged model results are presented in Figure 3. GIFs providing a side-by-side comparison of the thresholded time-averaged and time-specific model projections for each algorithm for the 1980–2010 primary study period and 2014–2015 supplemental evaluation period are available in the Supplementary Information (doi.org/10.6084/m9.figshare.8160290.v2).

Time-specific models

All three time-specific models adequately predicted both the area of the core *Hylocichla mustelina* population and beyond to include areas of known vagrancy. On average, they predicted greater proportions of the study area climatically suitable for both evaluation periods than time-averaged models (Supp. Table 5). GAM and GLM models had the lowest overall mean omission rates during the 1980–2010 study period (GAM 0.036; GLM 0.036; BRT 0.210; Supp. Table 6); however, overall omission rate for 2014–2015 was roughly equivalent for all three algorithms, with all three models performing well during model transfer (BRT 0.026, GAM 0.027, GLM 0.025).
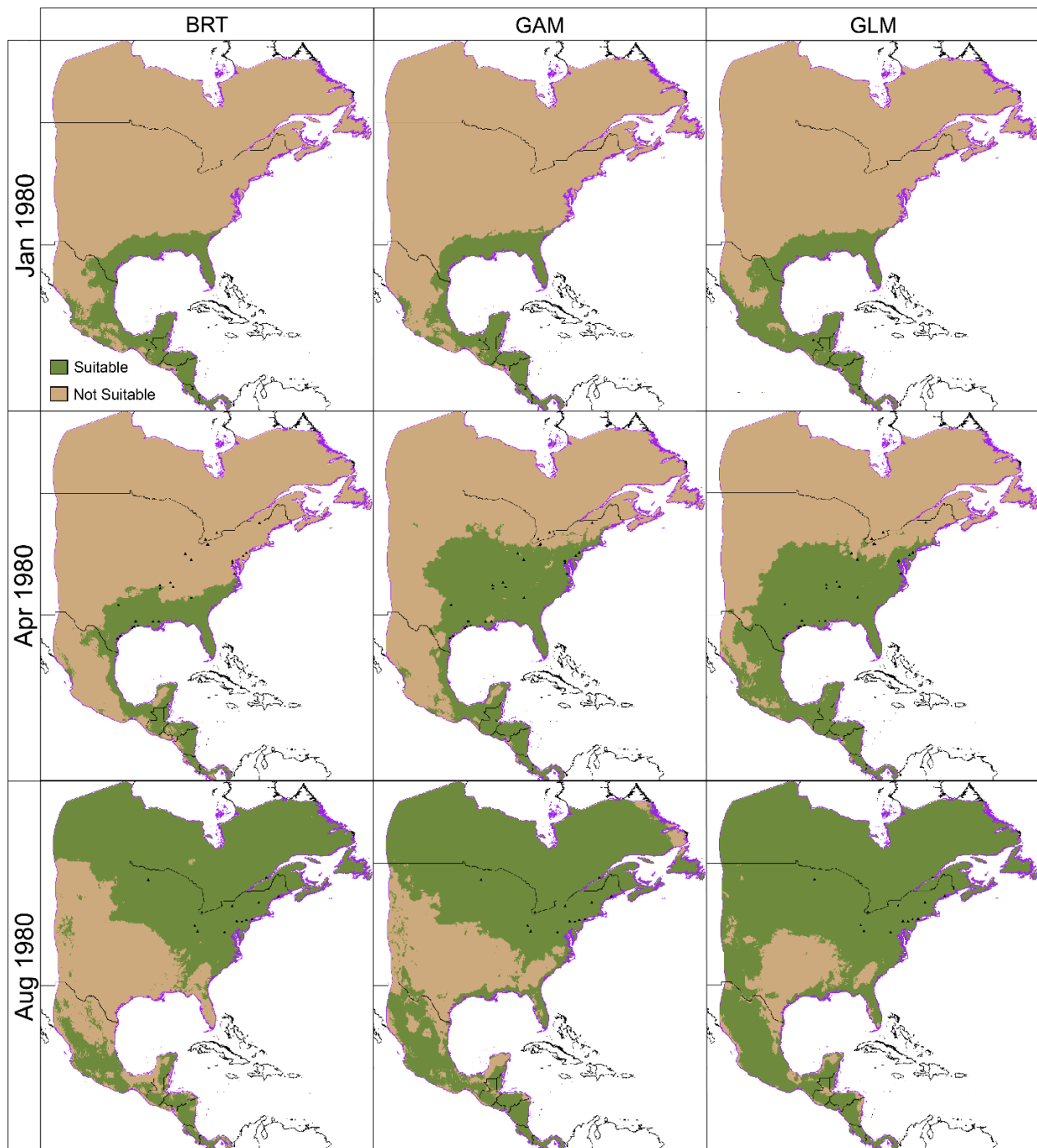
Figure 2. Snapshot of thresholded (E=1%) time-specific BRT (left column), GAM (center column), and GLM (right column) projections for three individual times steps from 1980 (January, top row; April, center row; August, bottom row). Green regions indicate areas predicted climatically suitable; tan denotes areas predicted unsuitable; black triangles denote *Hylocichla mustelina* test data.

Variability in model performance (omission rate) was greatest during the wintering months

for GAM and GLM (1980–2010), and for all three 2014–2015 projections (Supp. Figs. 5–7, Supp.

Table 7). Mean monthly area predicted suitable was most restricted during the wintering period for the GAM (12.4–41.8%) and GLM (14.6–46.4%) models, and greatest during the breeding period (GAM 80.1–81.5%; GLM 89.7–91.6%) for the primary study period (Supp. Figs. 8–10, Supp. Table 8). This same trend was evident in all three 2014–2015 time-specific model projections. The 1980–2010 BRT model had noticeably elevated omission rates during April (0.591) and May (0.401), coinciding with a tendency towards underpredicting the northernmost distributional extent of *H. mustelina*. While all three time-specific models failed to predict the full northern extent of the species, the area predicted suitable by the BRT model was particularly low (April – 19.7%; May – 30.0%) relative to the GAM (April – 30.5%; May – 56.7%) and GLM (April – 36.3%; May – 60.7%) models.

Time-averaged models

All three time-averaged models fit the core distribution of *Hylocichla mustelina*, but failed to predict into areas of known vagrancy, and tended to underpredict during wintering months, with patchy areas of predicted suitability in Central America and southeastern Mexico (Fig. 3). Model projections into 2014–2015 predicted more area climatically suitable (BRT 36.9%, GAM 42.3%, GLM 46.3%) than for 1980–2010 (BRT 32.8%, GAM 36.6%, GLM 39.3%; Supp. Figs. 8–10, Supp. Table 5). Overall omission rates were effectively the same for GAM (1980–2010: 0.029; 2014–2015: 0.020) and GLM (1980–2010: 0.030; 2014–2015: 0.020) models, and slightly elevated in the BRT model (1980–2010: 0.037; 2014–2015: 0.039; Supp. Figs. 5–7, Supp. Table 6). Model variability was greatest during the winter for both time periods, with area predicted suitable patchier in Central America and southeastern Mexico. Omission rates ranged 0.092–0.159 (BRT), 0.074–0.178 (GAM), and 0.087–0.283 (GLM) during 1980–2010 and 0.087–0.177 (BRT),

0.049–0.158 (GAM), and 0.045–0.157 (GLM) during 2014–2015. Model variability was lowest for all three models during the breeding season (0.025–0.326 for BRT, 0.018–0.044 for GAM, and 0.008–0.026 for GLM) for 1980–2010, as well as for GAM (0.007–0.023) and GLM (0.008–0.023) in 2014–2015.
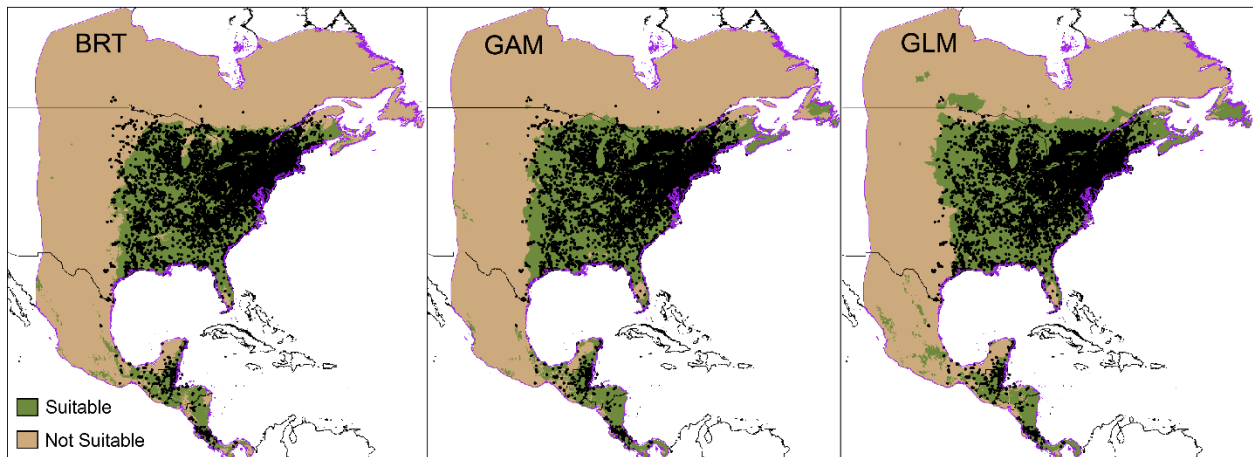
Figure 3. Thresholded (E=1%) time-averaged 1980–2010 BRT (left), GAM (center), and GLM (right) model projections. Green regions indicate areas predicted climatically suitable; tan denotes areas predicted unsuitable; black triangles denote *Hylocichla mustelina* test data.

DISCUSSION

All three time-specific models successfully yielded dynamic (monthly) predictions reflecting known distributional shifts in *Hylocichla mustelina*'s annual cycle (Collar 2005; BirdLife International 2017). On average, the majority of the study region (> 75%) was predicted climatically suitable during the breeding season (June – August) and included areas of known vagrancy in the central United States; a moderate proportion of the study region (60–75%) was predicted suitable during migration (May, September); and areas of bioclimatic suitability during the wintering period (November – April) were restricted to the southeastern United States, eastern Mexico, and Central America. In contrast, the time-averaged models predicted 32–39% (1980–2010) and 37–46% (2014–2015) of the study region (including the eastern United States,

southeastern Canada, and Central America) climatically suitable, successfully capturing the geographic breadth of *H. mustelina*'s core population; but the static view of predicted climatic suitability failed to reflect the dynamic nature of *H. mustelina*'s annual distribution. Both time-averaged and time-specific models exhibited increased model variability (elevated omission rates) during the wintering period potentially as a reflection of strong temporal bias in the primary observation data (Supp. Fig. 4), and omission rates were notably elevated in April and May (1980–2010) for time-specific BRT and GLM models.

Temporally-explicit approaches to correlative niche modeling methods have been at the core of movement ecology analyses for some time (Gschweng *et al.* 2012), and yet the distributional ecology community has yet to adopt a similar approach. Indeed, despite long-standing understanding that traditional (time-averaged) correlative modeling approaches lead to over-generalization of climatic niches (Peterson *et al.* 2005; Barve *et al.* 2014; Ingenloff 2017), efforts to incorporate time-specificity into the modeling framework have a fairly punctuated history. Seasonal modeling has been the gold star method for some time (Laube, Graham & Böhning-Gaese 2015; Skov *et al.* 2016; Soriano-Redondo *et al.* 2019). However, because these methods subset data, resulting models often provide a less than comprehensive overview of the study species' full niche. Methods introduced to account for these gaps include the STEM approach (stacking of seasonally time-averaged models; Fink *et al.* 2010), and full modeling framework (assessing time-averaged monthly intervals; Williams, Willemoes & Thorup 2017). Despite the well-documented need for a temporally-inclusive approach to modeling that avoids time-averaging across study periods (Peterson *et al.* 2005), techniques didn't appear in the literature until 2018 (Welch, Pressey & Reside 2018; Abrahms *et al.* 2019). Our contribution establishes (and makes more broadly accessible) a set of temporally-explicit input data preparation

techniques that improves the overall utility of the traditional correlative niche modeling framework for non-sedentary species. We note that this approach can be applied at many temporal resolutions, depending on the questions being asked and the data availability: centuries for species responding to broad, historical climate shifts (e.g., in the Pleistocene); years for long-lived species that respond to environmental changes very generally (e.g., El Niño events); months for behaviorally complex species or seasonal migrants; or even days for short-lived species (e.g., mosquitoes).

The workflow presented here builds upon the traditional modeling framework to improve ability to characterize species' niches for any situation in which a species' distribution may respond to changing environmental conditions, and considers the full range of a species' distributional dynamics relative to climatic suitability in a single modeling endeavor. It also incorporates the full suite of available observational data without subjective subsetting of data or running multiple series of model calibrations to capture bioclimatic suitability of a species for individual time steps (Peterson *et al.* 2005). Further, where the traditional framework requires averaging of environmental covariates across large timeframes (long-term climate means), rendering some climatic covariates useless (e.g., variables with large variances), time-specific modeling readily allows for the incorporation of higher resolution weather and remotely sensed covariates which have already shown improved performance in time-averaged modeling applications (Bateman, VanDerWal & Johnson 2012; Feldmeier *et al.* 2018). Finally, derivation of a time-specific pseudo-absence dataset, or "bias cloud", provides a dataset reflective of both spatial *and* temporal facets of relative sampling effort. These improvements can provide a significant advantage over previous methods, such as for application to conservation or management of highly mobile species, assessments of species with short lifespans and

spatiotemporally variable populations (e.g., mosquito populations), and species responding to large-scale climate variation.

As with any modeling effort, several limitations are associated with time-explicit modeling First, the derivation of temporally-explicit pseudo-absence datasets can be computationally demanding. This limitation ultimately resulted in our abridging the study period from 2015 to 2010, although relatively few species will have such enormous quantities of distributional data available. Further, this approach still results in some degree of temporal averaging due to the limitations of available primary species observation data and relevant covariate data. This issue can be alleviated with improved data precision and quality perhaps from high resolution weather and remotely sensed data. Finally, these methods are not necessary or appropriate for all species or modeling applications. Rather, we recommend application (a) for species where traditional methods either fail to capture underlying distributional dynamics or (b) when the questions underpinning the modeling require more insight into a species' distribution through time. Indeed, both algorithm selection and parameterization, and the decision to engage in time-averaged, seasonal, or time-specific modeling should be approached as an iterative, hypothesis- or question-driven process. In spite of these limitations, this approach provides a critical template for capturing the distributional dynamics of highly mobile or behaviorally complex species.

Future research should assess the utility of these methods for niche-tracking species that move in geographic space in concert with changing bioclimatic conditions (Tingley *et al.* 2009) versus niche-shifting species (Nakazawa *et al.* 2004), particularly as regards the need for separate models in cases in which qualitatively distinct niches are used in different parts of the year (Batalden, Oberhauser & Peterson 2007). These methods could be adapted into a hypothesis testing framework easily, similar to tests developed by Warren, Glor and Turelli (2008). Further

application has potential to elucidate drivers of movement patterns and improve our understanding of migratory connectivity, a critical component of effective conservation plans for mobile species (Runge *et al.* 2014).

Sample size.—Correlational distribution modeling methods assume systematic sampling of the full model calibration region, but this rarely happens in practice. In time-averaged approaches, small sample sizes are associated with increased model variability and decreased model accuracy (Stockwell & Peterson 2002; Wisz *et al.* 2008). We purposely chose a study species for which available data were plenty and completely representative of the species' realized niche, but availability of such robust datasets are limited to relatively few taxonomic groups. Indeed, correlative modeling is often used to help fill gaps where distributional knowledge is limited and sampling incomplete, and small sample sizes often correspond to species of increased conservation concern (Gaubert, Papeş & Peterson 2006). Further, data available for mobile species are often biased towards particular seasons or behaviors, as seen in our *H. mustelina* example where the overwhelming majority of available data were collected in the United States during breeding or migration (Supp. Fig. 4). By associating sample data with spatially and temporally relevant covariate data, a time-specific approach could maximize limited data through increased retention during the data cleaning process (e.g., data with duplicate locality but different time of collection) to decrease overall model variability. These issues of information content and retention warrant further exploration.

Temporal sampling bias.—Spatial and temporal biases are inherent in open-access primary occurrence data. Myriad studies illustrate strong links between spatial bias in primary species observation data and environmental bias in resulting distributional models (Phillips *et al.* 2009; Beck *et al.* 2014), but few assess impacts of temporal bias. Environmental bias may be introduced

into models as a result of uneven sampling in geographic space, and it stands to reason that we also risk inserting bias into models where strong biases exist in the temporal capture of data. Further research should treat the relationship between temporal bias and model accuracy. See supplementary information for further discussion.

Our ability to gain improved insight into the spatiotemporal dynamics of species distributions via temporally-explicit approaches can positively impact analyses in biodiversity management and conservation, as well as in public health. Consideration for the complexity involved with conserving migratory species is a relatively recent addition to conservation planning, and can be critical in ensuring that species which engage in long-distance movement patterns are protected adequately (Fink *et al.* 2010; Runge *et al.* 2014; Runge *et al.* 2016; Jetz *et al.* 2019). In particular, such approaches may be useful in identifying marine areas of conservation interest (Nur *et al.* 2011; Skov *et al.* 2016) or in other dynamic management applications such as establishing or evaluating marine time-area closures (Lascelles *et al.* 2014; Abrahms *et al.* 2019). Similarly, the ability to produce time-specific distributional models can also help inform decision-making and control measures for current and emerging zoonotic and vector-borne diseases when populations of species respond to environmental changes (Clements & Pfeiffer 2009; Giles *et al.* 2014; Ramsey *et al.* 2015; Parra-Henao *et al.* 2016).

AUTHOR CONTRIBUTIONS

KI and ATP conceived the ideas and designed methodology. KI led analyses and writing of the manuscript. Both authors contributed critically to the drafts and gave final approval for publication.

REFERENCES

Abatzoglou, J.T., Dobrowski, S.Z., Parks, S.A. & Hegewisch, K.C. (2018) Terraclimate, a high-resolution global dataset of monthly climate and climatic water balance from 1958–2015. *Scientific Data,* **5,** 170191.

Abrahms, B., Welch, H., Brodie, S., Jacox, M.G., Becker, E.A., Bograd, S.J., Irvine, L.M., Palacios, D.M., Mate, B.R. & Hazen, E.L. (2019) Dynamic ensemble models to predict distributions and anthropogenic risk exposure for highly mobile species. *Diversity and Distributions,* 25, 1182–1193.

Alvarado-Serrano, D.F. & Knowles, L.L. (2014) Ecological niche models in phylogeographic studies: applications, advances and precautions. *Molecular Ecology Resources,* **14,** 233–248.

Anderson, R.P. (2003) Real vs. artefactual absences in species distributions: tests for *Oryzomys albigularis* (Rodentia:Muridae) in Venezuela. *Journal of Biogeography,* **30,** 591–605.

Anderson, R.P., Araújo, M.B., Guisan, A., Lobo, J.M., Martínez-Meyer, E., Peterson, A.T. & Soberón, J. (2016) Are species occurrence data in global online repositories fit for modeling species distributions? The case of the Global Biodiversity Information Facility (GBIF). *Final Report of the Task Group on GBIF Data Fitness for Use in Distribution Modelling.* Global Biodiversity Information Facility (GBIF).

Barve, N., Barve, V., Jiménez-Valverde, A., Lira-Noriega, A., Maher, S.P., Peterson, A.T., Soberón, J. & Villalobos, F. (2011) The crucial role of the accessible area in ecological niche modeling and species distribution modeling. *Ecological Modelling,* **222,** 1810–1819.

Barve, N., Martin, C., Brunsell, N.A. & Peterson, A.T. (2014) The role of physiological optima in shaping the geographic distribution of Spanish moss. *Global Ecology and Biogeography,* **23,** 633–645.

Batalden, R.V., Oberhauser, K.S. & Peterson, A.T. (2007) Ecological niches in sequential generations of eastern North American monarch butterflies: the ecology of migration and likely climate change implications. *Environmental Entomology,* **36,** 1365–1373.

Bateman, B.L., VanDerWal, J. & Johnson, C.N. (2012) Nice weather for bettongs: using weather events, not climate means, in species distribution models. *Ecography,* **35,** 306–314.

Beck, J. (2013) Predicting climate change effects on agriculture from ecological niche modeling: Who profits, who loses? *Climatic Change,* **116,** 177–189.

Beck, J., Böller, M., Erhardt, A. & Schwanghart, W. (2014) Spatial bias in the GBIF database and its effect on modeling species' geographic distributions. *Ecological Informatics,* **19,** 10–15.

BirdLife International (2017) *Hylocichla mustelina* (amended version of 2016 assessment). *The IUCN Red List of Threatened Species 2017: e.T22708670A111170926.*

Calcagno, V. (2013) glmulti: Model selection and multimodel inference made easy. R package version 1.0.7.

Clements, A.C.A. & Pfeiffer, D.U. (2009) Emerging viral zoonoses: frameworks for spatial and spatiotemporal risk assessment and resource planning. *Veterinary Journal,* **182,** 21–30.

Collar, N.J. (2005) Family Turdidae (thrushes). *Handbook of the Birds of the World* (eds J. del Hoyo, A. Elliott & D.A. Christie), pp. 514–807. Lynx Edicions, Barcelona.

Dodge, S., Bohrer, G., Weinzierl, R., Davidson, S.C., Kays, R., Douglas, D., Cruz, S., Jiawei Han, Brandes, D. & Wikelski, M. (2013) The environmental-data automated track annotation

(Env-DATA) system: linking animal tracks with environmental data. *Movement Ecology,* **1**, 3.

Eaton, S., Ellis, C., Genney, D., Thompson, R., Yahr, R. & Haydon, D.T. (2018) Adding small species to the big picture: species distribution modelling in an age of landscape scale conservation. *Biological Conservation,* **217,** 251–258.

Elith, J., Kearney, M. & Phillips, S. (2010) The art of modelling range-shifting species. *Methods in Ecology and Evolution,* **1,** 330–342.

Feldmeier, S., Schefczyk, L., Hochkirch, A., Lötters, S., Pfeifer, M.A., Heinemann, G. & Veith, M. (2018) Climate versus weather extremes: temporal predictor resolution matters for future rather than current regional species distribution models. *Diversity and Distributions,* **24,** 1047–1060.

Fink, D., Hochachka, W.M., Zuckerberg, B., Winkler, D.W., Shaby, B., Munson, M.A., Hooker, G., Riedewald, M., Sheldon, D. & Kelling, S. (2010) Spatiotemporal exploratory models for broad-scale survey data. *Ecological Applications,* **20,** 2131–2147.

Franklin, J. (2013) Species distribution models in conservation biogeography: developments and challenges. *Diversity and Distributions,* **19,** 1217–1223.

Gaubert, P., Papeş, M. & Peterson, A.T. (2006) Natural history collections and the conservation of poorly known taxa: ecological niche modeling in central African rainforest genets (*Genetta* spp.). *Biological Conservation,* **130,** 106–117.

GBIF (24–26 March 2018) Data from: Global Biodiversity Information Facility Occurrence Download-"Turdidae". DOI: http://dx.doi.org/10.15468/dl.usjwfr, http://dx.doi.org/10.15468/dl.mzlu54, http://dx.doi.org/10.15468/dl.7tyi73, http://dx.doi.org/10.15468/dl.wbehpg, http://dx.doi.org/10.15468/dl.ewipqa, http://dx.doi.org/10.15468/dl.tdz842, http://dx.doi.org/10.15468/dl.3klver, http://dx.doi.org/10.15468/dl.jwmwmw.

GBIF (26 March 2018) Data from: Global Biodiversity Information Facility Occurrence Download - "*Hylocichla mustelina*". DOI: http://dx.doi.org/10.15468/dl.hdg0e2.

Giles, J.R., Peterson, A.T., Busch, J.D., Olafson, P.U., Scoles, G.A., Davey, R.B., Pound, J.M., Kammlah, D.M., Lohmeyer, K.H. & Wagner, D.M. (2014) Invasive potential of cattle fever ticks in the southern United States. *Parasites & Vectors,* **7,** 189.

Gschweng, M., Kalko, E.K.V., Berthold, P., Fiedler, W. & Fahr, J. (2012) Multi-temporal distribution modelling with satellite tracking data: predicting responses of a long-distance migrant to changing environmental conditions. *Journal of Applied Ecology,* **49,** 803–813.

Hayfield, T. & Racine, J.S. (2008) Nonparametric econometrics: The np package. *Journal of Statistical Software,* **27,** 1–32.

Hijmans, R.J., Phillips, S., Leathwick, J. & Elith, J. (2017) dismo: species distribution modeling. R package version 1.1-4. https://cran.r-project.org/web/packages/dismo/index.html.

Ingenloff, K. (2017) Biologically informed ecological niche models for an example pelagic, highly mobile species. *European Journal of Ecology,* **3,** 55–75.

Ingenloff, K., Hensz, C.M., Anamza, T., Barve, V., Campbell, L.P., Cooper, J.C., Komp, E., Jiménez, L., Olson, K.V., Osorio-Olvera, L., Owens, H.L., Peterson, A., T, Samy, A., Simões, M. & Soberón, J. (2017) Predictable invasion dynamics in North American populations of the Eurasian collared dove *Streptopelia decaocto*. *Proceedings of the Royal Society B,* **284,** 11–57.

Jetz, W., McGeoch, M.A., Guralnick, R., Ferrier, S., Beck, J., Costello, M.J., Fernandez, M., Geller10, G.N., Keil, P., Merow, C. & Meyer, C. (2019) Essential biodiversity variables for mapping and monitoring species populations. *Nature Ecology & Evolution,* **3,** 539–551.

Kadmon, R., Farber, O. & Danin, A. (2004) Effect of roadside bias on the accuracy of predictive maps produced by bioclimatic models. *Ecological Applications,* **14,** 401–413.

Kramer-Schadt, S., Niedballa, J., Pilgrim, J.D., Schroder, B., Lindenborn, J., Reinfelder, V., Stillfried, M., Heckmann, I., Scharf, A.K., Augeri, D.M., Cheyne, S.M., Hearn, A.J., Ross, J., Macdonald, D.W., Mathai, J., Eaton, J., Marshall, A.J., Semiadi, G., Rustam, R., Bernard, H., Alfred, R., Samejima, H., Duckworth, J.W., Breitenmoser-Wuersten, C., Belant, J.L., Hofer, H. & Wilting, A. (2013) The importance of correcting for sampling bias in MaxEnt species distribution models. *Diversity and Distributions,* **19,** 1366–1379.

Lascelles, B., Di Sciara, G.N., Agardy, T., Cuttelod, A., Eckert, S., Glowka, L., Hoyt, E., Llewellyn, F., Louzao, M., Ridoux, V. & Tetley, M.J. (2014) Migratory marine species: their status, threats and conservation management needs. *Aquatic Conservation: Marine and Freshwater Ecosystems,* **24,** 111–127.

Laube, I., Graham, C.H. & Böhning-Gaese, K. (2015) Niche availability in space and time: migration in *Sylvia* warblers. *J. Biogeogr,* **42,** 1896–1906.

Martínez-Meyer, E., Peterson, A.T. & Navarro-Sigüenza, A.G. (2004) Evolution of seasonal ecological niches in the Passerina buntings (Aves: Cardinalidae). *Proceedings of the Royal Society B,* **271,** 1151–1157.

Nakazawa, Y., Peterson, A.T., Martínez-Meyer, E. & Navarro-Sigüenza, A.G. (2004) Seasonal niches of Nearctic-Neotropical migratory birds: implications for the evolution of migration. *Auk,* **121,** 610–618.

Nur, N., Jahncke, J., Herzog, M.P., Howar, J., Hyrenbach, K.D., Zamon, J.E., Ainley, D.G., Wiens, J.A., Morgan, K., Ballance, L.T. & Stralberg, D. (2011) Where the wild things are: predicting hotspots of seabird aggregations in the California Current system. *Ecological Applications,* **21,** 2241–2257.

Ooms, J. (2018a) *gifski: highest quality GIF encoder. R package version 0.8.6. https://CRAN.R-project.org/package=gifski.*

Ooms, J. (2018b) *magick: advanced graphics and image-processing in R. R package version 2.0. https://CRAN.R-project.org/package=magick.*

Pacifici, M., Foden, W.B., Visconti, P., Watson, J.E., Butchart, S.H., Kovacs, K.M., Scheffers, B.R., Hole, D.G., Martin, T.G., Akcakaya, H.R. & Corlett, R.T. (2015) Assessing species vulnerability to climate change. *Nature Climate Change,* **5,** 215.

Parra-Henao, G., Quirós-Gómez, O., Jaramillo-O, N. & Cardona, Á.S. (2016) Environmental determinants of the distribution of Chagas disease vector *Triatoma dimidiata* in Colombia. *American Journal of Tropical Medicine and Hygiene,* **94,** 767–774.

Pearson, R.G., Raxworthy, C.J., Nakamura, M. & Peterson, A.T. (2007) Predicting species distributions from small numbers of occurrence records: a test case using cryptic geckos in Madagascar. *Journal of Biogeography,* **34,** 102–117.

Peterson, A.T. (2006) Uses and requirements of ecological niche models and related distribution models. *Biodiversity Informatics,* **3,** 59–72.

Peterson, A.T. (2014) *Mapping disease transmission risk*. Johns Hopkins University Press, Baltimore.

Peterson, A.T., Martínez-Campos, C., Nakazawa, Y. & Martínez-Meyer, E. (2005) Time-specific ecological niche modeling predicts spatial dynamics of vector insects and human dengue cases. *Transactions of the Royal Society of Tropical Medicine and Hygiene,* **99,** 647–655.

Peterson, A.T., Papeş, M. & Soberón, J. (2015) Mechanistic and correlative models of ecological niches. *European Journal of Ecology,* **1,** 28–38.

Phillips, S.J., Dudík, M., Elith, J., Graham, C.H., Lehmann, A., Leathwick, J. & Ferrier, S. (2009) Sample selection bias and presence-only distribution models: implications for background and pseudo-absence data. *Ecological Applications,* **19,** 181–197.

Qiao, H.J., Soberón, J. & Peterson, A.T. (2015) No silver bullets in correlative ecological niche modelling: insights from testing among many potential algorithms for niche estimation. *Methods in Ecology and Evolution,* **6,** 1126–1136.

R Development Core Team (2009) *R: A language and environment for statistical computing. R Foundation for Statistical Computing: http://www.r-project.org*.

Ramsey, J.M., Peterson, A.T., Carmona-Castro, O., Moo-Llanes, D.A., Nakazawa, Y., Butrick, M., Tun-Ku, E., la Cruz-Félix, K.D. & Ibarra-Cerdeña, C.N. (2015) Atlas of Mexican Triatominae (Reduviidae: Hemiptera) and vector transmission of Chagas disease. *Memórias do Instituto Oswaldo Cruz,* **110,** 339–352.

Rodríguez , J.P., Brotons, L., Bustamante, J. & Seoane, J. (2007) The application of predictive modelling of species distribution to biodiversity conservation. *Diversity and Distributions,* **13,** 243–251.

Runge, C.A., Martin, T.G., Possingham, H.P., Willis, S.G. & Fuller, R.A. (2014) Conserving mobile species. *Frontiers in Ecology and the Environment,* **12,** 395–401.

Runge, C.A., Tulloch, A.I.T., Possingham, H.P., Tulloch, V.J.D. & Fuller, R.A. (2016) Incorporating dynamic distributions into spatial prioritization. *Diversity and Distributions,* **22,** 332–343.

Searcy, C.A. & Shaffer, H.B. (2016) Do ecological niche models accurately identify climatic determinants of species ranges? *American Naturalist,* **187,** 423–435.

Signorell, A., Aho, K., Alfons, A., Anderegg, N., Aragon, T., Arppe, A., Baddeley, A., Barton, K., Bolker, B., Borchers, H.W., Caeiro, F., Champely, S., Chessel, D., Chhay, L., Cummins, C., Dewey, M., Doran, H.C., Dray, S., Dupont, C., Eddelbuettel, D., Enos, J., Ekstrom, C., Elff, M., Erguler, K., Farebrother, R.W., John Fox, R.F., Friendly, M., Galili, T., Gamer, M., Gastwirth, J.L., Gel, Y.R., Gross, J., Grothendieck, G., Jr, F.E.H., Heiberger, R., Hoehle, M., Hoffmann, C.W., Hojsgaard, S., Hothorn, T., Hui, M.H.W.W., Hurd, P., Hyndman, R.J., Iglesias, P.J.V., Jackson, C., Kohl, M., Korpela, M., Kuhn, M., Labes, D., Lang, D.T., Leisch, F., Lemon, J., Li, D., Maechler, M., Magnusson, A., Malter, D., Marsaglia, G., Marsaglia, J., Matei, A., Meyer, D., Miao, W., Millo, G., Min, Y., Mitchell, D., Naepflin, M., Navarro, D., Nilsson, H., Nordhausen, K., Ogle, D., Ooi, H., Parsons, N., Pavoine, S., Plate, T., Rapold, R., Revelle, W., Rinker, T., Ripley, B.D., Rodriguez, C., Russell, N., Sabbe, N., Venkatraman E. Seshan, Greg Snow, M.S., Soetaert, K., Stahel, W.A., Stephenson, A., Stevenson, M., Templ, M., Therneau, T., Tille, Y., Trapletti, A., Ulrich, J., Ushey, K., VanDerWal, J., Venables, B., Verzani, J., Warnes, G.R., Wellek, S., Wickham, H., Wilcox, R.R., Wolf, P., Wollschlaeger, D., Yee, T. & Zeileis, A. (2019) DescTools: tools for descriptive statistics. R package version 0.99.27.

Skov, H., Heinänen, S., Thaxter, C.B., Williams, A.E., Lohier, S. & Banks, A.N. (2016) Real-time species distribution models for conservation and management of natural resources in marine environments. *Marine Ecology Progress Series,* **542,** 221–234.

Soriano-Redondo, A., Jones-Todd, C.M., Bearhop, S., Hilton, G.M., Lock, L., Stanbury, A., Votier, S.C. & Illian., J.B. (2019) Understanding species distribution in dynamic populations: a new approach using spatio-temporal point process models. *Ecography,* 42, 1092–1102.

Stockwell, D.R. & Peterson, A.T. (2002) Effects of sample size on accuracy of species distribution models. *Ecological Modelling,* **148,** 1–13.

Thuiller, W., Georges, D., Engler, R. & Breiner, F. (2016) biomod2: ensemble platform for species distribution modeling. R package version 3.3-7. https://CRAN.R-project.org/package=biomod2.

Tingley, M.W., Monahan, W.B., Beissinger, S.R. & Moritz, C. (2009) Birds track their Grinnellian niche through a century of climate change. *Proceedings of the National Academy of Sciences, USA,* **106,** 19637–19643.

Warren, D.L., Glor, R.E. & Turelli, M. (2008) Environmental niche equivalency versus conservatism: quantitative approaches to niche evolution. *Evolution,* **62,** 2868–2883.

Warren, D.L. & Seifert, S.N. (2011) Ecological niche modeling in Maxent: the importance of model complexity and the performance of model selection criteria. *Ecological Applications,* **21,** 335–342.

Welch, H., Pressey, R.L. & Reside, A.E. (2018) Using temporally explicit habitat suitability models to assess threats to mobile species and evaluate the effectiveness of marine protected areas. *Journal for Nature Conservation,* **41,** 106–115.

Williams, H.M., Willemoes, M. & Thorup, K. (2017) A temporally explicit species distribution model for a long distance avian migrant, the common cuckoo. *Journal of Avian Biology,* **48,** 1624–1636.

Wisz, M.S., Hijmans, R.J., Li, J., Peterson, A.T., Graham, C.H., Guisan, A. & Group, N.P.S.D.W. (2008) Effects of sample size on the performance of species distribution models. *Diversity and Distributions,* **14,** 763–773.

Wood, S.N. (2011) Fast stable restricted maximum likelihood and marginal likelihood estimation of semiparametric generalized linear models. *Journal of the Royal Statistical Society (B),* **73,** 3–36.

CHAPTER 3. Assessing the utility of time-specific correlative ecological niche framework to produce dynamic distributional predictions for the nomadic Wandering Albatross (*Diomedea exulans*)

ABSTRACT

Background. Correlative ecological niche modeling is a commonly utilized method of estimating a species' ecological niche on the geographic landscape. Traditional time-averaged approaches tend to fail for migratory species and other less predictable, highly mobile species. Recent work incorporated temporal dimensions into the traditional niche modeling framework through a series of modifications to the input data preparation workflow. The initial proof-of-concept indicated that this modified workflow is able to predict more accurately the ecological niches of mobile species. This contribution assesses the utility of the modified time-specific niche modeling framework with a less predictable species.

Methods. Using open access primary biodiversity point observation data, we applied time-specific correlative niche modeling framework to a nomadic seabird species, the Wandering Albatross (*Diomedea exulans*). I compared traditional time-averaged modeling to the temporally-explicit approach alongside two methods of addressing sampling bias in open access species observation data.

Results. These modeling results provide further support for the improved utility of temporally-inclusive modeling framework for species with seasonally unstable geographic distributions.

INTRODUCTION

Correlative ecological niche modeling, broadly applied in the fields of movement ecology and distributional ecology, provides a statistical method of quantifying a species' niche and its footprint in geographic space. Applications range from modeling habitat suitability (e.g., Ceia *et al.* 2012; Scales *et al.* 2016), to estimating species' invasive potential (e.g., Ingenloff *et al.* 2017), to exploring more broad-scale phylogeographic questions (e.g., Alvarado-Serrano & Knowles 2014). In typical correlative modeling frameworks, environmental covariates are averaged across the study period such that each geographic location has only a single environmental value. However, this time-averaging of covariates can result in over-generalization of environmental variation (Peterson *et al.* 2005), decreasing reliability for highly mobile (Ingenloff 2017) and more ephemeral species.

Movement ecology studies assessing movements of individuals using tracking (movement) data incorporate the temporal dimension as standard protocol (Dodge *et al.* 2013); this step, however, is not common in species-level analyses in distributional ecology where the input data are point observation data derived from human or machine observations, or data associated with museum specimens (Andrew & Fox 2020; Ingenloff & Peterson 2021). Distributional ecologists have explored diverse methods to address issues in modeling highly mobile organisms at the species level, including spatiotemporal exploratory models (stacking of seasonally time-averaged models; Fink *et al.* 2010), incorporation of mechanistic models (Kearney *et al.* 2010; Barve *et al.* 2014), and a full-year modeling framework that evaluated series of monthly models averaged across the full study period (Williams, Willemoes & Thorup 2017). However, seasonal correlative niche modeling approaches—modeling a particular season or behavior state time-averaged over the full breadth of the study period—persist as the most commonly utilized approach (Laube,

Graham & Böhning-Gaese 2015; Soriano-Redondo *et al.* 2019). More recently, a few studies have made explicit efforts to incorporate the temporal dimension into species-level modeling to produce dynamic niche predictions (Welch, Pressey & Reside 2018; Abrahms *et al.* 2019; Andrew & Fox 2020; Ingenloff & Peterson 2021).

Ingenloff and Peterson (2021) introduced a modification to the data preparation process of traditional correlational modeling frameworks to incorporate the temporal dimension of species-level distributional dynamics. That study assessed impacts of these methodological improvements on a single well-studied, seasonal migratory bird (Wood Thrush, *Hylocichla mustelina*). However, migration is only one of four major classifications of large-scale species movement patterns. Of the four, migration and intergenerational relays ("regular migration over multiple generations") tend to be more predictable, whereas nomadism (wandering movements commonly under conditions of high inter-annual resource variability) and irruption (occasional long-distance movement by typically sedentary species) consist of more erratic, less predictable movement patterns (Runge *et al.* 2014). Increased unpredictability in movement patterns inherently increases the difficulty of developing effective conservation strategies for these species. Ingenloff (2017) established a series of seasonal, time-averaged baseline correlative niche models for the nomadic Wandering Albatross (*Diomedea exulans*, Linnaeus 1758). These baseline models provide an ideal starting point for which to evaluate the utility of the time-specific modeling framework of Ingenloff and Peterson (2021).

This study seeks to assess the utility of time-specific correlative niche modeling frameworks for the nomadic *Diomedea exulans*, using open-access primary occurrence data from the Global Biodiversity Information Facility (GBIF). We provide comparisons between traditional

time-averaged approaches to modeling and the time-averaged seasonal modeling of Ingenloff (2017) with the dynamic niche predictions resulting from the modified framework.

MATERIALS & METHODS

To maximize the reproducibility of analyses in this study, all analyses were run using open-access data and open-source tools in R v3.6.2 (R Development Core Team 2009). Relevant, generalized R scripts (modified from Ingenloff & Peterson 2021) are available at: https://github.com/kingenloff/dynamicENM. We used the same study period (February 2000 – December 2013 study period) and study region (-20˚S to -60˚S latitude) as Ingenloff (2017; Supplemental Figure 1) to facilitate direct comparisons.

STUDY SPECIES

The study species is a nomadic, Subantarctic, circumpolar, pelagic seabird. Long-lived and slow to mature, *Diomedea exulans* breeds biennially in large colonies on five Subantarctic island groups (South Georgia, Prince Edward Islands, Crozet Islands, Kerguelen Islands, and Macquarie Island) and exhibit high natal and breeding philopatry (i.e., they return to the colony where they hatched throughout their lifetime to breed; Prince *et al.* 1992; Jouventin & Dobson 2002; Milot, Weimerskirch & Bernatchez 2008). Their spatial distributions at any moment are a function of sex (Phillips *et al.* 2011; Åkesson & Weimerskirch 2014; Pereira *et al.* 2018), age (Åkesson & Weimerskirch 2005; Weimerskirch, Åkesson & Pinaud 2006; Weimerskirch *et al.* 2014; Froy *et al.* 2015), colony of origin (Wakefield *et al.* 2011), breeding phase (Phillips *et al.* 2005; Mackley *et al.* 2010; Rains, Weimerskirch & Burg 2011; Weimerskirch *et al.* 2014), and foraging strategy (Forslund & Pärt 1995). Traditional correlative niche modeling techniques fail to capture the

complexity of these factors, producing overly generalized models (Ingenloff 2017) due in part to the fact that this information (e.g., age, sex, breeding phase) is largely unavailable for species' point observation data (Camphuysen *et al.* 2012) which are collected opportunistically either as observational data (e.g., from research or fishing vessels or through citizen science initiatives) or from specimen records in museums or natural history collections (Camphuysen *et al.* 2012; Grecian *et al.* 2012; Meyer *et al.* 2016). Often, point observation data consist of no more than the species identification with a date/time and location of observation, thus lacking much biologically relevant information (Grecian *et al.* 2012). Further confounding species-level modeling efforts is the issue of accurate at-sea identification of *D. exulans* from the three other "great" albatross species in the Wandering Albatross complex—the Amsterdam Albatross (*D. amsterdamensis*, Joux, Jouventin, Mougin, Stahl & Weimerskirch 1983), Antipodean Albatross (*D. antipodensis*, Robertson & Warham 1992), and Tristan Albatross (*D. dabbenena* Matthews, 1929)—which are visually similar and with whom *D. exulans* have significant range overlap (Burg & Croxall 2004; Schodde *et al.* 2017). The at-sea distribution of *D. antipodensis* falls entirely within that of *D. exulans*; those of *D. amsterdamensis* and *D. dabbenena* are mostly within that of *D. exulans* (Supplemental Figure 2).

INPUT DATA

Primary Occurrence data.—A GBIF query for all available Diomedeidae (G.R. Gray 1840) occurrence data between 2000 and 2013 returned 122,058 occurrences, including 18,001 *Diomedea exulans* observations (GBIF 31 December 2018). Data were curated to remove occurrences with obvious inaccuracies (e.g., inconsistencies in species names, occurrences with imprecise or completely lacking coordinates), or occurrences lacking adequate temporal

information (e.g., sampling date), limited to include only those records collected during February 2000 – December 2013 and clipped to the study region. This reduced the data to 17,731 *D. exulans* and 102,845 Diomedeidae occurrences.

Pseudo-absence data.—Because true absence data are not available for *D. exulans*, we used the 102,845 cleaned Diomedeidae occurrences as a reference group from which to generate a temporally explicit pseudo-absence dataset, or bias cloud, to characterize the sampling bias that produced the study species' data (Anderson 2003) following the methods of Ingenloff and Peterson (2021). The temporal resolution of the pseudo-absence dataset was limited to monthly time steps matching the temporal resolution of the environmental covariate data. The pseudo-absence dataset for the February 2000 – December 2013 study period, totaling 167 time steps (months), included 26,685 pseudo-absences (~1.5x *D. exulans* occurrences).

Rarefication and subsetting of data.—We explored two levels of rarefication to address sampling bias in both the *D. exulans* observation data and the pseudo-absence data. Initially, we rarefied *D. exulans* occurrence data and pseudo-absences spatially only. Spatial rarefication reduced data to a single point per pixel (time-averaged data) and a single point per pixel per time step (time-specific data) relative to the spatial resolution of the environmental covariate data (Phillips *et al.* 2009; Kramer-Schadt *et al.* 2013). The spatial rarefication process produced a time-averaged dataset consisting of 3078 *D. exulans* occurrences and 11328 pseudo-absences, and a time-specific dataset with 3791 *D. exulans* occurrences and 9867 pseudo-absences (Table 1).

Table 1. Total *Diomedea exulans* occurrence data and pseudo-absence data available for time-averaged and time-specific spatially rarefied (SR) and spatially rarefied and thinned (STR) analyses.

		Raw, cleaned data		Model calibration		Model evaluation	
		SR	STR	SR	STR	SR	STR
Time-averaged	*D. exulans*	3078	2128	2315	1609	763	519
	Pseudo-absences	11328	8326	8488	6326	2840	2100
Time-specific	*D. exulans*	3791	3196	2822	2364	969	832
	Pseudo-absences	9867	7289	7397	5445	2470	1844

We thinned the spatially rarefied datasets as a means of assessing a second level of data thinning on model quality. During this, *D. exulans* occurrences were thinned such that, for each time step t_i, if the number of study species occurrences in t_i were greater than three times the mean number of presences per each time step (relative to the overall dataset), the presences in t_i were subsampled to three times the overall mean value. Pseudo-absences were thinned such that if the number of pseudo-absences in t_i was greater than double the mean number of pseudo-absences for each time step relative to the overall dataset, the pseudo-absences in t_i were subsampled to double the mean number of points (Supplemental Figures 3–4). This further reduced spatially rarefied datasets to 2128 *D. exulans* and 8426 pseudo-absence time-averaged spatially rarefied and thinned data points, and 3196 *D. exulans* and 7289 pseudo-absence time-specific spatially rarefied and thinned data points (Table 1).

We then randomly subset data such that 70% were set retained for model calibration and the remaining 30% set aside for model evaluation (Table 1). The spatially rarefied time-averaged model calibration data included 2315 *D. exulans* occurrence points and 8488 pseudo-absences and reserved 763 *D. exulans* and 2840 pseudo-absences for model evaluation. And, the time-specific model calibration dataset retained 2822 *D. exulans* occurrence points and 7397 pseudo-absences and set aside 969 *D. exulans* points and 2470 pseudo-absences for model evaluation. The spatial rarefication and thinning process further reduced time-averaged data to 2128 *D. exulans*

observations and 8326 pseudo-absences, and time-specific data to 3196 *D. exulans* observations and 7289 pseudo-absences.

Temporal information (e.g., month and year) were retained for all data through both rarefication processes. In the entire study period, four months held no *D. exulans* data for use in model calibration and 15 held no *D. exulans* data for model evaluation.

Covariate data.—We selected covariate data to summarize the complex environmental landscape of the high-latitude marine system under analysis, and allow for side-by-side comparison between time-averaged and dynamic approaches, and comparison with seasonal modeling results from Ingenloff (2017). Specifically, we used three dynamic covariates and one static covariate. Dynamic data included sea surface temperature (SST), and Chlorophyll-*a* (CHL; Hyrenbach *et al.* 2007; Wakefield, Phillips & Matthiopoulos 2009) and chromophoric dissolved organic matter (CDOM; Coble 2007; Nelson & Siegel 2013; Urtizberea *et al.* 2013), which were included as proxies of ocean productivity, downloaded from the NASA OceanColor Web at monthly temporal resolution for the February 2000 – December 2013 study period (NASA 2014). ETOPO1 global relief bathymetric data served as the static covariate (Amante & Eakins 2009). All covariate data were clipped to the study region and standardized to the native resolution of dynamic data (4.6 km). Unlike Ingenloff (2017), we used raw covariate data rather than generating principal components.

We extracted covariate data to all time-specific spatially rarefied and spatially rarefied and thinned *D. exulans* occurrence and pseudo-absences such that each point was associated with the environmental information specific to a point in space and time of observation. For time-averaged analyses, we derived a covariate dataset that included the mean and range for each of the three dynamic covariates over the duration of the February 2000 – December 2013 study period. This

step yielded six summary covariate layers for use in analyses in conjunction with the static bathymetry layer. Data from the six derived covariate layers and bathymetry data, corresponding to the time-averaged spatially rarefied and spatially rarefied and thinned *D. exulans* and pseudo-absence data were extracted for analyses.

CORRELATIONAL NICHE MODELING

　　Model calibration selection.—We explored a suite of calibration scenarios for three common modeling algorithms—generalized linear models (GLMs), generalized additive models (GAMs), and boosted regression trees (BRTs)—to identify the best model implementation for time-averaged and time-specific models (Qiao, Soberón & Peterson 2015). For each algorithm and modeling scenario (time-averaged spatially rarefied, time-averaged spatially rarefied and thinned, time-specific spatially rarefied, time-specific spatially rarefied and thinned), we explored a suite of parameter settings, wherein we generated a large suite of models, and then selected a final model among them using criteria of predictive ability and simplicity (see below).

　　We calibrated GLMs with both main effects and pairwise interactions using the 'glmulti' function in the glmulti package (Calcagno 2013). GAMs were calibrated using the 'gam' function in the mgcv package (Wood 2011). GAM calibrations assessed an array of smoothers (cubic splines, thin plate splines, P splines, and adaptive splines), two basis dimensions for the smoothers (default, $k = 25$), two smoothing parameters (default, restricted maximum likelihood), and covariate interactions (ranging from no interaction to full interaction). We assessed covariate responses visually for GLM and GAM calibrations using the 'response.plot2' function in the biomod2 package (Thuiller *et al.* 2016), and we used the Akaike information criterion (AIC) for within-algorithm model selection of GLM and GAM models (Warren & Seifert 2011). We

calibrated BRTs using the 'gbm.step' function in the dismo package (Hijmans *et al.* 2017), and evaluated a suite of settings for learning rate (default, 0.005, 0.0025, 0.001), bag fraction (default, 0.6, 0.7), and tree complexity (interaction depth; time-averaged: 1, 2, 3, 4, 5; time-specific: 1, 2, 3, 4). AIC is not an appropriate evaluation metric for tree-based algorithms so we used training and test data mean squares estimates (MSE) and *D. exulans* test data omission rate to evaluate BRTs. MSE values were calculated using the 'MSE' function in the DescTools package (Signorell *et al.* 2019).

Calibration of all three algorithms for both temporal and rarefaction scenarios assessed the impact of weighting *D. exulans* occurrences greater than pseudo-absence data versus equal weighting of *D. exulans* presences and pseudo-absences (see Supplemental Information for more detail). Range sea surface temperature was dropped from time-averaged model calibrations owing to high correlation with range chlorophyll ($r^2 = 1.00$; Supplemental Table 4, Supplemental Figures 5–8).

Model transfer.—The model selection process yielded three final models—one for each algorithm—for each temporal and rarefaction modeling scenario: time-averaged spatially rarefied, time-averaged spatially rarefied and thinned, time-specific spatially rarefied, time specific spatially rarefied and thinned. We thresholded each of the selected models to minimum training presence adjusted to allow 5% omission error ($E = 5\%$) to allow for some error in the occurrence data (Pearson *et al.* 2007) and transferred them to each step in the temporally corresponding covariate dataset.

Consensus models.—We generated a median consensus model using the corresponding thresholded final models for each unique temporal and rarefication scenario. This process produced four binary median consensus models. To facilitate visual assessment (i.e., a reality

check) of each model's ability to predict known areas of importance to *D. exulans*, we overlaid on each consensus model *D. exulans* range extent (BirdLife International and NatureServe 2015), important bird areas (IBAs) relevant to the broader Wandering Albatross complex as indicated by the Marine IBA E-atlas (Supplemental Figure 1; BirdLife International 2016; BirdLife International and NatureServe 2020), and the major Southern Ocean fronts, including the Subtropical Front (STF), Subantaractic Front (SAF), and Polar Front (PF; Orsi & Harris 2008). Time-specific spatially rarefied and spatially rarefied and thinned consensus projections were appended and aggregated into an image sequence in graphics interchange format (GIF) to produce a dynamic visualization of predicted climatic suitability through time using R packages 'magick' and 'gifski' (Ooms 2018b; Ooms 2018a).

Model evaluation.—We evaluated the four consensus using omission rate—percent of test data incorrectly predicted 'absent' by the model—as a key measure of model predictive performance, and partial receiver operating characteristic (pROC) as a measure of statistical significance. Model evaluation was conducted using custom functions. Partial ROC scores were calculated using a modification of the kuenm_proc() function (Cobos *et al.* 2019) with 500 bootstrapped replicates for time-averaged models, and 500 bootstrapped replicates for per time step for time-specific models.

RESULTS

The model selection process yielded 12 finals models (see Supplementary Tables 5–8 for model details) for use in generating the four consensus models. Weighting *D. exulans* presence data produced higher performing GLMs and GAMs but did not have any significant impact on BRTs for either time-averaged or time-specific models. The model calibration process dropped

sea surface temperature range from final time-averaged models owing to a high correlation with chlorophyll range ($r^2 = 1.0$). Chlorophyll range was dropped during the calibration process for both time-averaged GAMs owing to lack of significant effect in model build. All four covariates were retained in model calibration of time-specific models. See Supplemental Figures 9–11 for snapshots of final time-averaged models, and Supplemental Figures 12–14 for snapshots of final time-specific models. Dynamic visualizations of time-specific model predictions by algorithm are available at doi.org/10.6084/m9.figshare.12612431.v1.
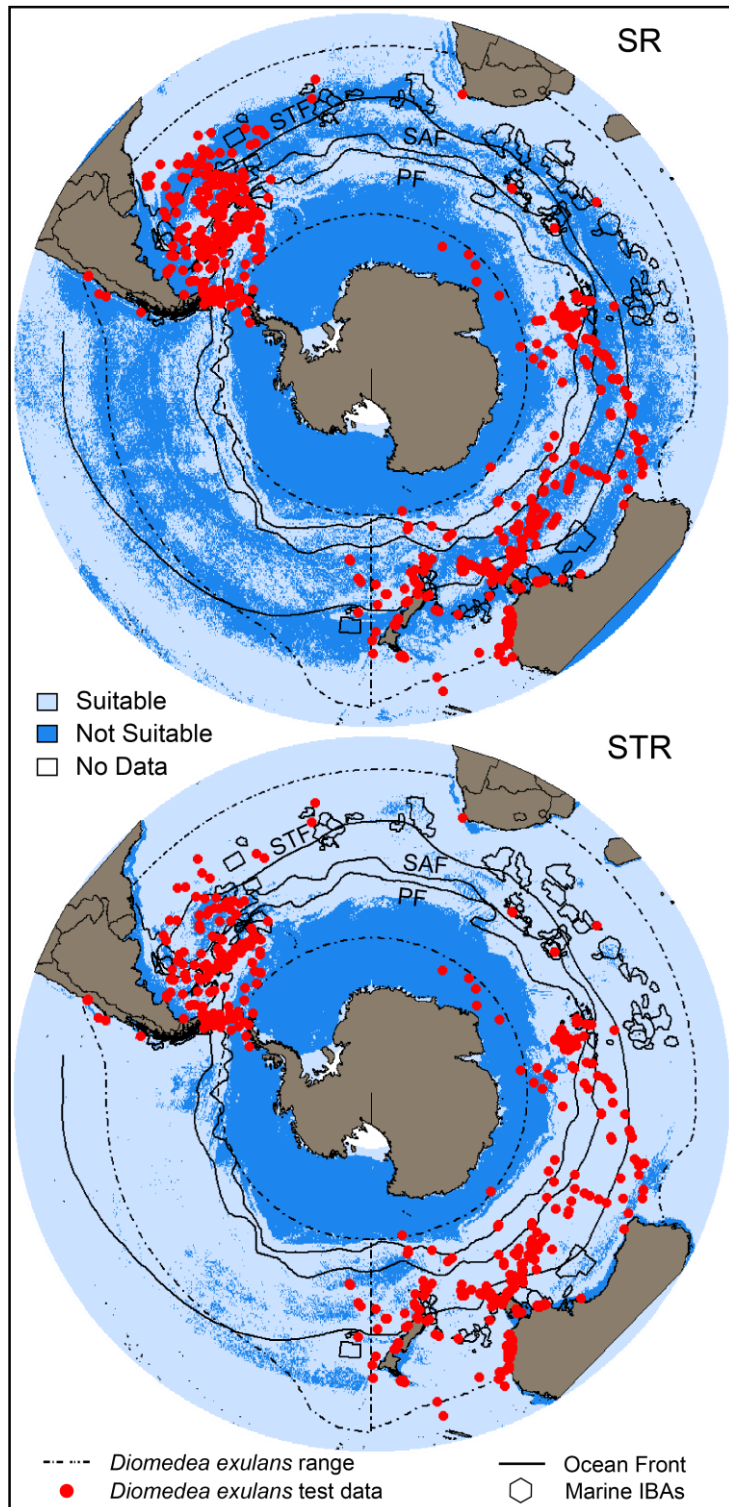
Figure 1. Time-averaged spatially rarefied (SR; top) and spatially rarefied and thinned (STR; bottom) consensus model predictions overlaid with *Diomedea exulans* range (dashed line; BirdLife International and NatureServe 2015), relevant marine IBAs (black polygons; BirdLife International 2016), and *D. exulans* test data (red points), and Subtropical (STF), Subantarctic (SAF) and Polar Fronts (PF; Orsi & Harris 2008).

Time-averaged models.—As expected, both time-averaged consensus models performed quite poorly, with neither model performing statistically better than random (Figure 1, Supplemental Table 9). The spatially rarefied consensus model omitted 273 of 761 (35.88%) *D. exulans* test occurrences (mean pROC = 1.12, *p*-value = 0.8); the spatially rarefied and thinned consensus omitted 108 of 517 (20.89%) *D. exulans* test data (mean pROC score = 0.995, pROC *p*-value = 0.67). Temporal rarefication of model calibration data relaxed model fit such that broader areas of the study region were predicted as bioclimatically suitable in the spatially rarefied and thinned consensus model than in the spatially

rarefied only model. The spatially rarefied consensus model predicted much of *D. exulans'* known distributional range as unsuitable, with the majority of areas predicted as suitable restricted predominantly to within the Subantarctic and Polar Fronts. Both consensus models predicted as unsuitable the colder Antarctic waters in the vicinity of the Antarctic Circumpolar Current and much of the eastern parts of the Argentine Basin.

Time-specific models.—Statistically, both time-specific consensus models performed better than random expectations (Supplemental Tables 10–11). A dynamic view of time-specific consensus models is available at doi.org/10.6084/m9.figshare.12612239.v1; a snapshot of the consensus models are provided in Figure 2. Overall, the spatially rarefied consensus model omitted only 24 of 969 (2.47%) test data points, and the spatially rarefied and thinned consensus model omitted 45 of 832 (5.41%) test data points.

For the 152 months for which *D. exulans* test data were available, monthly omission rates ranged 0–50.% for the spatially rarefied consensus model and 0–69.23% for spatially rarefied and thinned consensus model where OR = 0 for 137 months for the spatially rarefied model and 134 months for the spatially rarefied and thinned model. The monthly mean pROC score for the spatially rarefied consensus model ranged 0.82–1.23, with only 11 months with a pROC *p*-value > 0.0001. The monthly mean pROC score for the spatially rarefied and thinned consensus mode ranged 0.74–1.18, with *p*-value = 0 for 134 months.

In the spatially rarefied model, only a single point was omitted for ten of the 15 months for which OR > 0.0001.In the spatially rarefied and thinned model, only a single test point was omitted in each of 11 of 18 months for which OR > 0. The maximum number of *D. exulans* test data omitted in any individual timestep for both the spatially rarefied and s spatially rarefied and thinned time-specific consensus models was in June 2000, with the five of 13 *D. exulans* test occurrences

omitted by the spatially rarefied model, and nine of 13 occurrences omitted by the spatially rarefied and thinned model (Figure 2). This lowest performance also coincided with the month with the highest omission rate for the spatially rarefied and thinned model (OR = 69.23%), and the second highest omission rate for the spatially rarefied model (OR = 38.46%). The month with the highest omission rate (OR = 50%) for the spatially rarefied model was February 2000, with one of the only two total *D. exulans* test points omitted.

Feb 2000

Jun 2000

Oct 2000

SR Consensus

STR Consensus

	Suitable		Diomedea exulans range		Ocean Front
	Not Suitable		Diomedea exulans test data		Marine IBAs
	No Data				
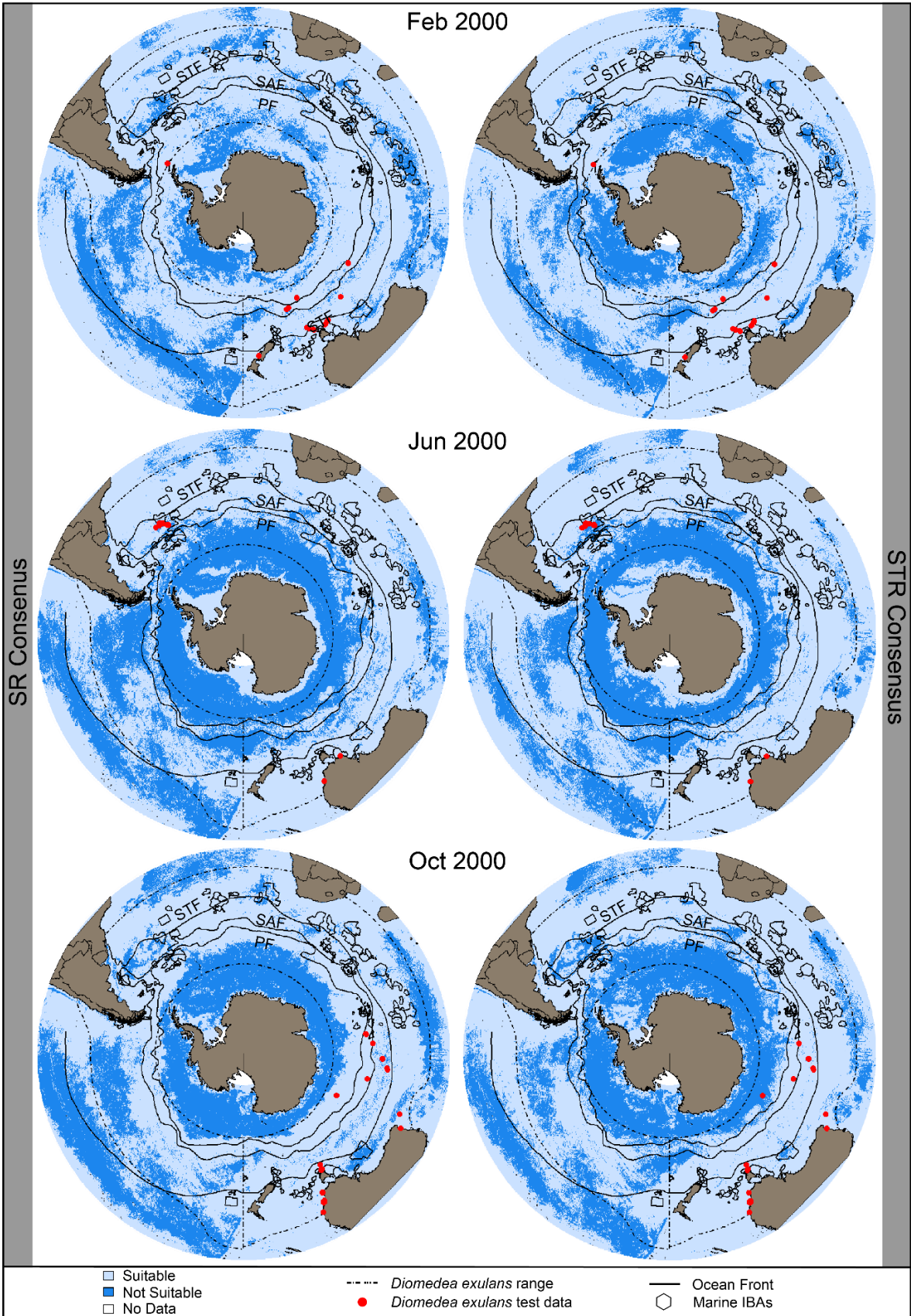
Figure 2. Snapshot of time-specific spatially rarefied (SR; left) and spatially rarefied and thinned (STR; right) consensus model predictions overlaid with *Diomedea exulans* range (dashed line; BirdLife International and NatureServe 2015), marine IBAs (black polygons; BirdLife International 2016), and *D. exulans* test data (red points), and the Subtropical Front (STF), the Subantarctic Front (SAF), and Polar Front (PF; CTOH 2019).

DISCUSSION

The results of this modeling exercise are not unexpected given the conceptual advantages of time-specific ecological niche modeling. On the other hand, both time-averaged consensus models performed poorly and showed high rates of omission. Both time-specific consensus models performed well statistically, with low rates of omission even without incorporating an environmental covariate known to constraining the distribution of this species in model calibration (wind; Pennycuick 1982). This study illustrates the potential for the modified time-specific correlational niche modeling framework to capture the breadth and dynamic nature of traditionally less predictable species' niches in greater detail and with more robust predictions.

Both time-averaged models performed poorly despite producing strikingly different results. Interestingly, the temporal rarefication of *D. exulans* occurrence data and pseudo-absence data resulted in a more relaxed model fit than the spatially rarefied model, predicting the vast majority of study region as environmentally suitable, including lower latitudes north of known areas of suitability. Compared to both time-specific consensus models, and to the seasonal modeling of Ingenloff (2017), the time-averaged spatially rarefied and thinned consensus model seriously over-predicted suitability of the study area. The areas predicted unsuitable and which included the greatest levels of omitted *Diomedea euxlans* data—areas of the subtropical waters of the Argentine Basin and colder Antarctic waters of the Antarctic Circumpolar Current—were the same for both time-averaged models. These results are not altogether surprising given that these

areas represent the relative edges of environmental suitability in *D. exulans* range relative to the suite of environmental covariates incorporated in the model and the fact that across the species as a whole, the breadth of environments exploited by *D. exulans* is quite broad. After fledging, juveniles often disperse from their natal colonies to warmer waters along the subtropical front (Weimerskirch *et al.* 2014) while more mature adults are more restricted to the Subantarctic region, which is characterized by stronger winds (Weimerskirch *et al.* 2012; Weimerskirch *et al.* 2014). During breeding, females tend to favor lower latitudes along the more northern extent of the Subantarctic front (Jaeger *et al.* 2009), while breeding males tend to gravitate towards the cold Antarctic waters in the more southerly reaches of the species' range (Weimerskirch *et al.* 2014). An important point is that while breeding populations are broadly disjunct, non-breeding populations overlap significantly (Rains, Weimerskirch & Burg 2011).

Even without additional biologically relevant information accompanying the *D. exulans* primary observation data (e.g., sex, breeding status, colony of origin), both time-specific consensus models performed well statistically with low overall omission rates. The spatially rarefied and thinned consensus model did have a greater omission rate than the spatially rarefied model (5.4% rather than 2.5%). Both models struggled to some degree in predicting in areas representing environmental extremes of the *D. exulans* range at the species level relative to the covariate data used in model calibration, including in the vicinity of the Antarctic Circumpolar Current (ACC) and the Argentine Basin. As with the time-averaged models, these areas account for the greatest proportion of *D. exulans* test data omitted. Other areas of environmental extremes, notably edges of ocean troughs (e.g., the South Shetland Trough), and around oceanic plateaus (specifically the Campbell Plateau and Naturaliste Plateau) correlated with smaller proportions of test data omitted. The failure of our models to predict fully into these areas is a reflection of the strong spatial and

temporal sampling bias inherent in the occurrence data, the relatively coarse temporal resolution applied in modeling, and the limitations on environmental covariate data available for use at coarser temporal resolutions.

Although the modified, temporally-explicit niche modeling framework retains more data for use in analyses, and allows for incorporation of finer resolution covariate data, it does raise some concern for data with very high sampling bias. This study only explored two methods of addressing what can only be described as extreme sampling bias. Spatial rarefication—reduction of point data to a single point per pixel—is already common practice in distributional ecology studies. The additional thinning step we explored, however, was a simple random process applied to each time step with arbitrary limits to the maximum number of presences and pseudo-absences regarded as acceptable. The resulting spatially rarefied and spatially rarefied and thinned data did have the same environmental ranges for the six time-averaged covariates (Supplemental Figure 15) and four time-specific covariates (Figure 3); however, because the thinning process randomly selected data for removal, unique covariate combinations were inevitably removed from model calibration. It is possible that this loss of covariate representation led to the higher omission rate in the spatially rarefied and thinned time-specific model relative to the spatially rarefied model. As such, future work should explore methods of subsampling such that representation of environmental breadth is retained.
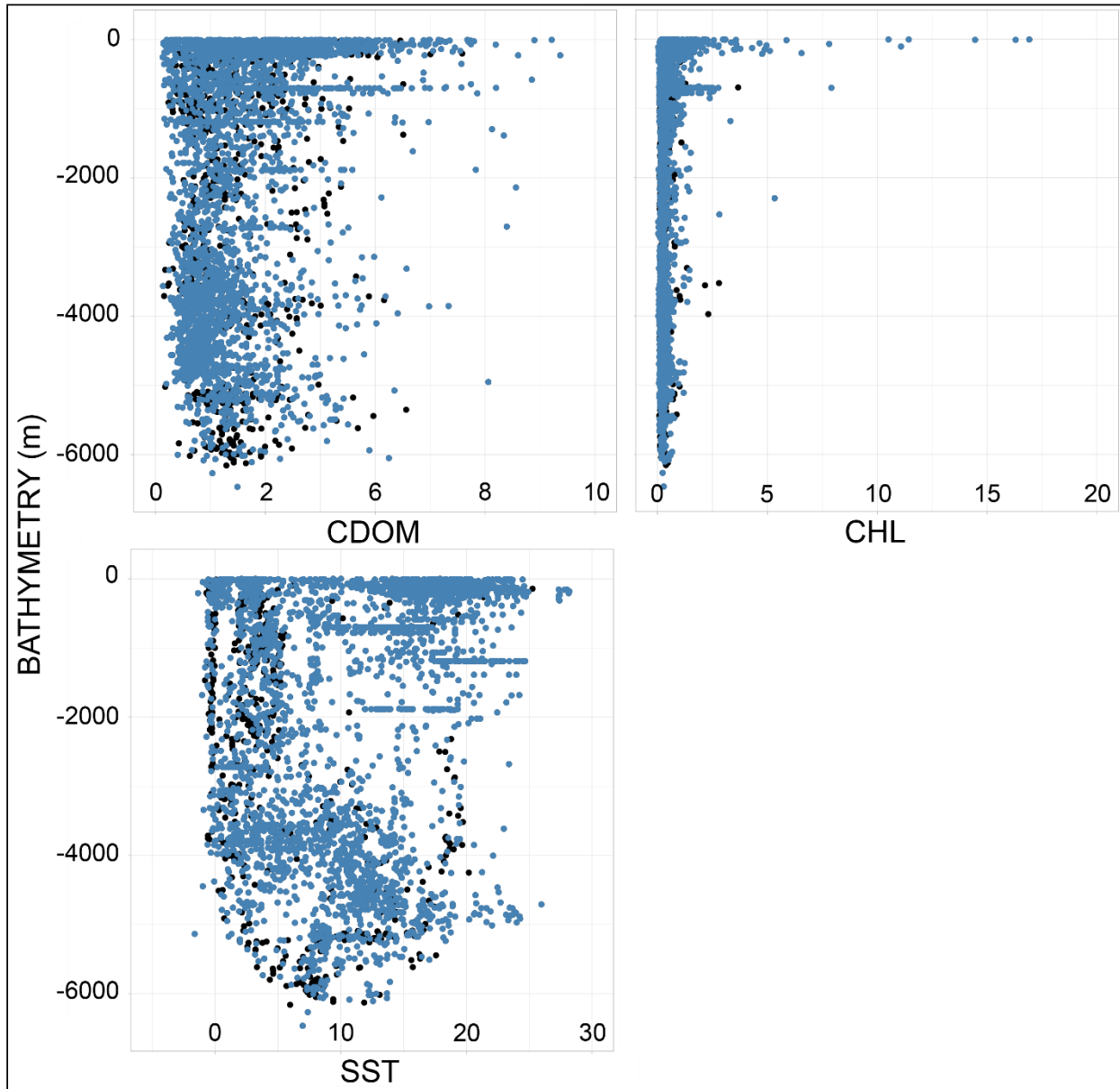
Figure 3. Covariate space for spatially rarefied (black) and spatially rarefied and thinned (blue) time-specific *Diomedea exulans* observation data. Visible black points denote unique covariate combinations lost during temporal rarefication.

Second, the distinct lack of biologically relevant contextual information associated with the primary occurrence data is problematic for behaviorally complex species such as pelagic seabirds (Ingenloff 2017). Species-level distributional ecology studies typically utilize primary point occurrence data—lists of localities at which individuals of a population/species are known

to have occurrence. These data may have been collected opportunistically, through coordinated at-sea surveys, or derived from data associated with specimens (Grecian *et al.* 2012), and typically consist of no more than species identification, date, and locality. For behaviorally complex species, this absence of contextual information impacts model calibration considerably. In the case of *D. exulans*, individual distribution is a function of sex, age, reproductive phase, and colony of origin, and the range of the species as whole extends from cold Antarctic waters to warm subtropical waters (Weimerskirch *et al.* 2014). Here, high sampling during a few time periods result in the capture only a portion of *D. exulans*' life history to any satisfactory extent. Until an accessible method of deriving these data is developed, statistical models built on open-access primary biodiversity point data will be at the mercy of these biases.

CONCLUSIONS

This study aimed to assess the utility of the modified, temporally-explicit correlative niche modeling framework with the challenge of a nomadic pelagic seabird. The dynamic niche predictions resulting from the time-specific modeling easily outperformed traditional, time-averaged approach and the seasonal modeling of Ingenloff (2017). Modeling limitations included high spatio-temporal sampling bias and lack of biologically relevant information with open-access point observation data. The results presented here strongly suggest that the modified framework of Ingenloff and Peterson (2021) does seem to overcome effectively the limitations of traditional, time-averaged modeling approaches for less predictable migratory species.

ACKNOWLEDGEMENTS

REFERENCES

Abrahms, B., Welch, H., Brodie, S., Jacox, M.G., Becker, E.A., Bograd, S.J., Irvine, L.M., Palacios, D.M., Mate, B.R. & Hazen, E.L. (2019) Dynamic ensemble models to predict distributions and anthropogenic risk exposure for highly mobile species. *Diversity and Distributions,* **25,** 1182–1193.

Åkesson, S. & Weimerskirch, H. (2005) Albatross longdistance navigation: comparing adults and juveniles. *Journal of Navigation,* **58,** 365–373.

Åkesson, S. & Weimerskirch, H. (2014) Evidence for sex-segregated ocean distributions of first-winter Wandering Albatrosses at Crozet Islands. *PLoS One,* **9**.

Alvarado-Serrano, D.F. & Knowles, L.L. (2014) Ecological niche models in phylogeographic studies: applications, advances and precautions. *Molecular Ecology Resources,* **14,** 233–248.

Amante, C. & Eakins, B.W. (2009) ETOPO1 1 arc-minute global relief model: procedures, data sources and analysis. *NOAA Technical Memorandum NESDIS NGDC-24*. NOAA, National Geophysical Data Center.

Anderson, R.P. (2003) Real vs. artefactual absences in species distributions: tests for Oryzomys albigularis (Rodentia: Muridae) in Venezuela. *Journal of Biogeography,* **30,** 591–605.

Andrew, M.E. & Fox, E. (2020) Modelling species distributions in dynamic landscapes: the importance of the temporal dimension. *Journal of Biogeography,* **00,** 1–20.

Barve, N., Martin, C., Brunsell, N.A. & Peterson, A.T. (2014) The role of physiological optima in shaping the geographic distribution of Spanish moss. *Global Ecology and Biogeography,* **23,** 633–645.

BirdLife International (2016) Important Bird and Biodiversity Area (IBA) digital boundaries: December 2015 version. BirdLife International, Cambridge, UK and NatureServe, Arlington, USA.

BirdLife International and NatureServe (2015) Bird species distribution maps of the world. BirdLife International, Cambridge, UK and NatureServe, Arlington, USA.

BirdLife International and NatureServe (2020) Marine IBA e-Atlas. https://maps.birdlife.org/marineIBAs/default.html.

Burg, T.M. & Croxall, J.P. (2004) Global population structure and taxonomy of the Wandering Albatross species complex. *Molecular Ecology,* **13,** 2345–2355.

Calcagno, V. (2013) glmulti: model selection and multimodel inference made easy. R package version 1.0.7.

Camphuysen, K., Shamoun-Baranes, J., Bouten, W. & Garthe, S. (2012) Identifying ecologically important marine areas for seabirds using behavioural information in combination with distribution patterns. *Biological Conservation,* **156,** 22–29.

Ceia, F.R., Phillips, R.A., Ramos, J.A., Cherel, Y., Vieira, R.P., Richard, P. & Xavier, J.C. (2012) Short- and long-term consistency in the foraging niche of Wandering Albatrosses. *Marine Biology,* **159,** 1581–1591.

Coble, P.G. (2007) Marine optical biogeochemistry: the chemistry of ocean color. *Chemical Reviews,* **107,** 402–418.

Cobos, M.E., Peterson, A.T., Barve, N. & Osorio-Olvera, L. (2019) kuenm: an R package for detailed development of ecological niche models using Maxent. *PeerJ,* **7:e6281**.

CTOH, C.f.T.S.o.t.O.a.H. (2019) Interpolated Southern Ocean fronts: 1993–2018. http://ctoh.legos.obs-mip.fr/applications/mesoscale/southern-ocean-fronts.

Dodge, S., Bohrer, G., Weinzierl, R., Davidson, S.C., Kays, R., Douglas, D., Cruz, S., Jiawei Han, Brandes, D. & Wikelski, M. (2013) The environmental-data automated track annotation (Env-DATA) system: linking animal tracks with environmental data. *Movement Ecology,* **1,** 3.

Fink, D., Hochachka, W.M., Zuckerberg, B., Winkler, D.W., Shaby, B., Munson, M.A., Hooker, G., Riedewald, M., Sheldon, D. & Kelling, S. (2010) Spatiotemporal exploratory models for broad-scale survey data. *Ecological Applications,* **20,** 2131–2147.

Forslund, P. & Pärt, T. (1995) Age and reproduction in birds hypotheses and tests. *Trends in Ecology & Evolution,* **10,** 374–378.

Froy, H., Lewis, S., Catry, P., Bishop, C.M., Forster, I.P., Fukuda, A., Higuchi, H., Phalan, B., Xavier, J.C., Nussey, D.H. & Phillips, R.A. (2015) Age-related variation in foraging behaviour in the Wandering Albatross at South Georgia: no evidence for senescence. *PLoS One,* **10,** 10:e0116415.

GBIF (31 December 2018) GBIF Occurrence Download: Diomedeidae. DOI: 10.15468/dl.qozkal.

Grecian, W.J., Witt, M.J., Attrill, M.J., Bearhop, S., Godley, B.J., Grémillet, D., Hamer, K.C. & Votier, S.C. (2012) A novel projection technique to identify important at-sea areas for seabird conservation: an example using Northern Gannets breeding in the North East Atlantic. *Biological Conservation,* **156,** 43–52.

Hijmans, R.J., Phillips, S., Leathwick, J. & Elith, J. (2017) dismo: species distribution modeling. R package version 1.1-4. https://cran.r-project.org/web/packages/dismo/index.html.

Hyrenbach, K.D., Veit, R.R., Weimerskirch, H., Metzl, N. & Hunt, G.L. (2007) Community structure across a large-scale ocean productivity gradient: marine bird assemblages of the southern Indian Ocean. *Deep-Sea Research Part I-Oceanographic Research Papers,* **54,** 1129–1145.

Ingenloff, K. (2017) Biologically informed ecological niche models for an example pelagic, highly mobile species. *European Journal of Ecology,* **3,** 55–75.

Ingenloff, K., Hensz, C.M., Anamza, T., Barve, V., Campbell, L.P., Cooper, J.C., Komp, E., Jiménez, L., Olson, K.V., Osorio-Olvera, L., Owens, H.L., Peterson, A., T, Samy, A., Simões, M. & Soberón, J. (2017) Predictable invasion dynamics in North American populations of the Eurasian collared dove *Streptopelia decaocto. Proceedings of the Royal Society B,* **284,** 11–57.

Ingenloff, K. & Peterson, A.T. 2021. Incorporating time into the traditional correlational distributional modeling framework: a proof-of-concept using the Wood Thrush (*Hylocichla mustelina*). *Methods in Ecology and Evolution*, **12**, 311–321.

Jaeger, A., Blanchard, P., Richard, P. & Cherel, Y. (2009) Using carbon and nitrogen isotopic values of body feathers to infer inter- and intra-individual variations of seabird feeding ecology during moult. *Marine Biology,* **156,** 1233−1240.

Jouventin, P. & Dobson, F.S. (2002) Why breed every other year? The case of albatrosses. *Proceedings of the Royal Society Biological Sciences,* **269,** 1955–1961.

Kearney, M., Simpson, S.J., Raubenheimer, D. & Helmuth, B. (2010) Modelling the ecological niche from functional traits. *Philosophical Transactions of The Royal Society B Biological Sciences,* **365,** 3469–3483.

Kramer-Schadt, S., Niedballa, J., Pilgrim, J.D., Schroder, B., Lindenborn, J., Reinfelder, V., Stillfried, M., Heckmann, I., Scharf, A.K., Augeri, D.M., Cheyne, S.M., Hearn, A.J., Ross, J., Macdonald, D.W., Mathai, J., Eaton, J., Marshall, A.J., Semiadi, G., Rustam, R., Bernard, H., Alfred, R., Samejima, H., Duckworth, J.W., Breitenmoser-Wuersten, C.,

Belant, J.L., Hofer, H. & Wilting, A. (2013) The importance of correcting for sampling bias in MaxEnt species distribution models. *Diversity and Distributions,* **19,** 1366–1379.

Laube, I., Graham, C.H. & Böhning-Gaese, K. (2015) Niche availability in space and time: migration in *Sylvia* warblers. *J. Biogeogr,* **42,** 1896–1906.

Mackley, E., Phillips, R., Silk, J., Wakefield, E., Afanasyev, V., Fox, J. & Furness, R. (2010) Free as a bird? Activity patterns of albatrosses during the nonbreeding period. *Marine Ecology Progress Series,* **406,** 291–303.

Meyer, C., Jetz, W., Guralnick, R.P., Fritz, S.A. & Kreft, H. (2016) Range geometry and socio-economics dominate species-level biases in occurrence information. *Global Ecology and Biogeography,* **25,** 1181–1193.

Milot, E., Weimerskirch, H. & Bernatchez, L. (2008) The seabird paradox: dispersal, genetic structure and population dynamics in a highly mobile, but philopatric albatross species. *Molecular Ecology,* **17,** 1658–1673.

NASA (2014) MODIS-Terra Ocean Color Data. (ed. O.E.L. NASA Goddard Space Flight Center, Ocean Biology Processing Group).

Nelson, N.B. & Siegel, D.A. (2013) The global distribution and dynamics of chromophoric dissolved organic matter. *Annual Review of Marine Science,* **5,** 447–476.

Ooms, J. (2018a) *gifski: highest quality GIF encoder. R package version 0.8.6. https://CRAN.R-project.org/package=gifski*.

Ooms, J. (2018b) *magick: advanced graphics and image-processing in R. R package version 2.0. https://CRAN.R-project.org/package=magick*.

Orsi, A. & Harris, U. (2008) Locations of the various fronts in the Southern Ocean, Australian Antarctic Data Centre: CAASM Metadata. http://gcmd.nasa.gov/KeywordSearch/ Metadata.do?Portal=amd_au&MetadataView=Full&MetadataType=0&KeywordPath=& OrigMetadataNode=AADC&EntryId=southern_ocean_fronts.

Pearson, R.G., Raxworthy, C.J., Nakamura, M. & Peterson, A.T. (2007) Predicting species distributions from small numbers of occurrence records: a test case using cryptic geckos in Madagascar. *Journal of Biogeography,* **34,** 102–117.

Pennycuick, C.J. (1982) The flight of petrels and albatrosses (Procellariiformes), observed in South Georgia and its vicinity. *Philosophical Transactions of the Royal Society of London. Series B, Biological Sciences,* **300**.

Pereira, J.M., Paiva, V.H., Phillips, R.A. & Xavier, J.C. (2018) The devil is in the detail: small-scale sexual segregation despite large-scale spatial overlap in the wandering albatross. *Marine Biology,* **165**.

Peterson, A.T., Martínez-Campos, C., Nakazawa, Y. & Martínez-Meyer, E. (2005) Time-specific ecological niche modeling predicts spatial dynamics of vector insects and human dengue cases. *Transactions of the Royal Society of Tropical Medicine and Hygiene,* **99,** 647–655.

Phillips, R.A., McGill, R.A., Dawson, D.A. & Bearhop, S. (2011) Sexual segregation in distribution, diet and trophic level of seabirds: insights from stable isotope analysis. *Marine Biology,* **158,** 2199–2208.

Phillips, R.A., Silk, J.R.D., Croxall, J.P., Afanasyev, V. & Bennett, V.J. (2005) Summer distribution and migration of nonbreeding albatrosses: individual consistencies and implications for conservation. *Ecology,* **86,** 2386–2396.

Phillips, S.J., Dudík, M., Elith, J., Graham, C.H., Lehmann, A., Leathwick, J. & Ferrier, S. (2009) Sample selection bias and presence-only distribution models: implications for background and pseudo-absence data. *Ecological Applications,* **19,** 181–197.

Prince, P.A., Wood, A.G., Barton, T. & Croxall, J.P. (1992) Satellite tracking of Wandering Albatrosses (*Diomedea exulans*) in the South Atlantic. *Antarctic Science,* **4,** 31–36.

Qiao, H.J., Soberón, J. & Peterson, A.T. (2015) No silver bullets in correlative ecological niche modelling: insights from testing among many potential algorithms for niche estimation. *Methods in Ecology and Evolution,* **6,** 1126–1136.

R Development Core Team (2009) *R: a language and environment for statistical computing. R Foundation for Statistical Computing: http://www.r-project.org.*

Rains, D., Weimerskirch, H. & Burg, T.M. (2011) Piecing together the global population puzzle of Wandering Albatrosses: genetic analysis of the Amsterdam albatross *Diomedea amsterdamensis. Journal of Avian Biology,* **42,** 69–79.

Runge, C.A., Martin, T.G., Possingham, H.P., Willis, S.G. & Fuller, R.A. (2014) Conserving mobile species. *Frontiers in Ecology and the Environment,* **12,** 395–401.

Scales, K.L., Miller, P.I., Ingram, S.N., Hazen, E.L., Bograd, S.J. & Phillips, R.A. (2016) Identifying predictable foraging habitats for a wide-ranging marine predator using ensemble ecological niche models. *Diversity and Distributions,* **22,** 212–224.

Schodde, R., Tennyson, A.J.D., Groth, J.G., Lai, J., Scofield, P. & Steinheimer, F.D. (2017) Settling the name *Diomedea exulans* Linnaeus, 1758 for the Wandering Albatross by neotypification. *Zootaxa,* **4236,** 135–148.

Signorell, A., Aho, K., Alfons, A., Anderegg, N., Aragon, T., Arppe, A., Baddeley, A., Barton, K., Bolker, B., Borchers, H.W., Caeiro, F., Champely, S., Chessel, D., Chhay, L., Cummins, C., Dewey, M., Doran, H.C., Dray, S., Dupont, C., Eddelbuettel, D., Enos, J., Ekstrom, C., Elff, M., Erguler, K., Farebrother, R.W., John Fox, R.F., Friendly, M., Galili, T., Gamer, M., Gastwirth, J.L., Gel, Y.R., Gross, J., Grothendieck, G., Jr, F.E.H., Heiberger, R., Hoehle, M., Hoffmann, C.W., Hojsgaard, S., Hothorn, T., Hui, M.H.W.W., Hurd, P., Hyndman, R.J., Iglesias, P.J.V., Jackson, C., Kohl, M., Korpela, M., Kuhn, M., Labes, D., Lang, D.T., Leisch, F., Lemon, J., Li, D., Maechler, M., Magnusson, A., Malter, D., Marsaglia, G., Marsaglia, J., Matei, A., Meyer, D., Miao, W., Millo, G., Min, Y., Mitchell, D., Naepflin, M., Navarro, D., Nilsson, H., Nordhausen, K., Ogle, D., Ooi, H., Parsons, N., Pavoine, S., Plate, T., Rapold, R., Revelle, W., Rinker, T., Ripley, B.D., Rodriguez, C., Russell, N., Sabbe, N., Venkatraman E. Seshan, Greg Snow, M.S., Soetaert, K., Stahel, W.A., Stephenson, A., Stevenson, M., Templ, M., Therneau, T., Tille, Y., Trapletti, A., Ulrich, J., Ushey, K., VanDerWal, J., Venables, B., Verzani, J., Warnes, G.R., Wellek, S., Wickham, H., Wilcox, R.R., Wolf, P., Wollschlaeger, D., Yee, T. & Zeileis, A. (2019) DescTools: tools for descriptive statistics. R package version 0.99.27.

Soriano-Redondo, A., Jones-Todd, C.M., Bearhop, S., Hilton, G.M., Lock, L., Stanbury, A., Votier, S.C. & Illian., J.B. (2019) Understanding species distribution in dynamic populations: a new approach using spatio-temporal point process models. *Ecography,* **42,** 1092–1102.

Thuiller, W., Georges, D., Engler, R. & Breiner, F. (2016) biomod2: ensemble platform for species distribution modeling. R package version 3.3-7. https://CRAN.R-project.org/package=biomod2.

Urtizberea, A., Dupont, N., Rosland, R. & Aksnes, D.L. (2013) Sensitivity of euphotic zone properties to CDOM variations in marine ecosystem models. *Ecological Modelling,* **256,** 16–22.

Wakefield, E.D., Phillips, R.A. & Matthiopoulos, J. (2009) Quantifying habitat use and preferences of pelagic seabirds using individual movement data: a review. *Marine Ecology Progress Series,* **391,** 165–182.

Wakefield, E.D., Phillips, R.A., Trathan, P.N., Arata, J., Gales, R., Huin, N., Robertson, G., Waugh, S.M., Weimerskirch, H. & Matthiopoulos, J. (2011) Habitat preference, accessibility, and competition limit the global distribution of breeding Black-browed Albatrosses. *Ecological Monographs,* **81,** 141–167.

Warren, D.L. & Seifert, S.N. (2011) Ecological niche modeling in Maxent: the importance of model complexity and the performance of model selection criteria. *Ecological Applications,* **21,** 335–342.

Weimerskirch, H., Åkesson, S. & Pinaud, D. (2006) Postnatal dispersal of Wandering Albatrosses *Diomedea exulans*: implications for the conservation of the species. *Journal of Avian Biology,* **37,** 23–28.

Weimerskirch, H., Cherel, Y., Delord, K., Jaeger, A., Patrick, S.C. & Riotte-Lambert, L. (2014) Lifetime foraging patterns of the Wandering Albatross: life on the move! *Journal of Experimental Marine Biology and Ecology,* **450,** 68–78.

Weimerskirch, H., Louzao, M., de Grissac, S. & Delord, K. (2012) Changes in wind pattern alter albatross distribution and life-history traits. *Science,* **335,** 211–214.

Welch, H., Pressey, R.L. & Reside, A.E. (2018) Using temporally explicit habitat suitability models to assess threats to mobile species and evaluate the effectiveness of marine protected areas. *Journal for Nature Conservation,* **41,** 106–115.

Williams, H.M., Willemoes, M. & Thorup, K. (2017) A temporally explicit species distribution model for a long distance avian migrant, the common cuckoo. *Journal of Avian Biology,* **48,** 1624–1636.

Wood, S.N. (2011) Fast stable restricted maximum likelihood and marginal likelihood estimation of semiparametric generalized linear models. *Journal of the Royal Statistical Society (B),* **73,** 3–36.

CONCLUSION

The body of research presented here iteratively assesses and builds upon the traditional distributional ecology framework to incorporate the temporal dimension and more accurately characterize the environmental niche for highly mobile, behaviorally complex, and ephemeral taxa at the species level. Seasonal time-averaged modeling of *Diomedea exulans* in Chapter 1 established a baseline of model performance and highlighted two major challenges for current species' level modeling approaches: (1) the loss of complexity and detail resulting from over-generalization of covariate data in traditional time-averaged niche modeling methods, and (2) the lack of relevant biological information associated with open-access primary species occurrence data. Based on these insights, Chapter 2 proposed a series of improvements for the input data preparation process of the canonical niche modeling framework to incorporate the temporal dimension into model calibration, significantly reducing the over-generalization of explanatory covariates, and producing dynamic niche predictions. Initial success when applied to the well-studied seasonal migrant *Hylocichla mustelina* suggested the potential value for less predictable migratory species and ephemeral species. Finally, Chapter 3 assessed the utility of the temporally explicit correlative niche modeling framework of Chapter 2 with *D. exulans*. The results indicate that by addressing only one of the two major challenges highlighted in the first chapter, that of environmental over-generalization resulting from time-averaging, we can indeed produce reliable species level distributional models for highly mobile taxa such as pelagic seabirds at the species level. The development of a step-wise methodology that works for highly mobile species will facilitate the development of more biologically informed strategies for a whole suite of taxa that might otherwise be neglected as a result of data deficiency.

The collective suite of analyses presented here provide an accessible framework for incorporating the temporal dimension into species level predictive models. All research was conducted using open access data and programs to ensure maximum transferability and accessibility to the broader research and resource planning and management communities. And, although this particular body of work focuses on pelagic seabirds in the southern oceans, this modified methodological framework is readily transferrable across taxonomic groups, providing researchers and natural resource managers with a framework by which to produce more robust, biologically-informed models that are more appropriate for informing the development of spatially-explicit management plans applicable to multiple species and responsive to global change. Further, these techniques have the potential to play a role in public health applications, particularly as regards monitoring of climate sensitive arthropod disease vectors, such as mosquitoes.

REFERENCES

Alvarado-Serrano, D.F. & Knowles, L.L. (2014) Ecological niche models in phylogeographic studies: applications, advances and precautions. *Molecular Ecology Resources,* **14,** 233–248.

Barve, N., Martin, C., Brunsell, N.A. & Peterson, A.T. (2014) The role of physiological optima in shaping the geographic distribution of Spanish moss. *Global Ecology and Biogeography,* **23,** 633–645.

Bellard, C., Bertelsmeier, C., Leadley, P., Thuiller, W. & Courchamp, F. (2012) Impacts of climate change on the future of biodiversity. *Ecology Letters,* **15,** 365–377.

Brandão-Filho, S.P., Donalisio, M.R., Silva, F.J.d., Valença, H.F., Costa, P.L., Shaw, J.J. & Peterson, A.T. (2011) Spatial and temporal patterns of occurrence of Lutzomyia sand fly species in an endemic area for cutaneous leishmaniasis in the Atlantic Forest region of northeast Brazil. *Journal of Vector Ecology,* **36,** S71–S76.

Catry, P., Lemos, R.T., Brickle, P., Phillips, R.A., Matias, R. & Granadeiro, J.P. (2013) Predicting the distribution of a threatened albatross: the importance of competition, fisheries and annual variability. *Progress in Oceanography,* **110,** 1–10.

Ceia, F.R., Phillips, R.A., Ramos, J.A., Cherel, Y., Vieira, R.P., Richard, P. & Xavier, J.C. (2012) Short- and long-term consistency in the foraging niche of Wandering Albatrosses. *Marine Biology,* **159,** 1581–1591.

Cook, B.I., Wolkovich, E.M., Davies, T.J., Ault, T.R., Betancourt, J.L., Allen, J.M., Bolmgren, K., Cleland, E.E., Crimmins, T.M., Kraft, N.J.B., Lancaster, L.T., Mazer, S.J., McCabe, G.J., McGill, B.J., Parmesan, C., Pau, S., Regetz, J., Salamin, N., Schwartz, M.D. & Travers, S.E. (2012) Sensitivity of spring phenology to warming across temporal and spatial climate gradients in two independent databases. *Ecosystems,* **15,** 1283–1294.

Croxall, J.P., Butchart, S.H.M., Lascelles, B., Stattersfield, A.J., Sullivan, B., Symes, A. & Taylor, P. (2012) Seabird conservation status, threats and priority actions: a global assessment. *Bird Conservation International,* **22,** 1–34.

Dias, M.P., Martin, R., Pearmain, E.J., Burfield, I.J., Small, C., Phillips, R.A., Yates, O., Lascelles, B., Borboroglu, P.B., & Croxall, J.P. (2019) Threats to seabirds: a global assessment. *Biological Conservation*, **237**, 525–537.

Dodge, S., Bohrer, G., Weinzierl, R., Davidson, S.C., Kays, R., Douglas, D., Cruz, S., Jiawei Han, Brandes, D. & Wikelski, M. (2013) The environmental-data automated track annotation (Env-DATA) system: linking animal tracks with environmental data. *Movement Ecology,* **1,** 1–3.

Eaton, S., Ellis, C., Genney, D., Thompson, R., Yahr, R. & Haydon, D.T. (2018) Adding small species to the big picture: species distribution modelling in an age of landscape scale conservation. *Biological Conservation,* **217,** 251–258.

Edwards, M. & Richardson, A.J. (2004) Impact of climate change on marine pelagic phenology and trophic mismatch. *Nature,* **430,** 881–884.

Franklin, J. (2013) Species distribution models in conservation biogeography: developments and challenges. *Diversity and Distributions,* **19,** 1217–1223.

Grecian, W.J., Witt, M.J., Attrill, M.J., Bearhop, S., Godley, B.J., Grémillet, D., Hamer, K.C. & Votier, S.C. (2012) A novel projection technique to identify important at-sea areas for seabird conservation: an example using Northern Gannets breeding in the North East Atlantic. *Biological Conservation,* **156,** 43–52.

Guisan, A. & Zimmermann, N.E. (2000) Predictive habitat distribution models in ecology. *Ecological Modelling, 135,* 147–186.

Heikkinen, R.K., Marmion, M. & Luoto, M. (2012) Does the interpolation accuracy of species distribution models come at the expense of transferability? *Ecography, 35,* 276–288.

Hughes, L. (2000) Biological consequences of global warming: is the signla already apparent? *Trends in Ecology & Evolution, 15,* 56–61.

Knudsen, E., Lindén, A., Both, C., Jonzén, N., Pulido, F., Saino, N., Sutherland, W.J., Bach, L.A., Coppack, T., Ergon, T., Gienapp, P., Gill, J.A., Gordo, O., Hedenström, A., Lehikoinen, E., Marra, P.P., Møller, A.P., Nilsson, A.L.K., Péron, G., Ranta, E., Rubolini, D., Sparks, T.H., Spina, F., Studds, C.E., Sæther, S.A., Tryjanowski, P. & Stenseth, N.C. (2011) Challenging claims in the study of migratory birds and climate change. *Biological Reviews, 86,* 928–946.

Lascelles, B.G., Langham, G.M., Ronconi, R.A. & Reid, J.B. (2012) From hotspots to site protection: identifying Marine Protected Areas for seabirds around the globe. *Biological Conservation, 156,* 5–14.

Lemoine, N. & Böhning-Gaese, K. (2003) Potential impact of global climate change on species richness of long-distance migrants. *Conservation Biology, 17,* 577–586.

Lewison, R., Oro, D., Godley, B., Underhill, L., Bearhop, S., Wilson, R.P., Ainley, D., Arcos, J.M., Boersma, P.D., Borboroglu, P.G., Boulinier, T., Frederiksen, M., Genovart, M., González-Solís, J., Green, J.A., Grémillet, D., Hamer, K.C., Hilton, G.M., Hyrenbach, K.D., Martínez-Abraín, A., Montevecchi, W.A., Phillips, R.A., Ryan, P.G., Sagar, P., Sydeman, W.J., Wanless, S., Watanuki, Y., Weimerskirch, H. & Yorio, P. (2012) Research priorities for seabirds: improving conservation and management in the 21st century. *Endangered Species Research, 17,* 93–121.

Louzao, M., Aumont, O., Hothorn, T., Wiegand, T. & Weimerskirch, H. (2013) Foraging in a changing environment: habitat shifts of an oceanic predator over the last half century. *Ecography, 36,* 57–67.

McGowan, J., Hines, E., Elliott, M., Howar, J., Dransfield, A., Nur, N. & Jahncke, J. (2013) Using seabird habitat modeling to inform marine spatial planning in central California's National Marine Sanctuaries. *PLoS One, 8,* e71406.

Møller., A.P., Fiedler, W., Berthold, P. & eds. (2010) *Effects of Climate Change on Birds*. Oxford University Press, Oxford, UK

Oppel, S., Meirinho, A., Ramírez, I., Gardner, B., O'Connell, A.F., Miller, P.I. & Louzao, M. (2012) Comparison of five modelling techniques to predict the spatial distribution and abundance of seabirds. *Biological Conservation, 156,* 94–104.

Pacifici, M., Foden, W.B., Visconti, P., Watson, J.E., Butchart, S.H., Kovacs, K.M., Scheffers, B.R., Hole, D.G., Martin, T.G., Akcakaya, H.R. & Corlett, R.T. (2015) Assessing species vulnerability to climate change. *Nature Climate Change, 5,* 215.

Parmesan, C. & Yohe, G. (2003) A globally coherent fingerprint of climate change impacts across natural systems. *Nature, 421,* 37–42.

Pearson, R.G. & Dawson, T.P. (2003) Predicting the impacts of climate change on the distribution of species: are bioclimate envelope models useful? *Global Ecology and Biogeography, 12,* 361–371.

Pecl, G.T., Araújo, M.B., Bell, J.D., Blanchard, J., Bonebrake, T.C., Chen, I.-C., Clark, T.D., Colwell, R.K., Danielsen, F., Evengård, B., Falconi, L., Ferrier, S., Frusher, S., Garcia, R.A., Griffis, R.B., Hobday, A.J., Janion-Scheepers, C., Jarzyna, M.A., Jennings, S.,

Lenoir, J., Linnetved, H.I., Martin, V.Y., McCormack, P.C., McDonald, J., Mitchell, N.J., Mustonen, T., Pandolfi, J.M., Pettorelli, N., Popova, E., Robinson, S.A., Scheffers, B.R., Shaw, J.D., Sorte, C.J.B., Strugnell, J.M., Sunday, J.M., Tuanmu, M.-N., Vergés, A., Villanueva, C., Wernberg, T., Wapstra, E. & Williams, S.E. (2017) Biodiversity redistribution under climate change: Impacts on ecosystems and human well-being. *Science,* **355,** eaai9214.

Peñuelas, J., Sardans, J., Estiarte, M., Ogaya, R., Carnicer, J., Coll, M., Barbeta, A., Rivas-Ubach, A., Llusià, J., Garbulsky, M., Filella, I. & Jump, A.S. (2013) Evidence of current impact of climate change on life: a walk from genes to the biosphere. *Global Change Biology,* **19,** 2303–2338.

Peterson, A.T. (2006) Uses and requirements of ecological niche models and related distribution models. *Biodiversity Informatics,* **3,** 59–72.

Peterson, A.T. (2014) *Mapping disease transmission risk*. Johns Hopkins University Press, Baltimore.

Peterson, A.T., Martínez-Campos, C., Nakazawa, Y. & Martínez-Meyer, E. (2005) Time-specific ecological niche modeling predicts spatial dynamics of vector insects and human dengue cases. *Transactions of the Royal Society of Tropical Medicine and Hygiene,* **99,** 647–655.

Peterson, A.T., Papeş, M. & Soberón, J. (2015) Mechanistic and correlative models of ecological niches. *European Journal of Ecology,* **1,** 28–38.

Phillips, R.A., Silk, J.R.D., Croxall, J.P., Afanasyev, V. & Bennett, V.J. (2005) Summer distribution and migration of nonbreeding albatrosses: individual consistencies and implications for conservation. *Ecology,* **86,** 2386–2396.

Piatt, J.F., Sydeman, W.J., & Wiese, F. (2007) Introduction: seabirds as indicators of marine ecosystems. *Marine Ecology Progress Series* 352, 199–204.

Robinson, R.A., Crick, H.Q.P., Learmonth, J.A., Maclean, I.M.D., Thomas, C.D., Bairlein, F., Forchhammer, M.C., Francis, C.M., Gill, J.A., Godley, B.J., Harwood, o., Hays, G.C., Huntley, B., Hutson, A.M., Pierce, G.J., Rehfisch, M.M., Sims, D.W., Santos, M.B., Sparks, T.H., Stroud, D.A. & Visser, M.E. (2009) Travelling through a warming world: climate change and migratory species. *Endangered Species Research,* **7,** 87–99.

Rodríguez , J.P., Brotons, L., Bustamante, J. & Seoane, J. (2007) The application of predictive modelling of species distribution to biodiversity conservation. *Diversity and Distributions,* **13,** 243–251.

Root, T.L., Price, J.T., Hall, K.R., Schneider, S.H., Rosenzweig, C. & Pounds, J.A. (2003) Fingerprints of global warming on wild animals and plants. *Nature,* **421,** 57–60.

Scales, K.L., Miller, P.I., Ingram, S.N., Hazen, E.L., Bograd, S.J. & Phillips, R.A. (2016) Identifying predictable foraging habitats for a wide-ranging marine predator using ensemble ecological niche models. *Diversity and Distributions,* **22,** 212–224.

Searcy, C.A. & Shaffer, H.B. (2016) Do ecological niche models accurately identify climatic determinants of species ranges? *American Naturalist,* **187,** 423–435.

Tancell, C., Phillips, R.A., Xavier, J.C., Tarling, G.A. & Sutherland, W.J. (2013) Comparison of methods for determining key marine areas from tracking data. *Marine Biology,* **160,** 15–26.

Taylor, F.E., Ryan, P.G., Makhado, A.B., De Bruyn, P.J.N. & Weimerskirch, H. (2011) The seasonal distribution and habitat use of marine top predators in the southern Indian Ocean. *Habitat of Marine Top Predators. Southern Indian Ocean Regional Workshop to Facilitate*

the Description of Ecologically or Biologically Significant Marine Areas (EBSAs). Flic en Flac, Mauritius.

Thackeray, S.J., Sparks, T.H., Frederiksen, M., Burthe, S., Bacon, P.J., Bell, J.R., Botham, M.S., Brereton, T.T., Bright, P.W., Carvalho, L., Clutton-Brock, T., Dawson, A., Edwards, M., Elliott, J.M., Harrington, R., Johns, D., Jones, I.D., Jones, J.T., Leech, D.I., Roy, D.B., Scott, W.A., Smith, M., Smithers, R.J., Winfield, I.J. & Wanless, S. (2010) Trophic level asynchrony in rates of phenological change for marine, freshwater and terrestrial environments. *Global Change Biology,* **16,** 3304–3313.

Thomas, C.D., Cameron, A., Green, R.E., Bakkenes, M., Beaumont, L.J., Collingham, Y.C., Erasmus, B.F.N., Siqueira, M.F.d., Grainger, A., Hannah, L., Hughes, L., Jaarsveld, B.H.A.S.v., Midgley, G.F., Miles, L., Ortega-Huerta, M.A., Peterson, A.T., Phillips, O.L. & Williams, S.E. (2004) Extinction risk from climate change. *Nature,* **427,** 145–148.

Weimerskirch, H., Åkesson, S. & Pinaud, D. (2006) Postnatal dispersal of Wandering Albatrosses *Diomedea exulans*: implications for the conservation of the species. *Journal of Avian Biology,* **37,** 23–28.

Weimerskirch, H., Inchausti, P., Guinet, C. & Barbraud, C. (2003) Trends in bird and seal populations as indicators of a system shift in the Southern Ocean. *Antarctic Science,* **15,** 249–256.

APPENDICES

APPENDIX 1: Supplementary Information – Biologically-informed ecological niche models for

highly mobile species: non-breeding Wandering Albatrosses (*Diomedea exulans*)

distributions in the southern oceans

Supplementary Information

Author: Kate Ingenloff (ORCid: 0000-0001-5942-9053)

Supplementary Materials

Appendix S1 Additional model calibration and parameterization information.

Appendix S2 Additional tables and figures.

Appendix S3 R code for running minimum volume ellipsoids as niche models.

APPENDIX S1 Data Preparation and Model Calibration

Input Data - Occurrence Data

Data Acquisition. Occurrence data for all members of the order Procellariiformes were obtained from the Global Biodiversity Information Facility (GBIF; accessed 5/26/2015, doi:10.15468/dl.fquf8g). GBIF search was restricted to observation data for all error-free procellariiform records within the study period of December 2000–November 2011 between -20˚ and -70˚ latitude requested 26 May 2015. The search returned 144,850 observations of 105 species from 28 genera and 4 families (Diomedeidae, Procellariidae, Hydrobatidae, Pelecanoididae) species from 31 collections/institutions. Occurrence data were derived from human and machine observations, and preserved specimens.

Table S1.1. GBIF procellariiform occurrence data contributors.

GBIF Institution Code	Institution
AADC	Australia Antarctic Data Centre
ABBBS	Bird Banding Records, Australian Antarctic Territory & Heard Island
AM	Australian Museum
AMNH	American Museum of Natural History
ANWC	Australian National Wildlife Collection
Anymals.org	Anymals.org; Anymals+Plants Mobile Application
APN-AR	*Administración de Parques Nacionales, Argentina*
BAS	British Antarctic Survey
BGBM	Botanical Garden and Botanical Museum Berlin-Dahlem
Birds Australia, Birdata	BirdLife Australia, BirdLife International
CAML	Census of Antarctic marine Life
CLO	Cornell Laboratory of Ornithology
CTALA_LB	*Ministerio del Medio Ambiente de Chile*
CUML	Cornel University Macaulay Library
Eremaea Pty Ltd	Eremaea eBird
iNaturalist	iNaturalist.org
Individual Sightings	Individual sightings
IRSNB	*Institut Royal des Sciences Naturelles de Belgique*
naturgucker	*Natur Gucker*
NMR	*Natuurhistorisch Museum*
NMV	National Museum Victoria
OBIS-SEAMAP	Ocean Biogeographic Information System: Spatial Ecological Analysis of Megavertebrate Populations
SAMA	South Australia Museum
SA Fauna	South Australia Department of Environment & Natural Resources
TMAG	Tasmanian Museum & Art Gallery
UCT-ADU	University of Cape Town Animal Demography Unit
USNM	Smithsonian Institution Natural History Museum
UWBM	University of Washington Burke Museum
QM	Queensland Museum, Australia
QVMAG	Queen Victoria Museum & Art Gallery
ZMA	Zoological Museum Amsterdam, University of Amsterdam

Input Data - Environmental Data

Four MODIS Terra L3 standard mapped image (SMI) environmental datasets at 4.6 km spatial resolution were downloaded from the NASA OceanColor Web (Table S1.2; NASA 2014). Imagery were converted from native HDFs to ASCII grids and reprojected to WGS 84 using the Marine Geospatial Ecology Tools (MGET) ArcGIS toolbox extension (Roberts et al 2010). 'NoData' values were filled using a temporal filter followed by a spatial filter. The mean, maximum, minimum, and range of values were calculated by season for each variable; the resulting time-averaged rasters were then incorporated into a series of principle component analyses (PCA).

Table S1.2. MODIS Terra raster data accessed from NASA's OceanColor Web.

Variable		Unit	Date accessed
Sea Surface Temperature	(SST)	11 μm	18 Feb 2015
Nightly Sea Surface Temperature	(NSST)	11 μm	14 Feb 2015
Chromophoric Dissolved Organic Matter Index	(CDOM)		8 Feb 2015
Chlorophyll-a Concentration	(CHL)	mg/m^3	16 Feb 2015

PCAs: PCAs were run were run to reduce dimensionality and collinearity. The first five principle components (PCs) per season were used in analyses; in all three seasons, the first PC explained $\geq$ 95% of variation (Table S1.3). The final PCs selected for use in analyses were resampled from 0.041667 to 0.20833 for analyses.

Table S1.3. PCA Loadings for the first five components of each set utilized in analyses by season.

Season	Variable	PC1	PC2	PC3	PC4	PC5
I	CDOM_max	0.034	-0.235	0.636	0.217	-0.005
	CDOM_range	0.041	-0.238	0.621	0.218	0.009
	CHL_max	0.012	-0.677	-0.246	-0.011	-0.008
	CHL_range	0.011	-0.648	-0.246	-0.010	-0.009
	NSST_max	-0.418	-0.039	0.096	-0.268	-0.201
	NSST_mean	-0.412	-0.015	0.020	0.014	-0.059
	NSST_min	-0.405	0.013	-0.085	0.309	0.340
	NSST_range	-0.013	-0.052	0.182	-0.576	-0.541
	SST_max	-0.410	-0.039	0.092	-0.245	0.285
	SST_mean	-0.406	-0.015	0.026	0.016	-0.061
	SST_min	-0.393	0.019	-0.067	0.274	-0.317
	SST_range	-0.017	-0.058	0.158	-0.520	0.602
	Cumulative Proportion	96.69	98.30	99.10	99.83	99.93
G	CDOM_max	0.053	-0.602	-0.335	0.003	0.008
	CDOM_range	0.056	-0.638	-0.334	0.010	0.006
	CHL_max	0.002	-0.068	0.109	-0.715	-0.013
	CHL_range	0.001	-0.059	0.099	-0.677	-0.018
	NSST_max	-0.428	-0.168	0.225	0.051	-0.309
	NSST_mean	-0.411	-0.016	-0.061	-0.005	-0.054
	NSST_min	-0.394	0.112	-0.282	-0.063	0.250
	NSST_range	-0.034	-0.280	0.507	0.114	-0.559
	SST_max	-0.420	-0.144	0.222	0.039	0.368
	SST_mean	-0.402	0.002	-0.055	-0.006	-0.043
	SST_min	-0.383	0.117	-0.268	-0.044	-0.216
	SST_range	-0.036	-0.261	0.490	0.084	0.585
	Cumulative Proportion	96.15	98.32	99.23	99.81	99.92
P	CDOM_max	0.0680	-0.5201	0.4385	-0.1618	0.0130
	CDOM_range	0.0751	-0.5295	0.4426	-0.1546	0.0038
	CHL_max	0.0084	-0.4177	-0.5581	-0.1779	-0.0147
	CHL_range	0.0078	-0.3955	-0.5410	-0.1803	-0.0236
	NSST_max	-0.4173	-0.1304	0.0061	0.2663	-0.2843
	NSST_mean	-0.4081	-0.0322	0.0374	-0.0378	-0.0660
	NSST_min	-0.4033	0.0682	0.0268	-0.3055	0.2590
	NSST_range	-0.0140	-0.1986	-0.0208	0.5718	-0.5432
	SST_max	-0.4108	-0.1214	-0.0081	0.2468	0.3756
	SST_mean	-0.4020	-0.0313	0.0360	-0.0287	-0.0676
	SST_min	-0.3942	0.0677	0.0392	-0.2645	-0.2218
	SST_range	-0.0166	-0.1891	-0.0472	0.5113	0.5974
	Cumulative Proportion	95.84	97.79	99.04	99.81	99.92

Model Calibration

Table S1.4. Cell value ranges for raw and Log_2 kernel smoothed seasonal bias layers tested in Maxent model calibrations.

Season	Bias layer	
	Raw	Log_2 Smoothed
I	0:1604	0:114.0237
G	0:469	0:39.2755
P	0:1070	0:84.2523

Table S1.5. MVE model calibration parameterizations.

Parameter	Parameter Range	
Threshold (T)	0.90	
	0.95	
	0.99	
Variables Included (Run)	Bathymetry, Bathymetry Slope, PC 1-5	Run 1
	Bathymetry, PC 1-5	Run 2
	Bathymetry, Bathymetry Slope, PC 1-4	Run 3
	Bathymetry, PC 1-4	Run 4
	Bathymetry, PC 1-3	Run 5
	Bathymetry, PC 1-2	Run 6

Table S1.6. Pseudo-absence levels used in boosted regression tree calibrations. The first level, PA-1, was standardized at 1500 randomly selected points in the calibration region; PA-2 values were calculated at double the total *Diomedea exulans* observation data available for use in model calibration and testing.

Season	PA-1	PA-2
I	1500	1106
G	1500	562
P	1500	280

REFERENCES

Global Biodiversity Informatics Facility (2015) www.gbif.org. Accessed 5/26/2015. DOI: 10.15468/dl.fquf8g

NASA Goddard Space Flight Center, Ocean Ecology Laboratory, Ocean Biology Processing Group (2014) MODIS-Terra Ocean Color Data; NASA Goddard Space Flight Center, Ocean Ecology Laboratory, Ocean Biology Processing Group. DOI: 10.5067/TERRA/MODIS_OC.2014.0. Accessed 2/8–18/2015.

Roberts JJ, Best BD, Dunn DC, Treml EA, Halpin PN (2010) Marine Geospatial Ecology Tools: An integrated framework for ecological geoprocessing with ArcGIS, Python, R, MATLAB, and C++. *Environmental Modelling & Software*, 25: 1197–1207. DOI: 10.1016/j.envsoft.2010.03.029.

APPENDIX S2 Results

Table S2.1. Model transfer summary statistics–mean pROC score and the overall significance–for the top five model parameterizations from each algorithm by season.

Season	Algorithm	Parameterizations	mean pROC	*P-val*
Model Transfer: I	BRT	PA-2, TC=1, LR=0.01, BF=0.5	1.0714	0.000
		PA-2, TC=1, LR=0.01, BF=0.6	1.0703	0.000
		PA-2, TC=1, LR=0.01, BF=0.75	1.0654	0.000
		PA-2, TC=2, LR=0.005, BF=0.5	1.0627	0.000
		PA-2, TC=1, LR=0.01, BF=0.5	1.0627	0.000
	Maxent	Bias=None, P=0.3, RM=2	1.0019	0.127
		Bias=None, P=0.5, RM=2	1.0018	0.2245
		Bias=None, P=0.7, RM=2	1.0018	0.2465
		Bias=None, P=0.6, RM=1	1.0017	0.1975
		Bias=None, P=0.4, RM=2	1.0017	0.172
	MVE	T=0.9, Run=2	1.0631	0.000
		T=0.99, Run=2	1.0630	0.000
		T=0.95, Run=2	1.0622	0.000
		T=0.99, Run=1	1.0619	0.000
		T=0.99, Run=5	1.0616	0.000
Model Transfer: G	BRT	PA-2, TC=5, LR=0.0025, BF=0.6	1.0276	0.000
		PA-2, TC=3, LR=0.001, BF=0.7	1.0259	0.000
		PA-2, TC=3, LR=0.001, BF=0.6	1.0255	0.000
		PA-2, TC=4, LR=0.001, BF=0.6	1.0251	0.000
		PA-2, TC=3, LR=0.0025, BF=0.5	1.0240	0.000
	Maxent	Bias=Log2, P=0.7, RM=2	1.1287	0.000
		Bias=Log2, P=0.3, RM=2	1.1083	0.000
		Bias=Log2, P=0.5, RM=2	1.0913	0.000
		Bias=Log2, P=0.5, RM=1.5	1.0833	0.000
		Bias=Log2, P=0.7, RM=1.5	1.0711	0.000
	MVE	T=0.9, Run=3	1.0631	0.000
		T=0.95, Run=4	1.0615	0.000
		T=0.9, Run=4	1.0615	0.000
		T=0.95, Run=3	1.0588	0.000
		T=0.9, Run=2	1.0576	0.000
Model Transfer: P	BRT	PA-2, TC=1, LR=0.005, BF=0.6	1.0592	0.000
		PA-2, TC=2, LR=0.005, BF=0.5	1.0530	0.000
		PA-2, TC=1, LR=0.005, BF=0.5	1.0465	0.000
		PA-2, TC=1, LR=0.01, BF=0.5	1.0361	0.002
		PA-2, TC=5, LR=0.0025, BF=0.5	1.0233	0.000
	Maxent	Bias=None, P=0.9, RM=1	1.0848	0.000
		Bias=Raw, P=0.7, RM=1	1.0707	0.000
		Bias=Raw, P=0.7, RM=1.5	1.0660	0.000
		Bias=Raw, P=0.7, RM=2	1.0651	0.000
		Bias=Raw, P=0.5, RM=2	1.0649	0.000
	MVE	T=0.9, Run=1	1.0327	0.021
		T=0.95, Run=1	1.0322	0.0215
		T=0.99, Run=1	1.0322	0.0265
		T=0.99, Run=2	1.0319	0.0255
		T=0.9, Run=3	1.0316	0.0215
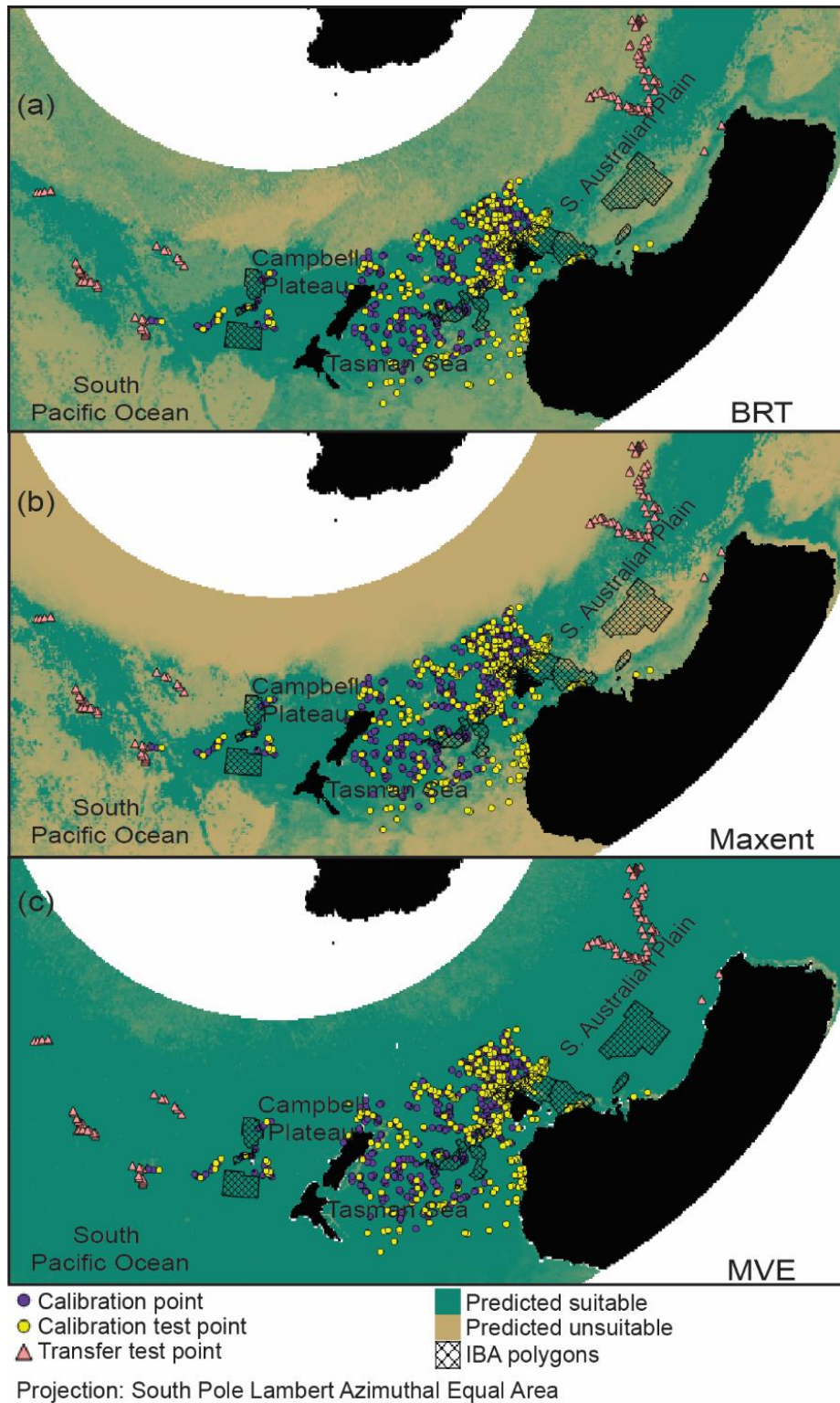
Figure S2.1. Season I projections for each algorithm: (a) BRT, (b) Maxent, and (c) MVE overlaid with *Diomedea exulans* IBAs in waters around Australia and New Zealand. Base layer: Global Administrative Areas global shapefile (http://www.gadm.org).
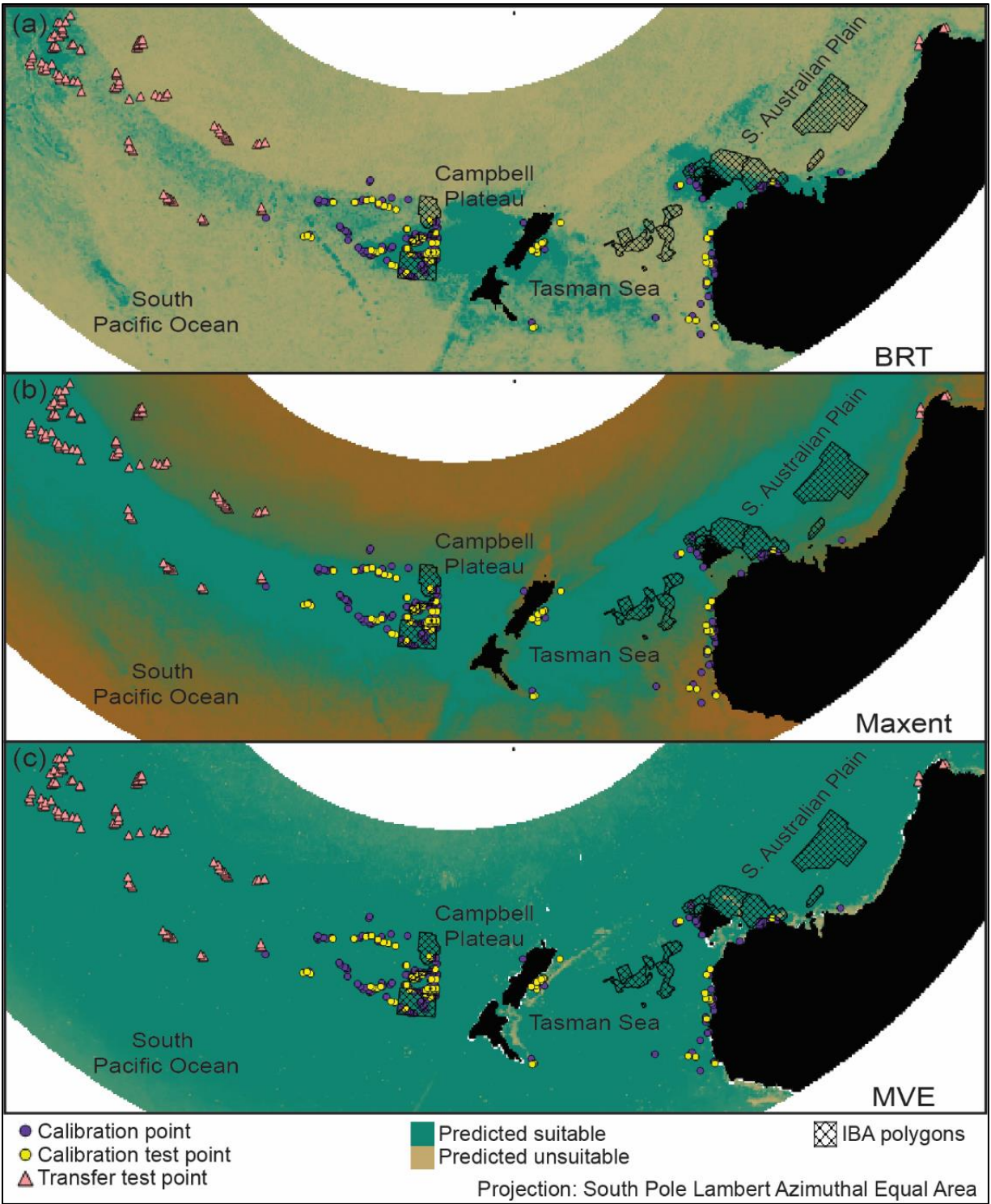
Figure S2.2. Season G projections for each algorithm: (a) BRT, (b) Maxent, and (c) MVE overlaid with *Diomedea exulans* IBAs in waters around Australia and New Zealand. Base layer: Global Administrative Areas global shapefile (http://www.gadm.org).
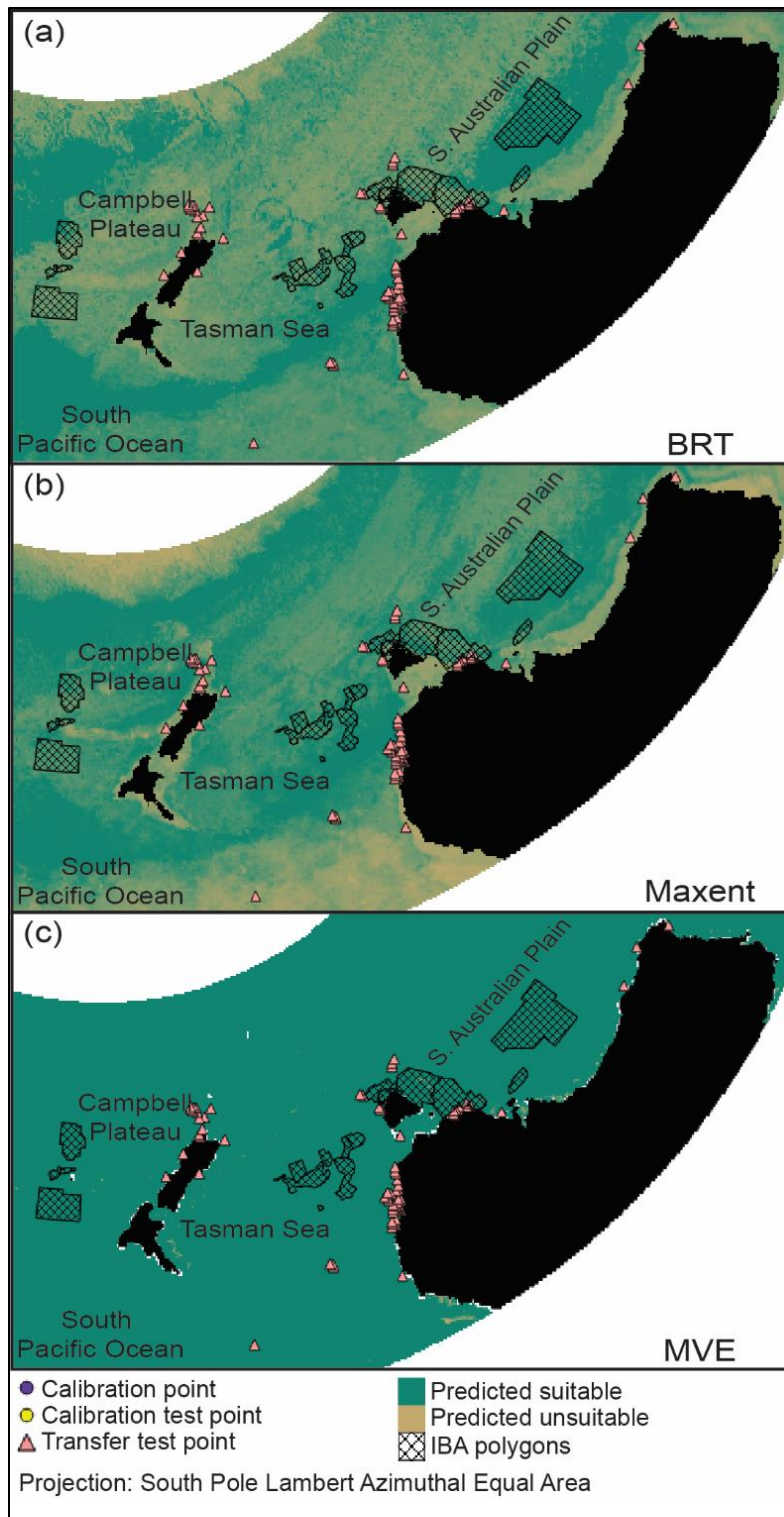
Figure S2.3. Season P projections for each algorithm: (a) BRT, (b) Maxent, and (c) MVE overlaid with *Diomedea exulans* IBAs in waters around Australia and New Zealand. Base layer: Global Administrative Areas global shapefile (http://www.gadm.org).
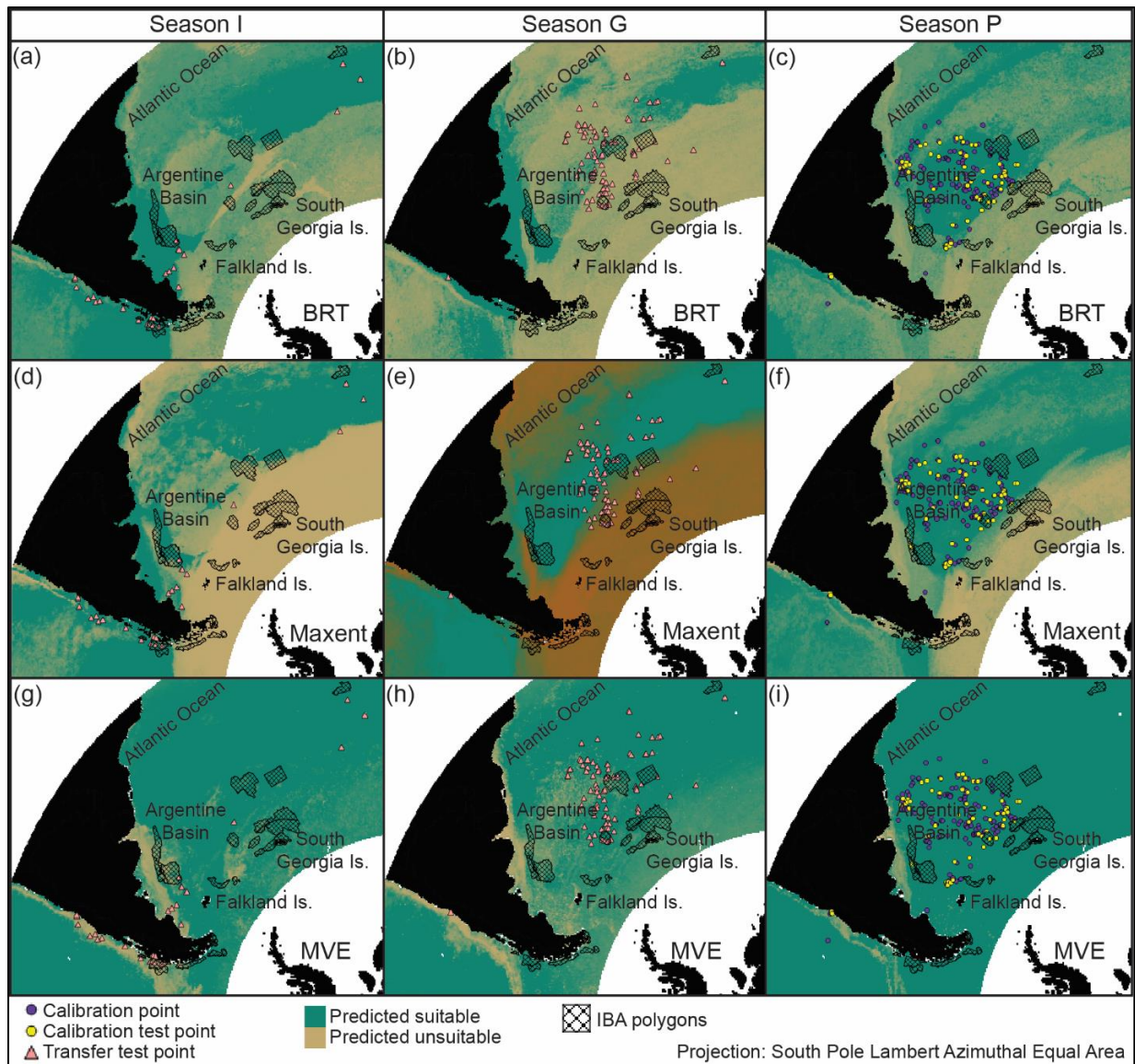
Figure S2.4. Binary model predictions for *Diomedea exulans* in the waters east of southern South America for (a,d,g) season I, (b,e,h) season G, and (c,f,i) season P for (a–c) BRT, (d–f) Maxent, and (g–i) MVE. Base layer: Global Administrative Areas global shapefile (http://www.gadm.org).
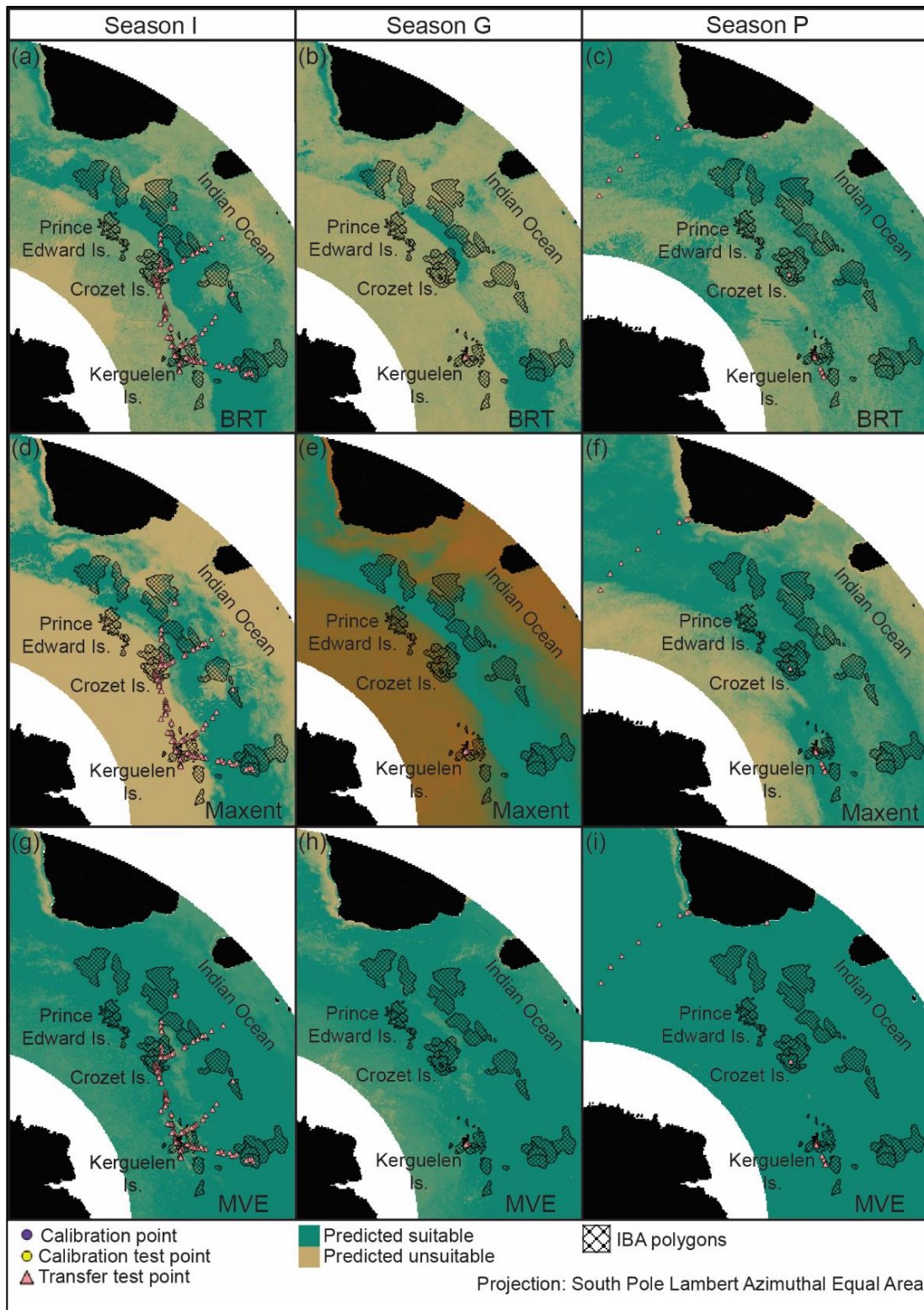
Figure S2.5. *Diomedea exulans* IBAs in marine regions southeast of southern Africa for (a,d,g) for season I, (b,e,h) season G, and (c,f,i) season P by algorithm: (a-c) BRT (d-f) Maxent (g-i) MVE. Base layer: Global Administrative Areas global shapefile (http://www.gadm.org).

REFERENCES

Birdlife International and NatureServe. (2015) Marine IBA e-Atlas: http://maps.birdlife.org/marineIBAs/default.html

Birdlife International and NatureServe. (2016) Marine IBAs. Birdlife International, Cambridge, UK and NatureServe, Arlington, USA.

APPENDIX S3 R Scripts

\# --------------------Fitting Minimum Volume Ellipsoids as Niche Models--------------------
\# Original code provided by Jorge Soberón, August 2015
\#\# Minimum Volume Ellipsoids (MVE) can be used as niche models, mostly when one is
interested in fitting a niche not too constrained by the details of the observed data. To do this,
we must (1) calculate ellipsoids, and (2) calculate, for all pixels in a region of interest, the
environmental distance of each pixel to a centroid of the ellipse.
\#\# Ellipsoids can be calculated in many dimensions, and are characterized by a centroid and by a
matrix (symmetric) that describes the directions of the axes and their lengths.

\# load required libraries
```
library(raster)
library(sp)
library(rgdal)
library(maptools)
library(MASS)
library(foreign)
```

\# Define the Mahalanobis function that calculates the distance from a point ('p') to an ellipse of
centroid ('m') and matrix ('s'). The parameters then are: *p*, the test point, *m*, the centroid of the
ellipse (of a distribution), and *s,* which is the INVERSE of the covariance matrix of the ellipse.
```
maja = function(p, m, s)((p - m)%*%s%*%t(p - m))^0.5;
```

\# --------------- DATA PREPARATION ---------------
\# Set working directory
```
setwd("<path to chosen working directory>");
```

\# load environmental rasters (ASCII format)
```
EnvArchives <- list.files(path = "<path to environmental variables>", pattern = "*.asc$",
full.names = F);
EnvArchives;
```

\# Rasterize and name each environmental variable to be used in analyses
```
V1 = raster(EnvArchives[1]);
V2 = raster(EnvArchives[2]);
V3 = raster(EnvArchives[3]);
V4 = raster(EnvArchives[4]);
V5 = raster(EnvArchives[5]);
…<and so forth>…
```

\# Stack the environmental layers
```
layers = stack(V1, V2, V3, V4, V5, …);
layers;
```

Read in the .csv file containing the 'training points" (species occurrence data to be used in model calibration) and check formatting. The .csv should contain 3 columns: species ID, longitude, and latitude.
```
refined = read.csv("<path to occurrence data file>.csv", header = T);
head(refined);
```

Index by species ID. This is *only* necessary if there are point observation data for multiple species in the .csv.
```
i1 = which(refined[, 1] == "<speciesID>");
i2 = which(refined[, 1] == "<speciesID>");
…
```

Convert to matrix
```
refined = as.matrix(refined[, 2:3]);
```

Extract the values of the environmental variables (using the raster stack) to the observation points. NOTE: specifying 'i#' here is not necessary if the occurrence data file only includes one species.
```
vars = extract(layers, refined[i1, 2:3]);
crds_vrs = cbind(refined, vars);
```

check that the new matrix contains SpeciesID, longitude, latitude, and extracted environmental data for each point
```
head(crds_vrs);
```

--------------- CALCULATING MVEs ---------------
Define the function to calculate the number of points to be included in MVE calculation. NOTE: "nD" designates the species (i.e., 'i1') and 'level' designates the model threshold.
```
NDquantil = function(nD, level) return(round(nD * level/1))
```

Specify the species, assign a threshold, and calculate the number of points to include in analyses. In the code below, the threshold is 0.95, or E = 5%. What you're doing here calculating the number of occurrence points for species 'il' excluding the most extreme 5%, which will then be used to generate the minimum volume ellipsoids to be used in model calibration.
only one species in occurrence dataset
```
n1 = NDquantil(refined, 0.95);
n1;
```

for occurrence datasets with multiple species, run a count for each species
```
n1 = NDquantil(length(i1), 0.95);
n1;
…
```

Generate ellipsoids. Ellipsoids are represented by a (1) centroid and (2) matrix of covariance. NOTE: The values of the highlighted column range below will depend on the number of

environmental variables to be extracted. The range below (4:8) indicate that ellipsoids are being generated based on 5 variables.

only one species in occurrence dataset
```
mve1 = cov.mve(crds_vrs[i1, 4:8], quantile.used = n1);
```

for occurrence datasets with multiple species, run a count for each species
```
mve1 = cov.mve(crds_vrs[i1, 4:8], quantile.used = n1);
…
```

Create a matrix of the covariances
```
mu1 = matrix(mve1$center, nrow=1);
```

Take the inverse of the covariances
```
invs1 = solve(s1);
```

--------------- MODEL CALIBRATION ---------------
To proceed with model calibration, you must first generate a regular grid (a.k.a., "fishnet") of the training/calibration region. QGIS is highly recommended for this process because it is (a) non-proprietary (read, open-source), and (b) a lot more efficient in this process than the competing ESRI product.
NOTE: The grid must be set to match the spatial resolution of the environmental data; be sure to add XY coordinates to labels. The resulting .dbf will be used to then apply the defined ellipsoids to every point in raster.

---- Creating the regular grid in QGIS (v 2.8.2 Wien):
  # [1] Load one of the environmental rasters that will be used in analyses
  # [2] Navigate to: Vector → Research Tools → Vector Grid
  # [3] Set the "Grid extent" to match the environmental raster
  # [4] Check "Align extents and resolution to selected raster layer"
  # [5] Select "Update extents from layer"
  # [6] Check "Output grid as polygons"
  # [7] Assign a name to and pathway to the output shapefile
  # [8] Press "OK" … processing does take a few minutes with processing time increasing as resolution and geographic area increase.

Read in regular grid .dbf file for the calibration region
```
randT = read.dbf("<path to regular grid of calibration region>.dbf");
head(randT); # check that the grid read in properly (e.g., the longitude and latitude are there)
```

Extract environmental data from the raster stack to the calibration region grid. NOTE: there will be A LOT will be NAs.
```
vrsT = extract(layers, randT[, 2:3]);
head(vrsT); # check that everything read in and extracted properly
```

For shits and giggles, you can calculate the percentage of NAs…
```
vrsTsna = na.omit(vrsT);
pNA = dim(vrsTsna) / TotalNumberPixelsInGrid;
```

```
pNA;
```

Create the matrix that will contain the distance of environment to centroid. The matrix size will be [Total number of pixels in grid x 1].
```
dT1 = matrix(0, ncol = 1, nrow = TotalNumberPixelsInGrid);
```

Calculate environmental distance of each ellipsoid from the centroid
```
for(i in 1:TotalNumberPixelsInGrid)dT1[i, 1] = maja(vrsT[i, ], mu1, invs1);
```

Check that it worked. The resulting table should have the following: longitude, latitude, one column for each environmental variable, and a column for dT1.
```
Mcalib = cbind(randT, vrsT, dT1);
head(Mcalib);
```

You're more than halfway through your application of MVEs to ENM approaches! Save model calibration in .csv to the path or your choosing then continue on to the final step of the process—model projection.
```
write.csv(Mcalib, "<YourAwesomeMVEmodelCalibrationFilenameHere.csv>");
```


--------------- MODEL PROJECTION ---------------
Again, a regularized grid is necessary to apply the defined ellipsoids to every point in the projection region.
If the model projection region is geographically different from the model calibration region, create a regularized grid of the full projection region at the spatial resolution of the environmental data (remember to add XY coordinates to labels).
If the model projection region is geographically the same as the model calibration region (e.g., if model projection is to different time periods only), you can use the same grid generated for model calibration.

Read in the regular grid
```
randT_fullproj = read.dbf("<path to regular grid of projection area>.dbf");
```

Extract environmental data from the raster stack to the calibration region grid. NOTE: there will be A LOT will be NAs.
```
vrsT_fullreg = extract(layers, randT_fullproj[, 2:3]);
head(vrsT_fullreg); # check that everything read in and extracted properly
```

For shits and giggles, let's calculate the percentage of NAs again.
```
vrsTsna_full = na.omit(vrsT_fullreg);
pNA_full = dim(vrsTsna_full) / TotalNumberPixelsInGrid;
pNA_full;
```

Create the matrix that will contain the distance of environment to centroid. The matrix size will be equivalent to the dimension of 'randT_fullproj' (e.g., TotalNumberPixelsInGrid x 1).
```
dT_full = matrix(0, ncol = 1, nrow = TotalNumberPixelsInGrid);
```

\# Calculate environmental distance of each ellipsoid from the centroid
```
for(i in 1:TotalNumberPixelsInGrid)dT_full[i, 1] = maja(vrsT_fullreg[i, ], mu1, invs1);
```

\# Check that it worked. The resulting table should have the following: longitude, latitude, one column for each environmental variable, and a column that is dT_full.
```
modProj = cbind(randT_fullproj, vrsT_fullreg, dT_full);
head(modProj);
```

\# Congratulations! You've now completed your application of MVEs to ENM approaches. Save full projection as .csv to the pathway of your choosing!
```
write.csv(modProj, "<YourAwesomeMVEmodelProjectionFilenameHere>.csv");
```

APPENDIX 2: Supplementary Information – Incorporating time into the traditional correlational

distributional modeling framework: a proof-of-concept using the Wood Thrush

(*Hylocichla mustelina*)

Supplementary Information

Authors: Kate Ingenloff (ORCid: 0000-0001-5942-9053) & A. Townsend Peterson (ORCid: 0000-0003-0243-2379)

METHODOLOGY
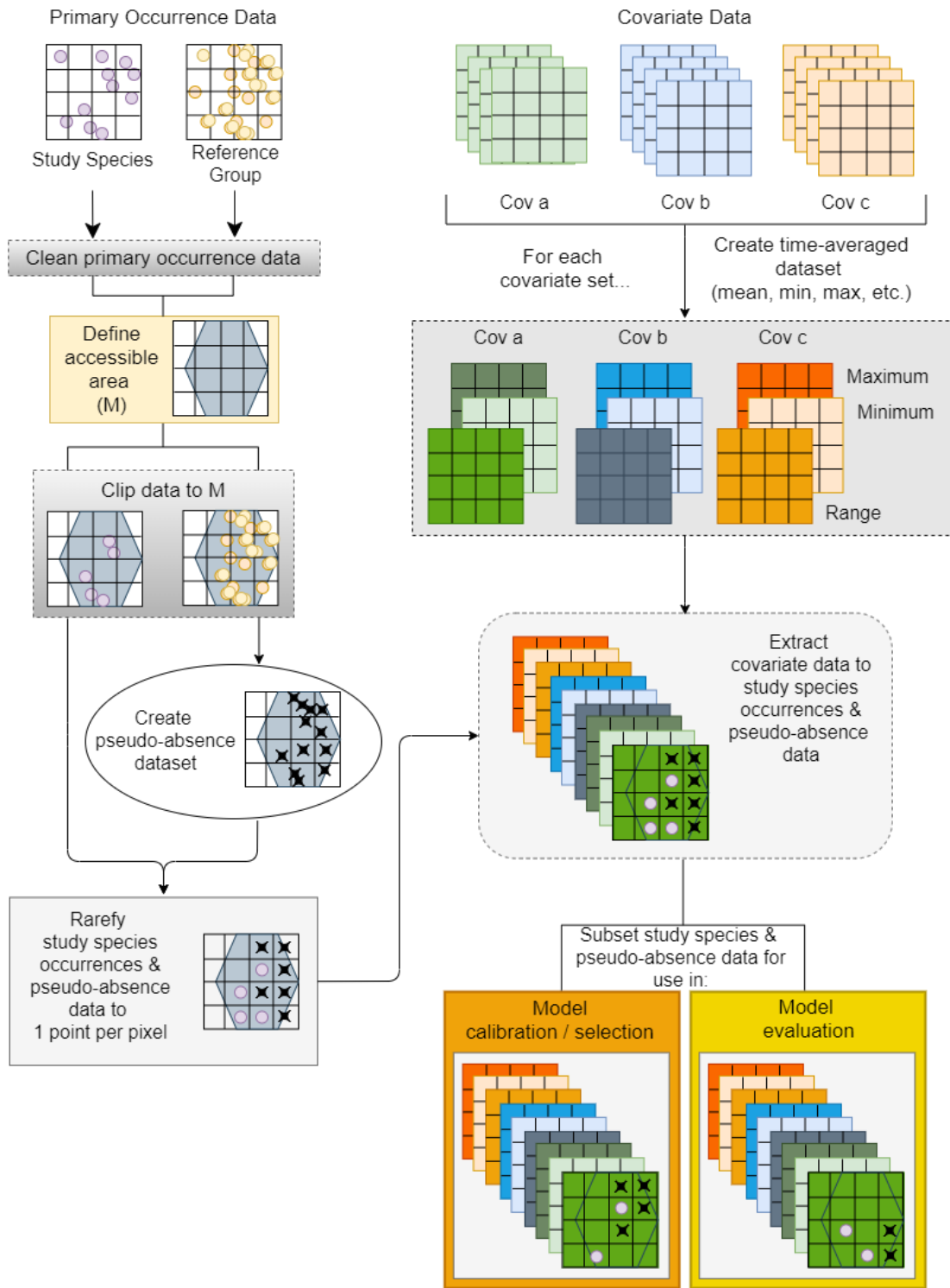
Supplementary Figure 1. Generalized methodological flowchart of the data preparation process in traditional time-averaged correlative modeling approaches.
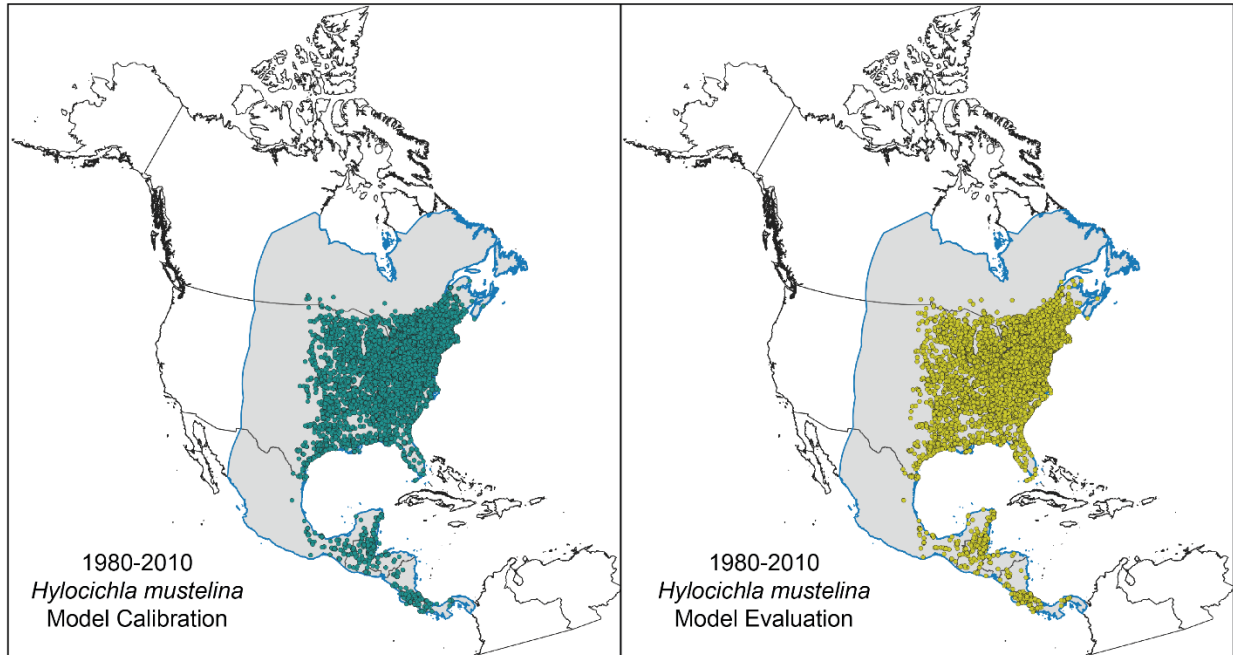
Supplementary Figure 2. Model calibration region (shaded gray, blue outline) overlaid with *Hylocichla mustelina* model calibration (left) and model evaluation (right) occurrences for January 1980 – March 2010. Country outline: Global Administrative Areas version 3.5 (GADM; https://gadm.org/). Projection: North America Lambert Conformal Conic.

Pseudo-absence dataset

Determining the number of pseudo-absences: To determine the total number of pseudo-absences generated for a given time step$_i$, we first calculate the "weight" of the time step (the number of reference group occurrence records in time step$_i$ divided by the number of study species occurrence records in time step$_i$). The calculated 'weight' for the time step is then multiplied by the total number of pseudo-absences desired for the full study period and rounded up to the nearest whole number.

R pseudo-code:

$$\text{Weight} = \text{\# reference group occurrences} / \text{\# study species occurrences}$$

$$\text{\# PAs [time step}_i] = \text{ceiling(weight * total \# of desired pseudo-absence dataset)}$$

For example, time step$_{363}$ (March 2010) had 11,866 Turdidae occurrences and 211 *H. mustelina* occurrences. Thus, the 'weight' to be used in calculated the number pseudo-absences to be sampled for time step$_{363}$ was 0.00393977. Because we sought to generate a pseudo-absence dataset approximately double the *H. mustelina* presence dataset, the total number of pseudo-absences created equaled the weight for time step 363 (0.00393977) multiplied by the total number of desired pseudo-absences (867,296) and rounded up to the nearest whole number, or 3,417.

$$\text{Weight} = 11,866 / 211$$
$$\text{[time step}_{363}] = 0.00393977$$

$$\text{\# PAs} = 0.00393977 * 867,296$$
$$\text{[time step}_{363}] = \text{ceiling}(3,416.94676)$$
$$= 3,417$$
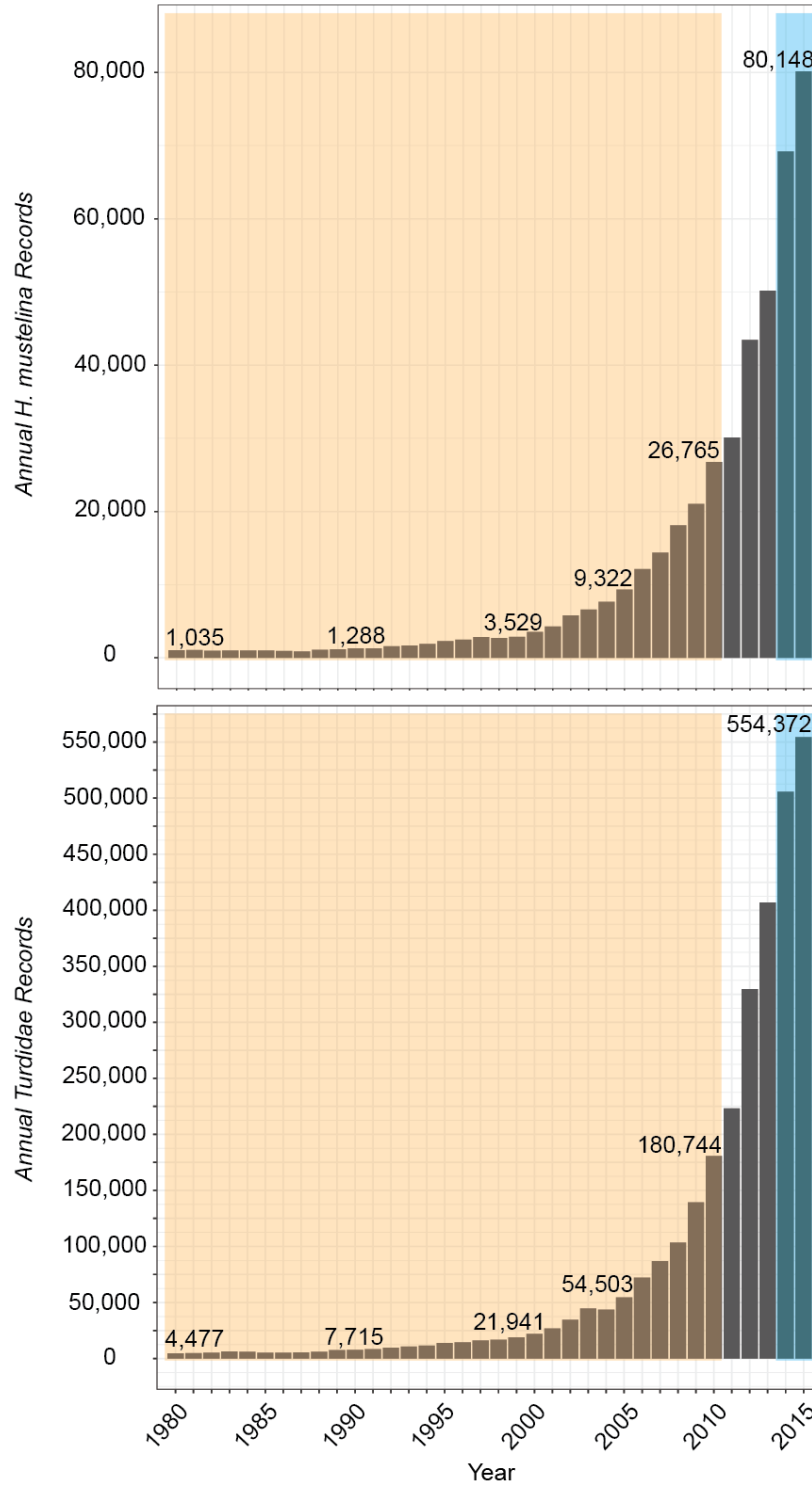
Supplementary Figure 3. Total annual *Hylocichla mustelina* (top) and Turdidae (bottom) observations 1980–2015 within the study area. Color blocks denote the January 1980 – March 2010 study period (tan) and supplemental 2014–2015 model evaluation period (blue).
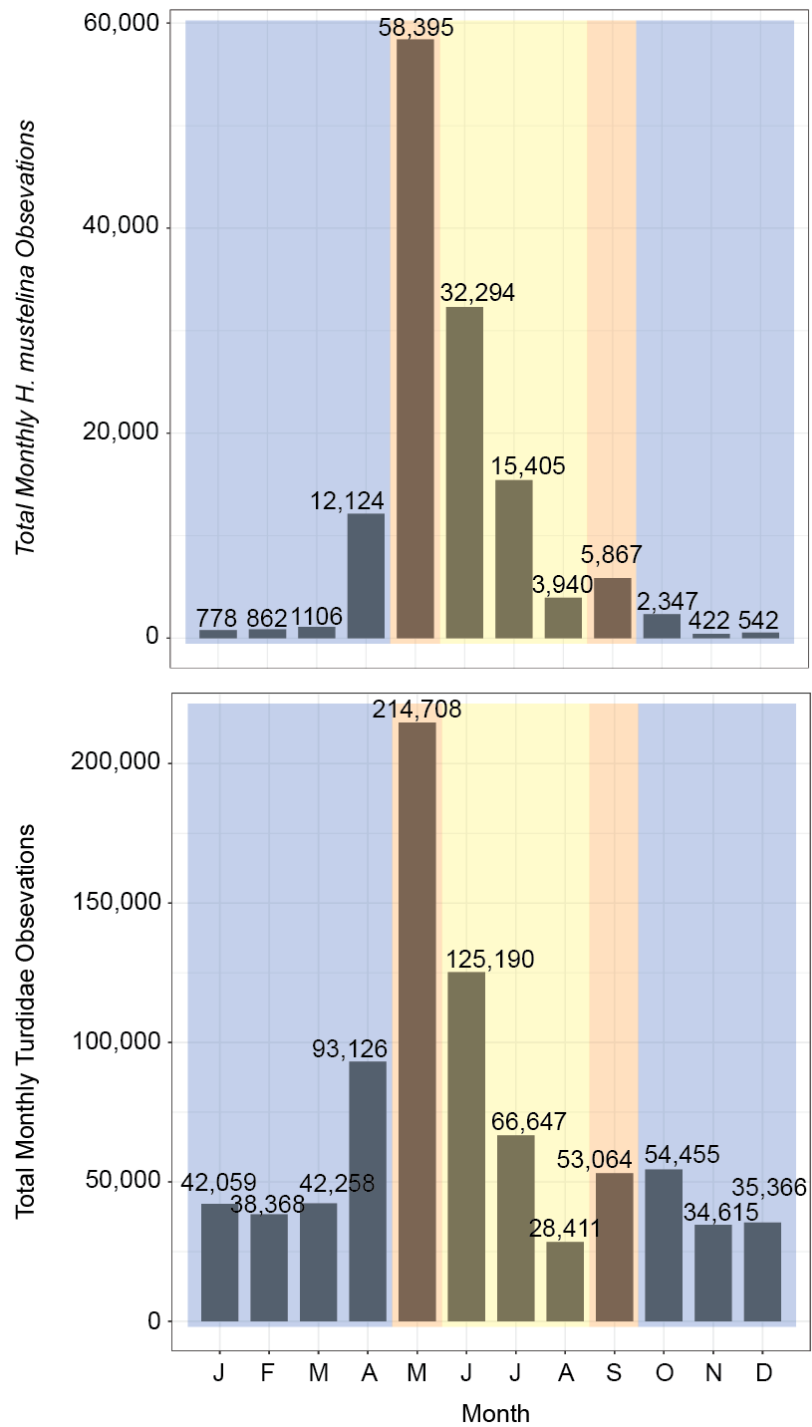
Supplementary Figure 4. Total monthly *Hylocichla mustelina* (top) and Turdidae (bottom) observations (1980–2010) within the study area. Color blocks denote season relative to *H. mustelina* behavior: breeding (yellow), migration (orange), and wintering/non-breeding (blue).

Supplementary Table 1. Time steps (months) with no *Hylocichla mustelina* observation data in the core population, and in the rarefied time-averaged and time-specific model evaluation datasets during the 1980–2010 study period.

Month	Core population	Model evaluation data	
		Time-averaged	Time-specific
January		'80, '82, '85, '89, '90	'81–'82, '85, '89
February	'80, '82, '84	'80–'84, '87–'88, '90, '94	'80–'82,'84–'85
March	'84	'83–'84, '86, '88, 2000	'84, '88
October		'83, '92, '95	
November	'81, '84, '86, '88	'81–'91, '93–'94, '98	'80–'82, '84, '86, '89–'88
December	'81–'82, '85, '89, '94	'80–'85, '89, '90, '92–'94, 2001	'81–'83, '85, '87, '89, '91–'92, '94

Supplementary Table 2. Total number of records in the final time-averaged and time-specific *Hylocichla mustelina* and pseudo-absence datasets for the January 1980 – March 2010 study period and the 2014–2015 supplemental model evaluation period.

	Evaluation period	Time-averaged		Time-specific	
		Presences	Pseudo-absences	Presences	Pseudo-absences
Calibration	1980–2010	16,983	102,918	38,011	120,979
Evaluation	1980–2010	16,980	102,918	38,017	120,979
	2014–2015	36,436	–	61,479	–

RESULTS

Supplementary Details: Final model calibration results

The model selection process yielded six final models (three time-averaged and three time-specific). Selected time-averaged models excluded minimum temperature range owing to high correlation with other covariates. The selected BRT model was calibrated at default bag fraction, default learning rate, tree complexity of four, and excluded mean minimum temperature. The GAM model was calibrated with a smoother basis dimension (k) of 25 using the default smoothing parameter estimation method and no covariate interaction. The GLM model was calibrated with pairwise interactions. Selected time-specific models were calibrated with all three time-specific covariates (precipitation, minimum temperature, maximum temperature). The BRT model was calibrated with default bag fraction, default learning rate, and a tree complexity of three. The GAM model was calibrated with a default basis dimension for the smoother, default smoothing parameter estimation method, and full covariate interactions. See the supplementary tables 3 and 4 for explicit time-averaged and time-specific parameter settings for each of the six models.

Supplementary Table 3. Time-averaged model calibration settings for the selected model for each of the three algorithms calibrated.

Time-Averaged	GLM	`m2 <- glm(Presence ~ 1 + meanPPT + meanTMIN + meanTMAX + rangePPT + rangeTMAX,`
		`            family = binomial,  data = p.train);`
		`summary(m2); # AIC 77811`
		`# Deviance Residuals:`
		`#    Min     1Q     Median    3Q     Max`
		`# -2.4563  -0.5435  -0.3088  -0.1691   7.6034`
		
		`# Coefficients:`
		`#              Estimate     Std. Error  z value     Pr(>|z|)`
		`# (Intercept)    -3.0904348  0.1367030  -22.61   <2e-16 ***`
		`# meanPPT     0.0585929   0.0007026   83.39   <2e-16 ***`
		`# meanTMIN   0.4954462   0.0088365   56.07   <2e-16 ***`
		`# meanTMAX  -0.2490662   0.0068807  -36.20   <2e-16 ***`
		`# rangePPT     -0.0198802   0.0002183  -91.08   <2e-16 ***`
		`# rangeTMAX   0.0957327   0.0026304   36.39   <2e-16 ***`
		
		`# Null deviance: 97823  on 119900  degrees of freedom`
		`# Residual deviance: 77799  on 119895  degrees of freedom`
		
		`var.m2 <- (1 - (m2$deviance / m2$null.deviance)) * 100;`
		`var.m2; # total variation explained by the model: 20.46986%`

	GAM	`model <- gam(Presence ~ 1 + s(meanPPT, k=25) + s(meanTMIN, k=25) + s(meanTMAX, k=25)`
		`+`
		`            s(rangePPT, k=25) + s(rangeTMAX, k=25),`
		`            family = binomial, data = p.train, select = TRUE);`
		
		`summary(model);`
		`# R-sq.(adj) =  0.358   Deviance explained = 41.2%`
		`# -ML =  29010  Scale est. = 1        n = 119901`

	BRT	`model <- gbm.step(data = p.train, gbm.x = c(5:8),  gbm.y = 1,`
		`            family = "bernoulli",  tree.complexity = 4); # bf default`
		
		`Training MSE;   # 0.283373`
		`Test MSE;    # 0.284127`
		`Test OR;    # 99.99% (MTP)     94.89% (E=5%)      89.9% (E=10%)`
		
		`summary(model)`
		`#                 var          rel.inf`
		`# meanTMAX    meanTMAX     42.91145`
		`# meanPPT       meanPPT        32.06410`
		`# rangeTMAX    rangeTMAX     13.61995`
		`# rangePPT       rangePPT        11.40451`

Supplementary Table 4. Time-specific model calibration settings for the selected model for each of the three algorithms calibrated.

Time-Specific	GLM	model <- glm(Presence ~ 1 + ppt + tmin + tmin:ppt + tmax:ppt + tmax:tmin,
		      family = "binomial", data = p.train);
		summary(model);
		# Deviance Residuals:
		# Min 1Q Median 3Q Max
		# -2.2953 -0.7595 -0.2016 0.0000 3.9889
		
		# Coefficients:
		# Estimate Std. Error z value Pr(>|z|)
		# (Intercept) -5.075e+00 4.322e-02 -117.43 <2e-16 ***
		# ppt -7.278e-03 6.565e-04 -11.09 <2e-16 ***
		# tmin 1.127e+00 9.106e-03 123.72 <2e-16 ***
		# ppt:tmin -1.780e-03 4.125e-05 -43.15 <2e-16 ***
		# ppt:tmax 1.249e-03 4.072e-05 30.66 <2e-16 ***
		# tmin:tmax -2.910e-02 2.567e-04 -113.37 <2e-16 ***
		# ---
		# Signif. codes: 0 '***' 0.001 '**' 0.01 '*' 0.05 '.' 0.1 ' ' 1
		
		#(Dispersion parameter for binomial family taken to be 1)
		
		# Null deviance: 174894 on 158989 degrees of freedom
		# Residual deviance: 128248 on 158984 degrees of freedom
		# AIC: 128260
		
		#Number of Fisher Scoring iterations: 8
		
		# calculate variance explained by the model
		model2 <- (1 - (model$deviance / model$null.deviance)) * 100;
		model2; # total variation explained by the model: 26.67086

	GAM	model <- gam(Presence ~ 1 + s(ppt, k=25) + s(tmin, k=25) + s(tmax, k=25), family = binomial, data = p.train, select = T); # summary(model); # R-sq.(adj) = 0.268 Deviance explained = 28.9% # UBRE = -0.2177 Scale est. = 1 n = 158990 AIC(model); # 124378.3

	BRT	model <- gbm.step(data = p.train,
		      gbm.x = c(5:7), gbm.y = 1,
		      family = "bernoulli", tree.complexity = 3, bag.fraction = 0.5);
		
		Training MSE; # 0.318984971903624
		Testing MSE; # 0.322308923380982
		Test OR; # 99.99% (MTP) 94.76% (E=5%) 89.54% (E=10%)
		
		summary(model);
		# var rel.inf
		# tmin tmin 59.18960
		# tmax tmax 27.18494
		# ppt ppt 13.62546

Supplementary Table 5. Percentage of model calibration area predicted suitable for time-averaged and time-specific models for the January 1980 – March 2010 primary study period and the 2014–2015 supplemental evaluation period.

	Model	Evaluation period	Minimum	Maximum	Median	Average
Time-averaged	BRT	1980–2010	–	–	–	32.8%
		2014–2015	–	–	–	36.9%
	GAM	1980–2010	–	–	–	36.6%
		2014–2015	–	–	–	42.3%
	GLM	1980–2010	–	–	–	39.3%
		2014–2015	–	–	–	46.4%
Time-specific	BRT	1980–2010	7.8%	92.5%	34.1%	45.2%
		2014–2015	7.1%	88.8%	39.9%	46.5%
	GAM	1980–2010	8.5%	89.9%	34.4%	43.6%
		2014–2015	7.9%	91.8%	42.1%	48.7%
	GLM	1980–2010	10.0%	97.3%	40.0%	50.1%
		2014–2015	9.1%	94.1%	45.7%	51.2%

Supplementary Table 6. Mean omission rates for time-averaged and time-specific models for the January 1980 – March 2010 primary study period and the 2014–2015 supplemental evaluation period.

	Model	Evaluation Period	Mean Omission Rate
Time-Averaged	BRT	1980–2010	0. 037
		2014–2015	0.039
	GAM	1980–2010	0.029
		2014–2015	0.020
	GLM	1980–2010	0.030
		2014–2015	0.020
Time-Specific	BRT	1980–2010	0.210
		2014–2015	0.026
	GAM	1980–2010	0.036
		2014–2015	0.027
	GLM	1980–2010	0.036
		2014–2015	0.025

Supplementary Figure 5. Monthly omission rates for time-averaged (top) and time-specific (bottom) BRT model. Red boxplots indicate 1980–2010 and blue indicate 2014–2015. Color blocks denote season relative to *Hylocichla mustelina* behavior: breeding (yellow), migration (orange), and wintering (blue).
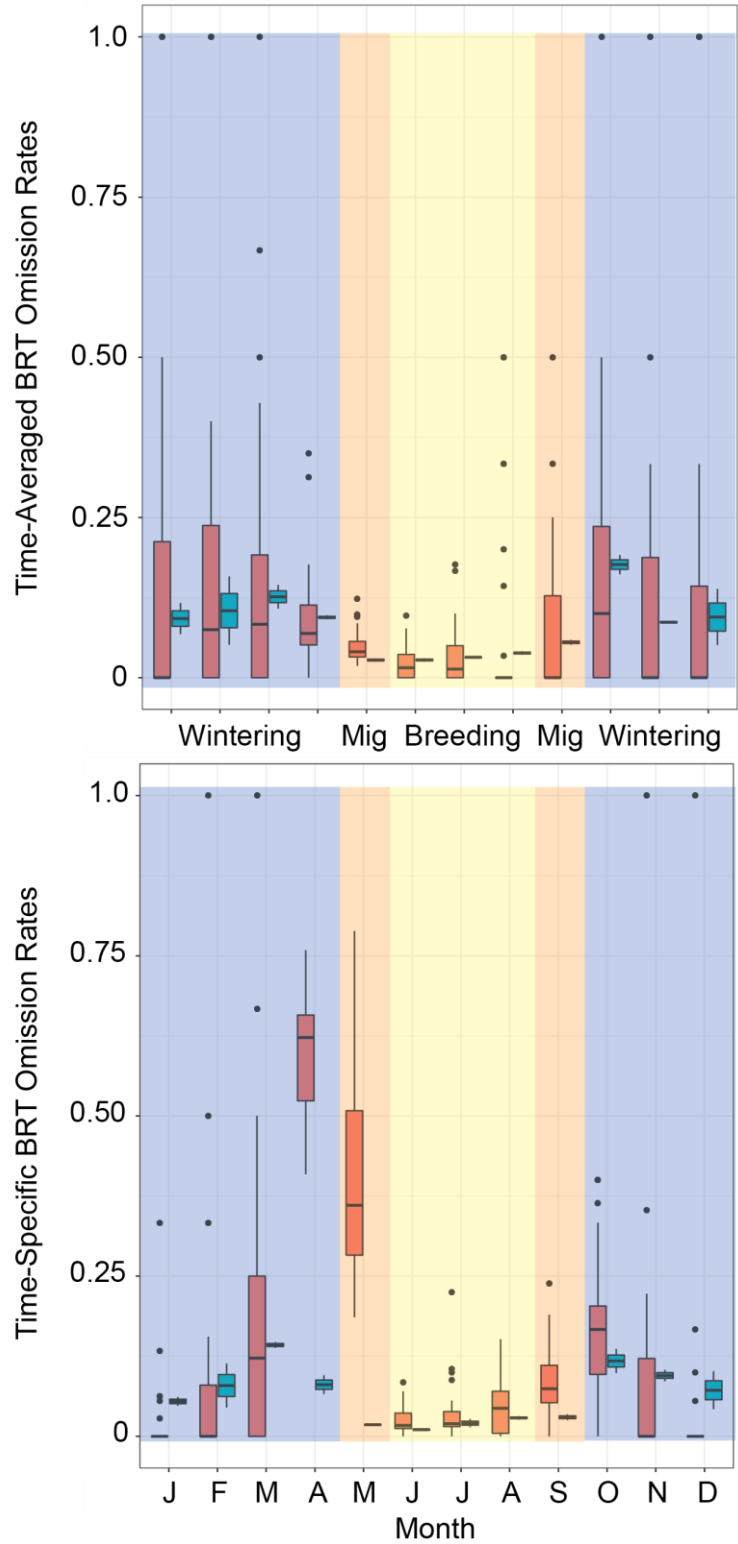
Supplemental Figure 6. Monthly omission rates for time-averaged (top) and time-specific (bottom) GAM models. Red boxplots indicate 1980–2010 and blue indicate 2014–2015. Color blocks denote season relative to *Hylocichla mustelina* behavior: breeding (yellow), migration (orange), and wintering (blue).
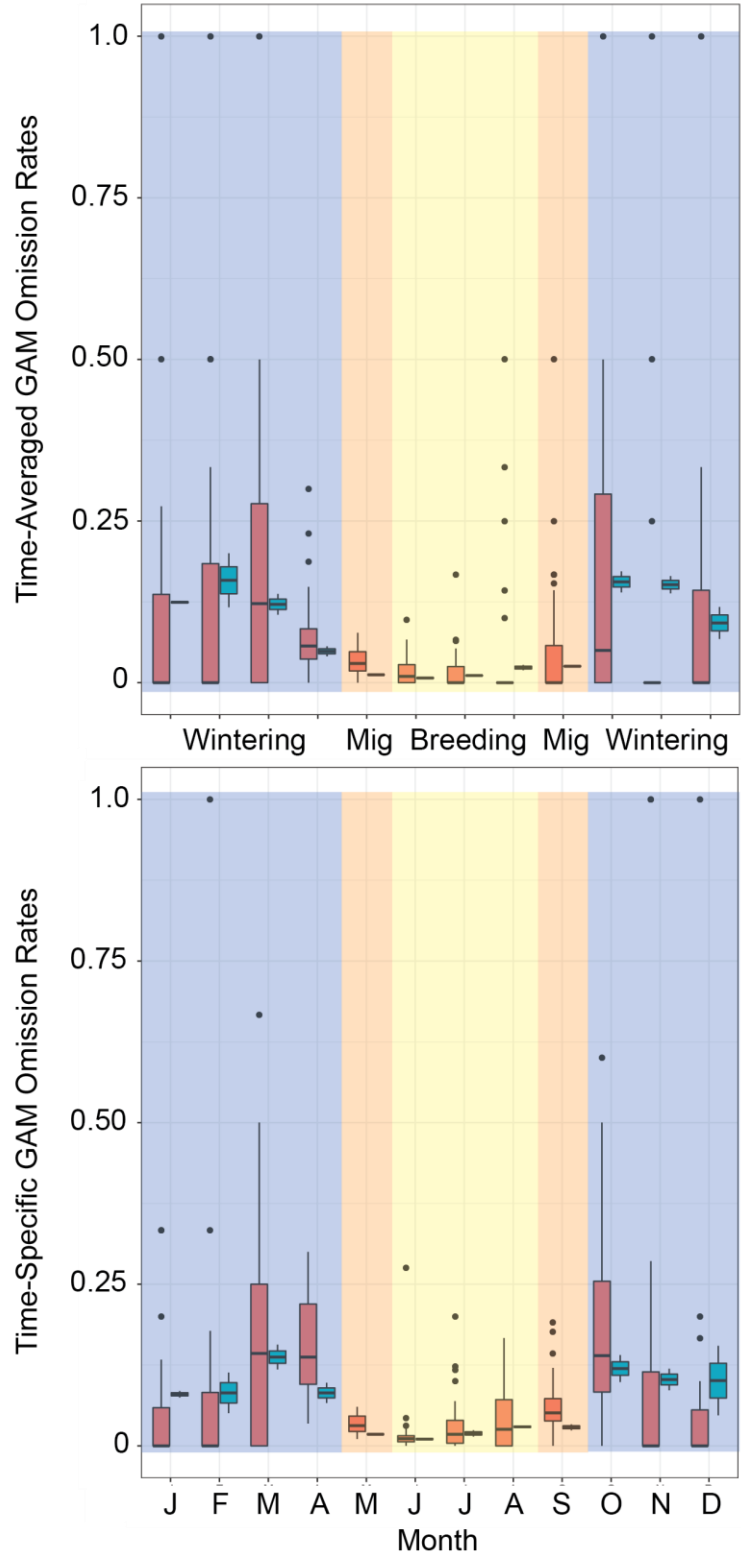
Supplementary Figure 7. Monthly omission rates for time-averaged (top) and time-specific (bottom) GLM model. Red boxplots indicate 1980–2010 and blue indicate 2014–2015. Color blocks denote season relative to *Hylocichla mustelina* behavior: breeding (yellow), migration (orange), and wintering (blue).
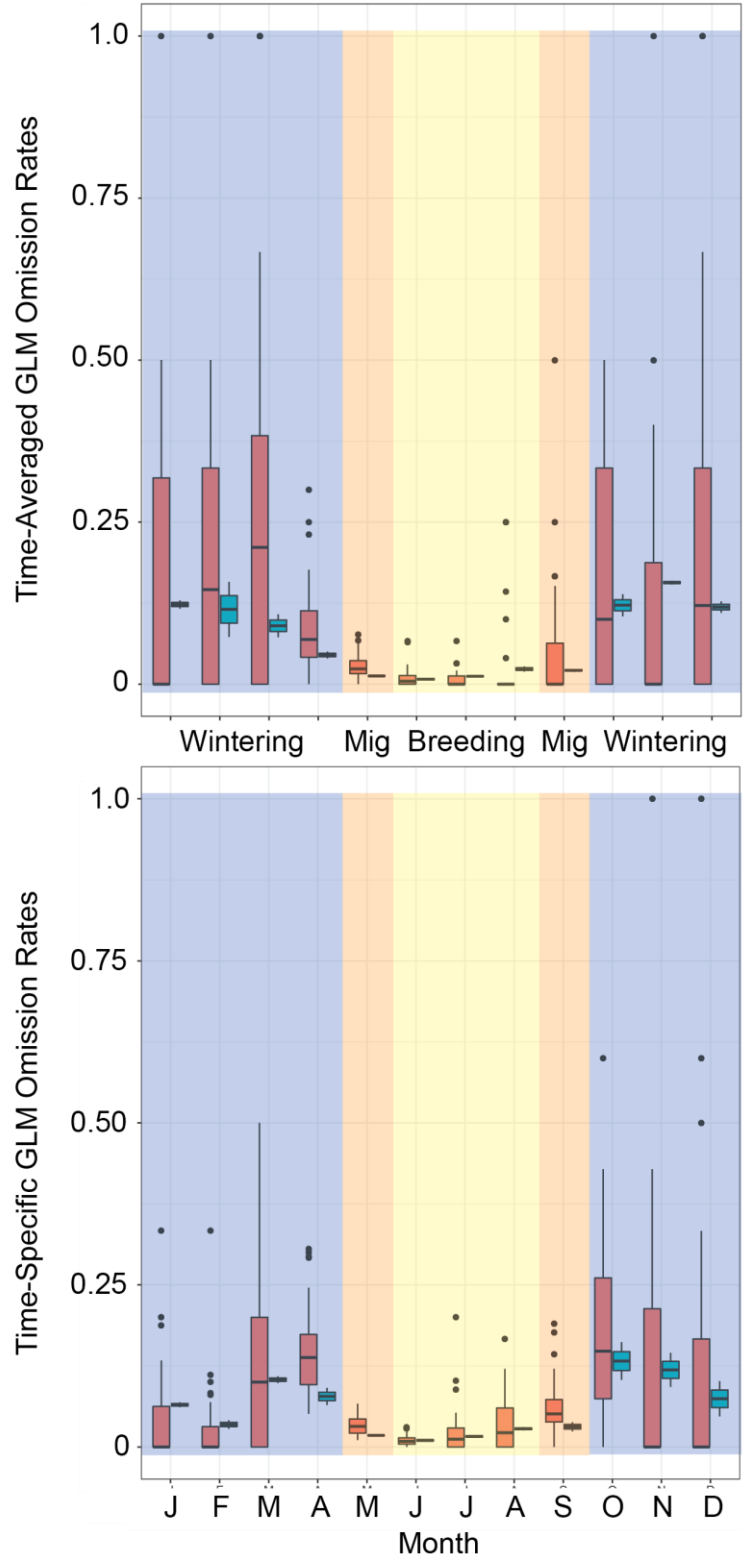
Supplementary Table 7. Seasonal mean monthly omission rate ranges and means for time-averaged and time-specific models for the January 1980 – March 2010 primary study period and the 2014–2015 supplemental evaluation period. Seasonal averages are presented in parentheses below range values.

	Model		Breeding (June–August)	Migratory (May, September)	Wintering (October–April)
Time-averaged	BRT	1980–2010	0.025–0.068 (0.042)	0.048–0.067 (0.057)	0.092–0.184 (0.154)
		2014–2015	0.028–0.055 (0.033)	0.028–0.039 (0.041)	0.087–0.176 (0.111)
	GAM	1980–2010	0.018–0.044 (0.027)	0.034–0.053 (0.043)	0.074–0.178 (0.130)
		2014–2015	0.007–0.023 (0.014)	0.012–0.025 (0.019)	0.049–0.158 (0.122)
	GLM	1980–2010	0.008–0.026 (0.015)	0.029–0.052 (0.041)	0.087–0.283 (0.184)
		2014–2015	0.008–0.023 (0.014)	0.013–0.021 (0.017)	0.045–0.157 (0.110)
Time-specific	BRT	1980–2010	0.026–0.0047 (0.036)	0.086–0.401 (0.244)	0.025–0.591 (0.189)
		2014–2015	0.010–0.029 (0.020)	0.018–0.030 (0.024)	0.054–0.142 (0.092)
	GAM	1980–2010	0.021–0.042 (0.033)	0.034–0.060 (0.047)	0.047–0.185 (0.123)
		2014–2015	0.011–0.030 (0.020)	0.018–0.029 (0.023)	0.080–0.137 (0.101)
	GLM	1980–2010	0.010–0.036 (0.024)	0.033–0.060 (0.046)	0.032–0.179 (0.120)
		2014–2015	0.010–0.028 (0.018)	0.018–0.031 (0.025)	0.035–0.133 (0.087)
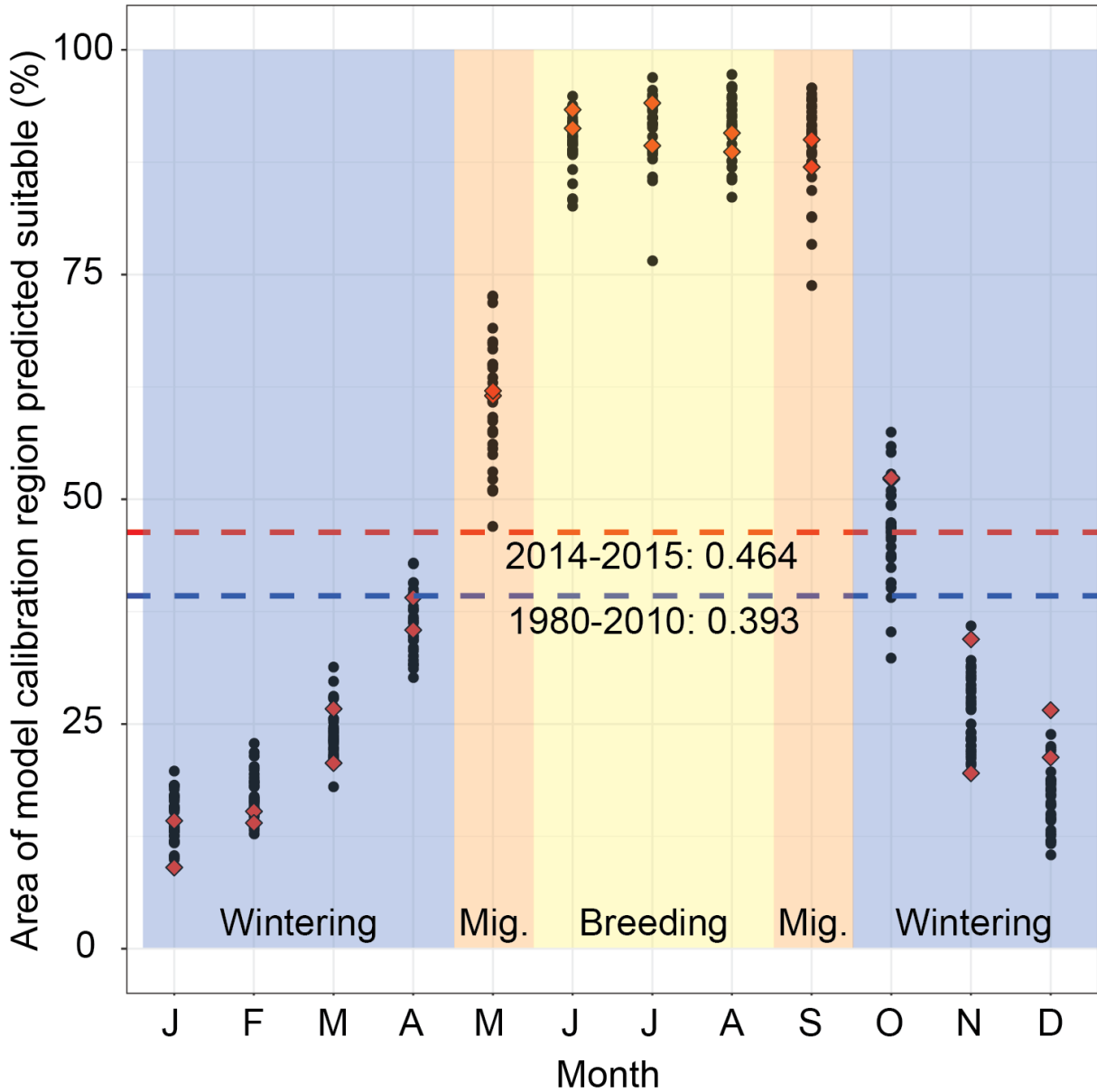
Supplementary Figure 8. Proportion of the study area predicted climatically suitable by GLM models by month. Black points indicate proportion of area predicted suitable for each month for the 1980–2010 study period and red diamonds represent proportion of area predicted suitable for the 2014–2015 model evaluation period for the time-specific model. Dashed lines denote proportion of area predicted suitable for the time-averaged model (blue, 1980–2010; red, 2014–2015). Color blocks denote season relative to *Hylocichla mustelina* behavior: breeding (yellow), migration (orange), and wintering (blue).
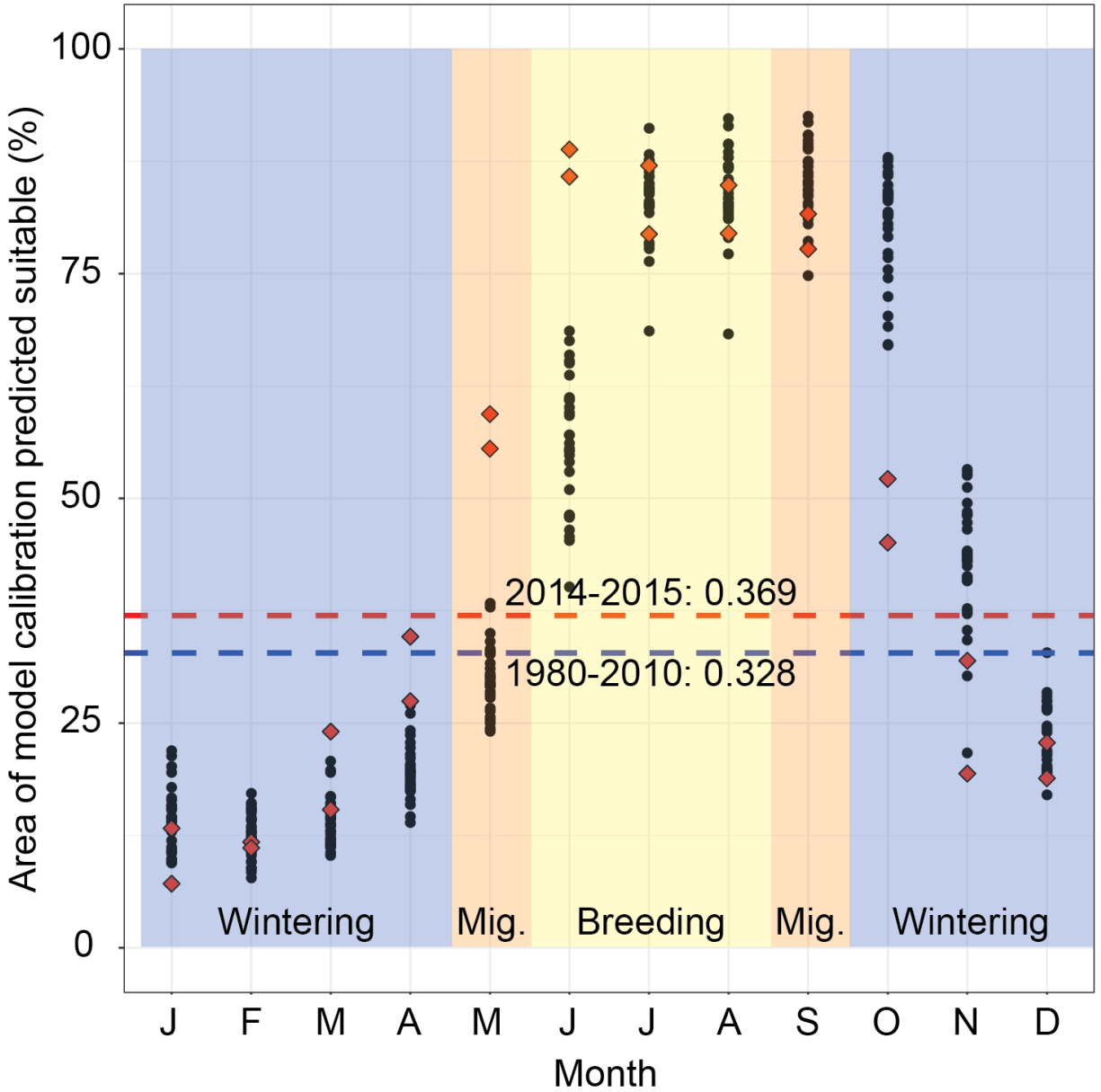
Supplementary Figure 9. Proportion of the study area predicted climatically suitable by BRT model by month. Black points indicate proportion of area predicted suitable for each month for the 1980–2010 study period and red diamonds represent proportion of area predicted suitable for the 2014–2015 model evaluation period for the time-specific model. Dashed lines denote proportion of area predicted suitable for the time-averaged model (blue, 1980–2010; red, 2014–2015). Color blocks denote season relative to *Hylocichla mustelina* behavior: breeding (yellow), migration (orange), and wintering (blue).
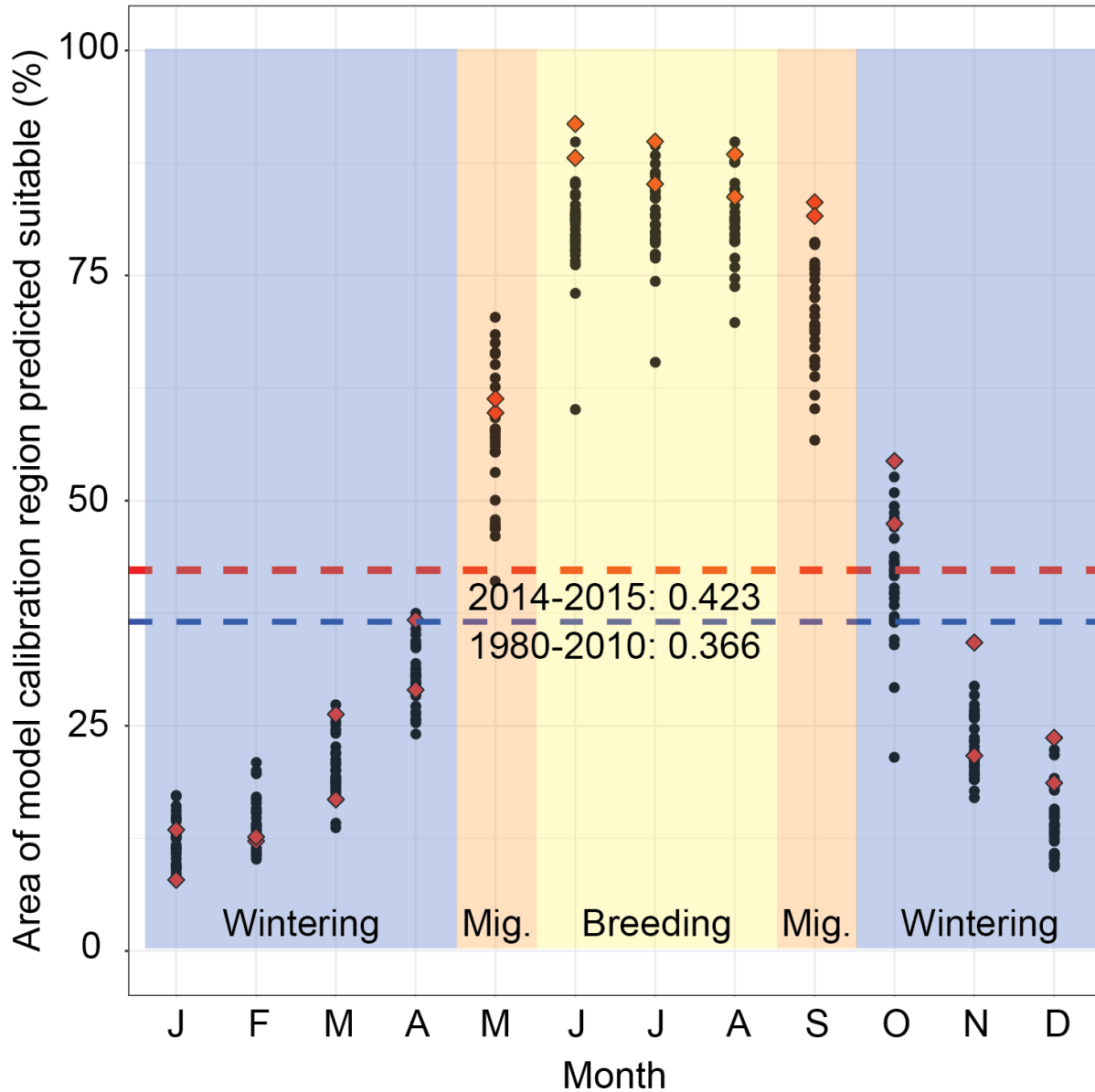
Supplemental Figure 10. Proportion of the study area predicted climatically suitable by GAM models. Black points indicate proportion of area predicted suitable for each month for the 1980–2010 study period and red diamonds represent proportion of area predicted suitable for the 2014–2015 model evaluation period for the time-specific model. Dashed lines denote proportion of area predicted suitable for time-averaged model (blue, 1980–2010; red, 2014–2015). Color blocks denote season relative to *Hylocichla mustelina* behavior: breeding (yellow), migration (orange), and wintering (blue).

Supplementary Table 8. Range of average monthly percentage of study region predicted suitable by season and time-specific algorithm for the January 1980 – March 2010 primary study period and the 2014–2015 supplemental evaluation period. Seasonal averages are presented in parentheses below range values.

Model	Evaluation period	Breeding (June–August)	Migratory (May, September)	Wintering (October–April)
BRT	1980–2010	56.0–94.0% (91.2%)	30.0–85.1% (75.1%)	12.5–80.2% (27.2%)
	2014–2015	82.2–87.3% (84.2%)	57.5–79.7% (68.6%)	10.2–48.6% (23.9%)
GAM	1980–2010	80.1–81.5% (81.0%)	56.7–70.6% (63.7%)	12.4–41.8% (22.2%)
	2014–2015	86.1–90.0% (87.9%)	60.5–82.4% (71.5%)	10.7–50.9% (25.4%)
GLM	1980–2010	89.7–91.6% (90.8%)	60.7–89.6% (75.2%)	14.6–46.4% (25.8%)
	2014–2015	89.7–92.3% (91.2%)	61.8–88.5% (75.1%)	11.6–52.3% (27.2%)

DISCUSSION

Discussion Point – Sample bias (continued)

For example, our *H. mustelina* occurrence data are 'complete' in that ample data are available representing the full geographic distribution of the species. However, there is a strong month-to-month bias in sampling intensity towards migration and breeding periods such that only 18,181 (13.5 %) of the 134,293 *H. mustelina* records available for the 1980–2010 study period were collected during what we loosely categorized as the wintering period (Supp. Fig. 3). Indeed, 47.9% of data (58,395 records) were collected during May alone, a 138-fold increase compared to data available for the month with the least total records (November, 422 records). Our spatial filtering process to one point per pixel (time-averaged) or one point per pixel per time step (time-specific) alleviates some of the spatial bias inherited from the original dataset (Dormann 2007; Phillips *et al.* 2009). This process also offsets some temporal bias by 1) reducing the data such that the time-specific data had a 131-fold difference between the lowest-sampled month (November, 99 records) and the highest-sampled month (May, 12,970 records), and 2) the time-averaged dataset had a 93-fold difference between the cumulative observations in the lowest-sampled month (November, 306 records) and the highest-sampled month (May, 28,601 records). However, the filtering process did not significantly impact the seasonal disparity in sampling intensity with only 13–15% of data in the final time-averaged and time-specific datasets from wintering period. This disparity illustrates the need for further research on accounting for temporal bias to ensure model accuracy.

APPENDIX 3: Supplementary Information – Assessing the utility of time-specific correlative

ecological niche framework to produce dynamic distributional predictions for the

nomadic Wandering Albatross (*Diomedea exulans*)

Authors: Kate Ingenloff (ORCid: 0000-0001-5942-9053) & A. Townsend Peterson (ORCid: 0000-0003-0243-2379)

Input Data
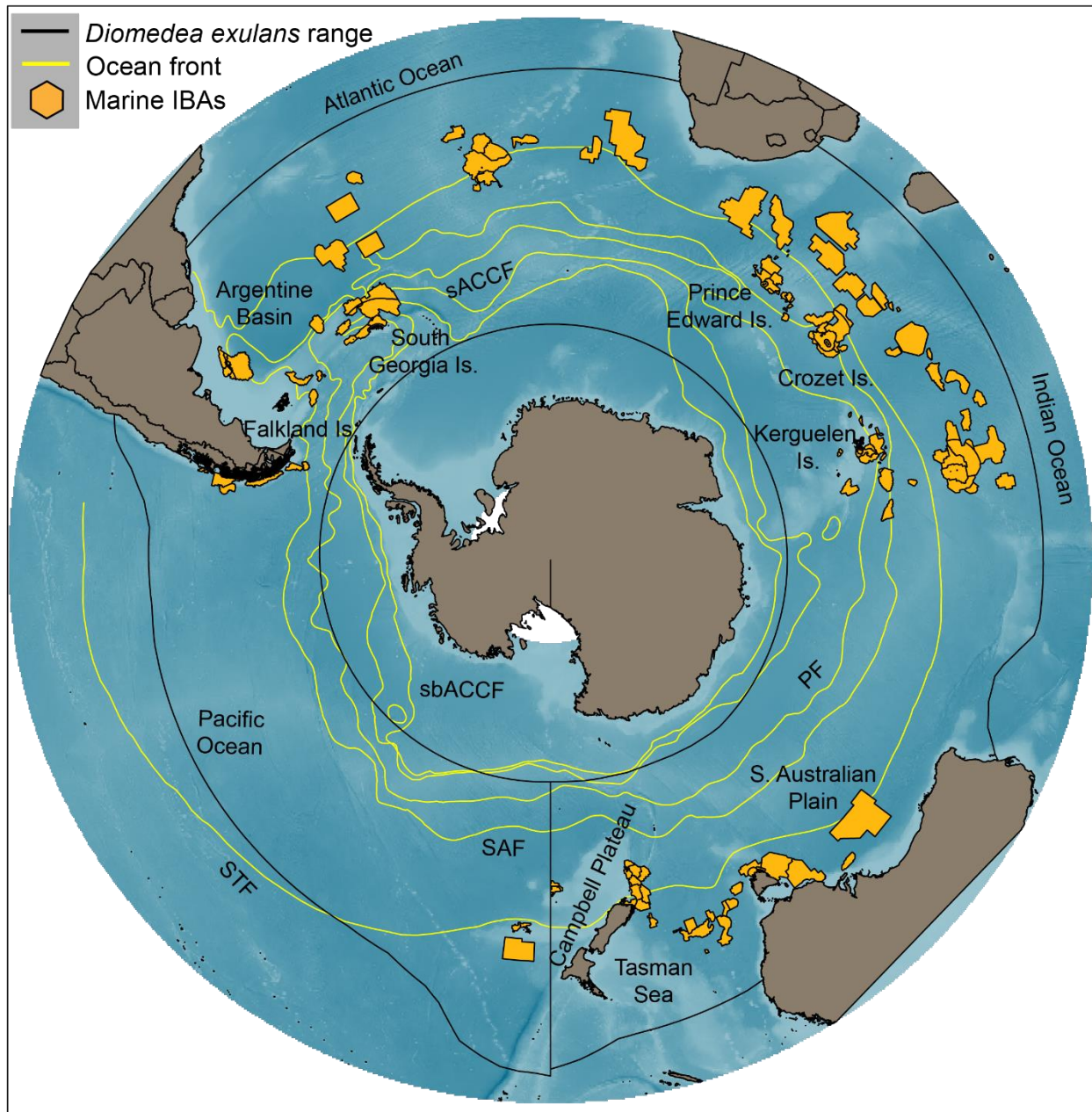
Supplemental Figure 1. Study region overlaid with *Diomedea exulans* range (black outline; BirdLife International and NatureServe 2015), marine IBAs relevant to wandering albatross complex (BirdLife International and NatureServe 2020), and averaged location of the Southern Ocean front lines (yellow lines: STF – subtropical front; SAF – sub-Antarctic front; PF – polar front; sACCF – southern Antarctic Circumpolar Current; sbACCF – southern boundary Antarctic Circumpolar Current; Orsi & Harris 2008).
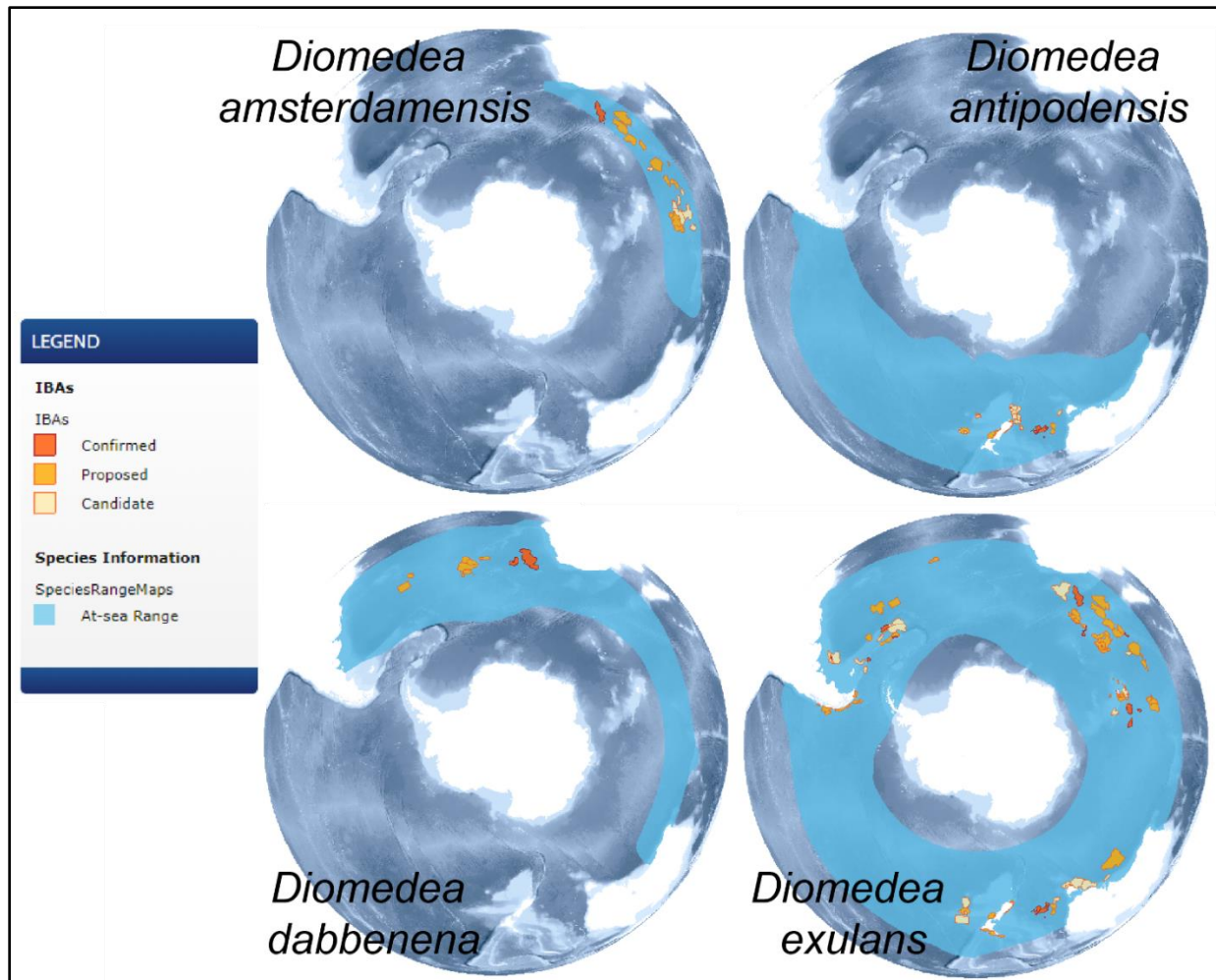
Supplemental Figure 2. At-sea distributions (light blue) and marine important bird areas (IBAs; confirmed IBAs denoted by red polygons, proposed IBAs denoted by orange polygons, and candidate IBAs represented by yellow polygons) for each of the four species in the Wandering Albatross complex: *Diomedea amsterdamensis* (top left), *D. antipodensis* (top right), *D. dabbenena* (bottom left), and *D. exulans* (bottom right). Maps are screenshots obtained from the Birdlife International Marine IBA e-Atlas (BirdLife International and NatureServe 2020).
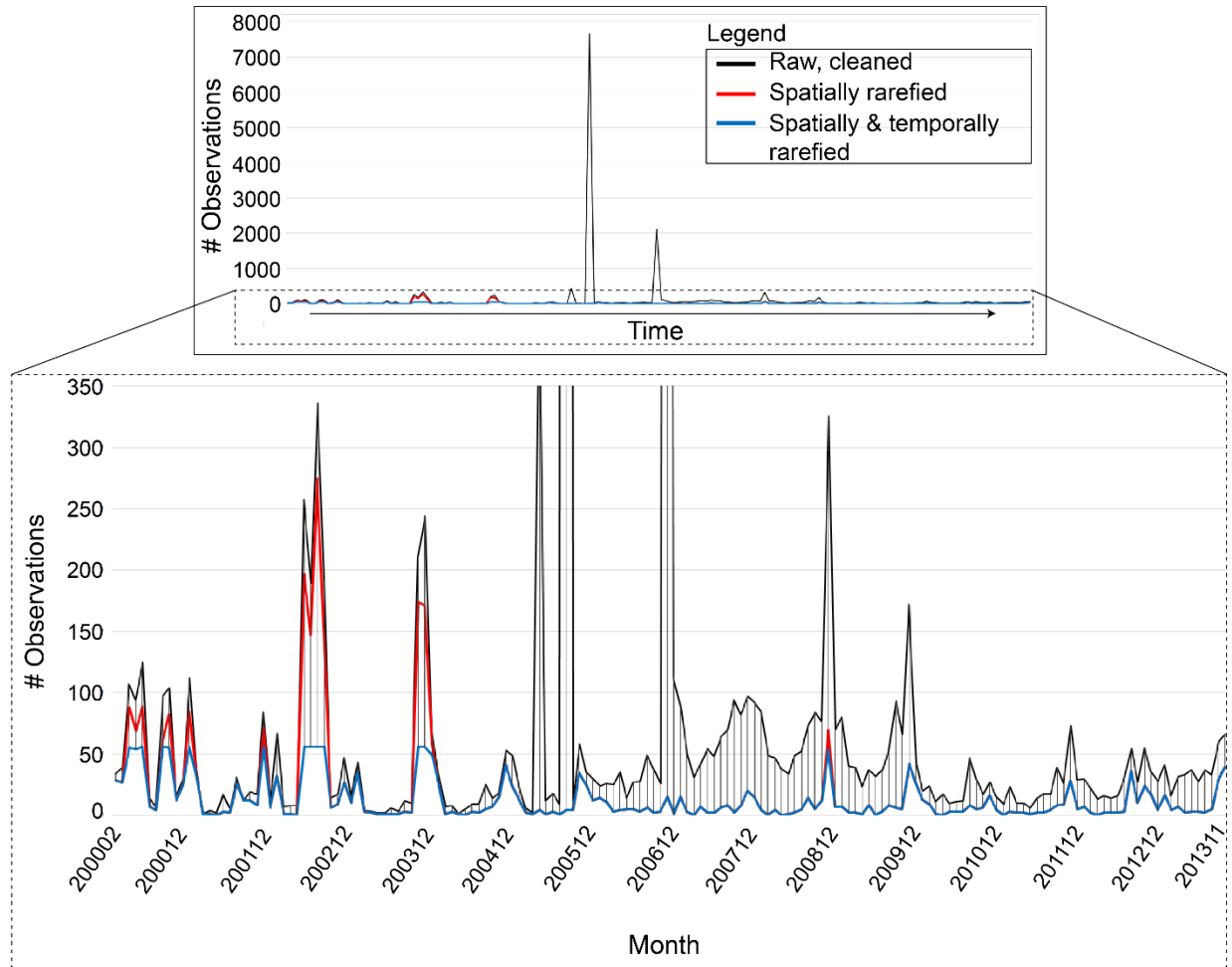
Supplemental Figure 3. *Diomedea exulans* observations by month for raw, cleaned (black), spatially rarefied (red), and spatially rarefied and thinned (blue) time-averaged data.
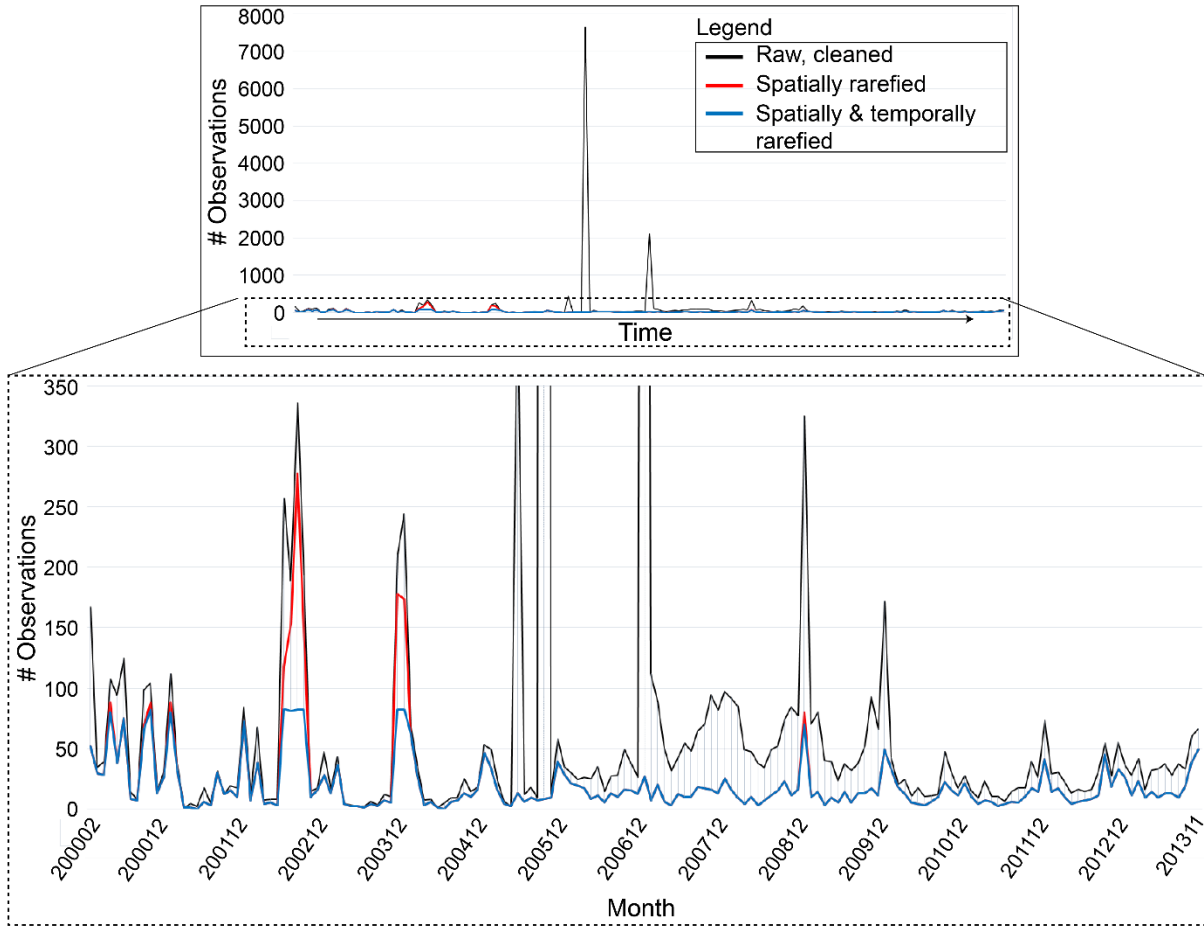
Supplemental Figure 4. *Diomedea exulans* observations by month for raw, cleaned (black), spatially rarefied (red), and spatially rarefied and thinned (blue) time-specific data.

Covariate Correlations

Covariate correlations were calculated for time-averaged and time-specific data using 'GGally' (Schloerke et al. 2018). We considered covariate correlations > 0.75 as overly high and were flagged for closer assessment during model calibration. High covariate correlations are noted below.

Supplemental Table 4. High covariate correlations ($r^2 > 0.75$) for spatially rarefied (SR) and spatially rarefied and thinned (STR) time-averaged and time-specific datasets.

Dataset		High Correlations
Time-Averaged	**SR**	rangeCHL:meanSST: $r^2 = 0.802$
		rangeCHL:rangeSST: $r^2 = 1.000$
		rangeCHL:meanCHL: $r^2 = 0.800$
		rangeSST:meanSST: $r^2 = 0.800$
	STR	rangeCHL:rangeSST: $r^2 = 1.000$
		rangeCHL:meanCHL: $r^2 = 0.820$
Time-Specific	**SR**	
	STR	

Supplemental Figure 5. Covariate correlation matrices for spatially rarefied time-averaged (a) *Diomedea exulans* and pseudo-absence data, (b) *Diomedea exulans* data, and (c) pseudo-absence data.
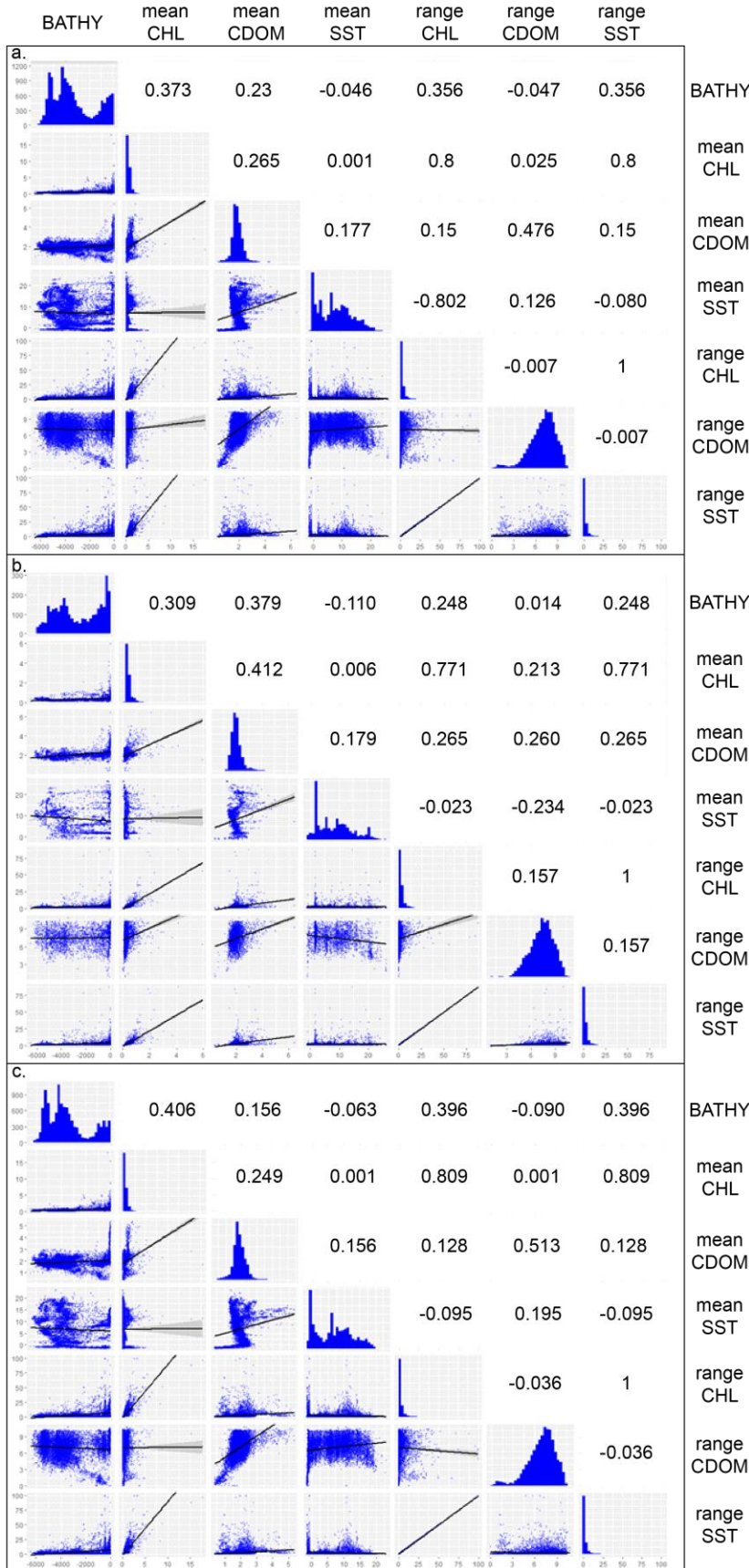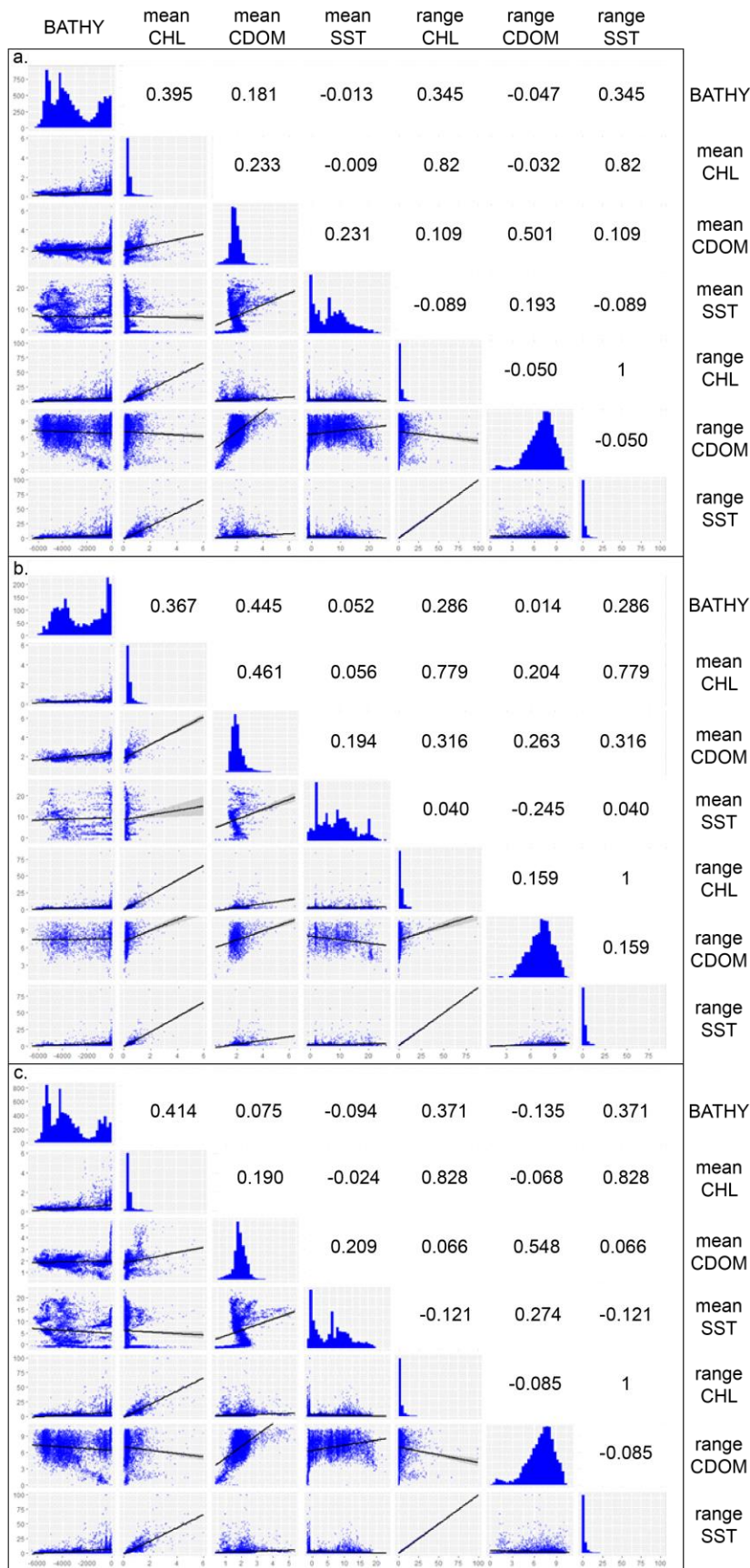
Supplemental Figure 6. Covariate correlation matrices for spatially rarefied and thinned time-averaged (a) *Diomedea exulans* and pseudo-absence data, (b) *Diomedea exulans* data, and (c) pseudo-absence data.
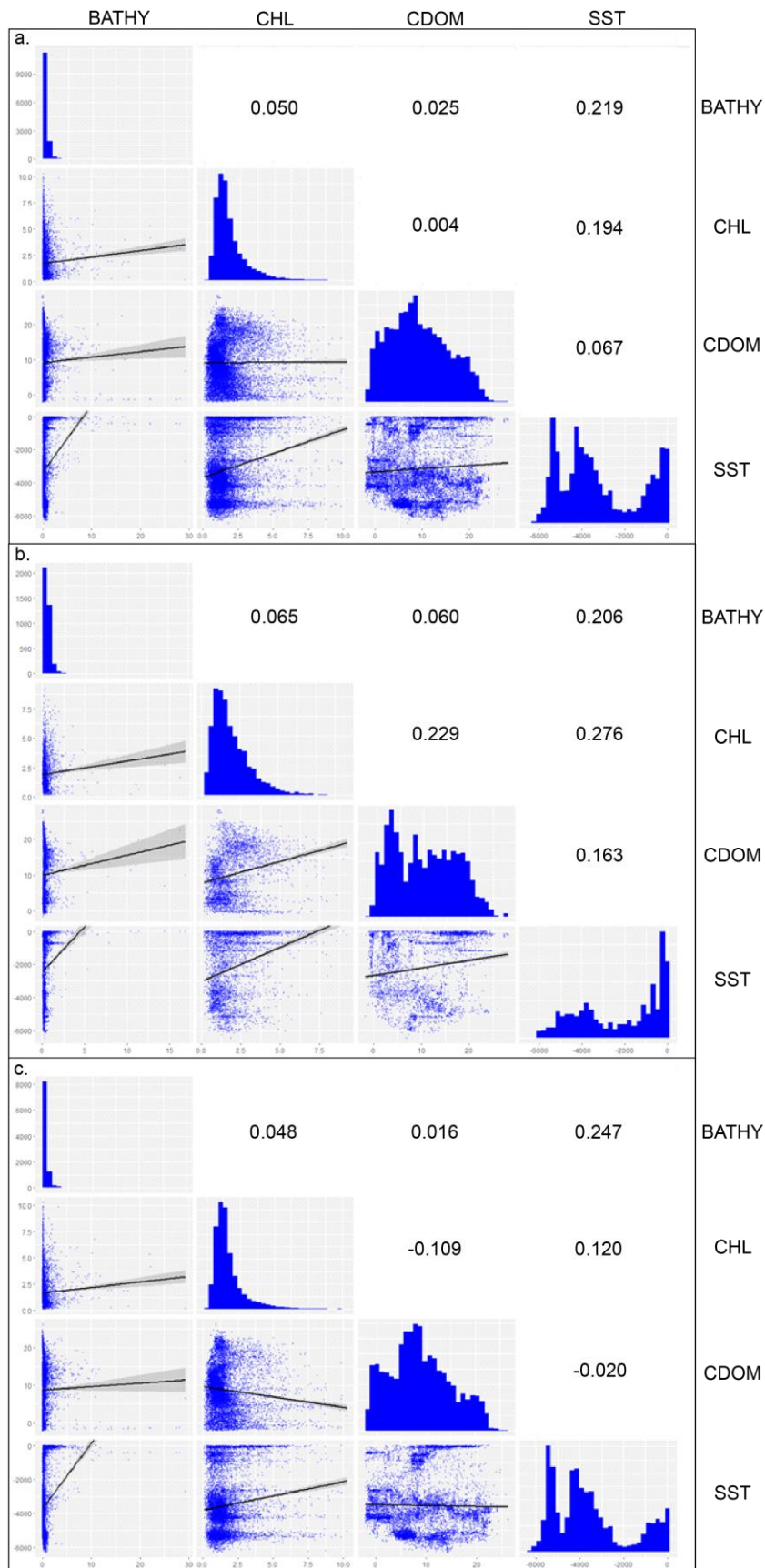
Supplemental Figure 7. Covariate correlation matrices for spatially rarefied time-specific (a) *Diomedea exulans* and pseudo-absence data, (b) *Diomedea exulans* data, and (c) pseudo-absence data.
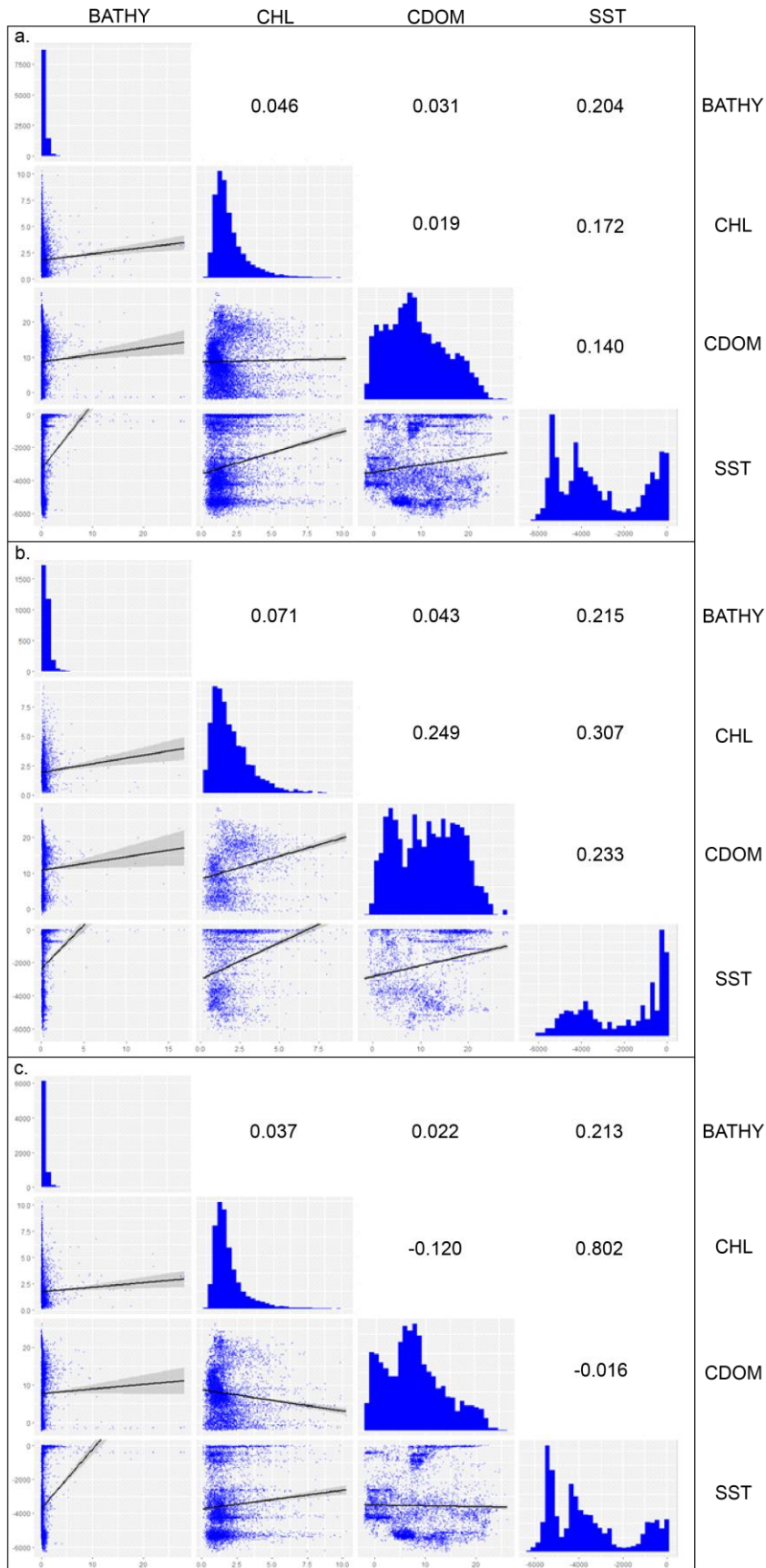
Supplemental Figure 8. Covariate correlation matrices for spatially rarefied and thinned time-specific (a) *Diomedea exulans* and pseudo-absence data, (b) *Diomedea exulans* data, and (c) pseudo-absence data.

Model Calibrations

Weighting input data

Weight scenario #1 weighted study species presence data greater than pseudo-absence data using the following R script:

```
w1 <- c(rep(1, nrow(modCal.Pres)), rep(nrow(modCal.Pres)/nrow(modCal.PAs), nrow(modCal.PAs)));
```

Weight scenario #2 weighted study species presence data and pseudo-absence data equally using the following R script:

```
w2 <- rep(1, nrow(modCal.Pres) + nrow(modCal.PAs));
```

Supplemental Table 5. Time-averaged spatially rarefied final model calibration settings for each algorithm.

GLM	model <- ta.pair.w1;
	model <- glm(formula = Presence ~ 1 + BATHY + meanCDOM + rangeCDOM + meanCHL:BATHY
	    + meanCDOM:BATHY + meanCDOM:meanCHL + meanSST:BATHY +
	    meanSST:meanCHL + meanSST:meanCDOM + rangeCDOM:BATHY +
	    rangeCDOM:meanCHL + rangeCDOM:meanCDOM + rangeCDOM:meanSST,
	    family = binomial, data = mcal, weights = w1)

summary(model);
Deviance Residuals:

Min	1Q	Median	3Q	Max
-1.9888	-0.3724	-0.2662	-0.1123	4.1274

Coefficients:

Variable	Estimate	Std. Error	z value	Pr(>|z|)
(Intercept)	-5.687e+00	7.198e-01	-7.901	2.76e-15 ***
BATHY	5.383e-04	1.466e-04	3.672	0.000241 ***
meanCDOM	4.164e+00	4.417e-01	9.428	< 2e-16 ***
rangeCDOM	2.052e-01	9.712e-02	2.113	0.034603 *
BATHY:meanCHL	-6.061e-04	1.098e-04	-5.519	3.42e-08 ***
BATHY:meanCDOM	6.411e-04	6.984e-05	9.179	< 2e-16 ***
meanCDOM:meanCHL	-3.137e+00	2.090e-01	-15.009	< 2e-16 ***
BATHY:meanSST	-4.513e-05	4.097e-06	-11.015	< 2e-16 ***
meanCHL:meanSST	1.685e-01	2.155e-02	7.820	5.28e-15 ***
meanCDOM:meanSST	8.712e-02	1.316e-02	6.621	3.56e-11 ***
BATHY:rangeCDOM	-1.168e-04	1.635e-05	-7.142	9.22e-13 ***
rangeCDOM:meanCHL	4.611e-01	5.177e-02	8.906	< 2e-16 ***
meanCDOM:rangeCDOM	-1.648e-01	4.381e-02	-3.761	0.000169 ***
rangeCDOM:meanSST	-4.332e-02	4.298e-03	-10.078	< 2e-16 ***

\# Signif. codes: 0 '***' 0.001 '**' 0.01 '*' 0.05 '.' 0.1 ' ' 1
(Dispersion parameter for binomial family taken to be 1)

Null deviance: 5336.6 on 10802 degrees of freedom
Residual deviance: 4222.0 on 10789 degrees of freedom
AIC: 2244.9

Number of Fisher Scoring iterations: 6

library(caret);
varImp(model);

Variable	Overall
meanCDOM:meanCHL	15.009195
BATHY:meanSST	11.014661
rangeCDOM:meanSST	10.078478
meanCDOM	9. 428055
BATHY:meanCDOM	9.178814
rangeCDOM:meanCHL	8.905823
meanCHL:meanSST	7.820008
BATHY:rangeCDOM	7.141671
meanCDOM:meanSST	6.621357
BATHY:meanCHL	5.518632
meanCDOM:rangeCDOM	3.761074
BATHY	3.671939
rangeCDOM	2.112976

GAM	model <- m1.25k.w1; model <- gam(Presence ~ 1 + s(BATHY, k = 25) + s(meanCHL, k = 25)+ s(meanCDOM, k = 25) + s(rangeCDOM, k = 25) + s(meanSST, k = 25),

| | family = binomial, data = mcal, select = TRUE, weights = w1);

AIC(model); # 1500.991

summary(model);
 Parametric coefficients:
                Estimate   Std. Error   z value   Pr($>$|z|)
 (Intercept)   -1.83679   0.06488   -28.31 $<$2e-16 *** |

Approximate significance of smooth terms:

	edf	Ref.df	Chi.sq	p-value
BATHY	15.709	24	180.563	< 2e-16 ***
meanCHL	15.024	24	273.360	< 2e-16 ***
meanCDOM	7.353	24	25.719	0.00015 ***
rangeCDOM	2.671	24	6.683	0.04203 *
meanSST	22.030	24	491.997	< 2e-16 ***

Signif. codes: 0 '***' 0.001 '**' 0.01 '*' 0.05 '.' 0.1 ' ' 1#

R-sq.(adj) =   0.44   Deviance explained = 38.4%
UBRE = -0.68409 Scale est. = 1   n = 10803

Variable response plot using 'response.plot2()' function (Biomod package)
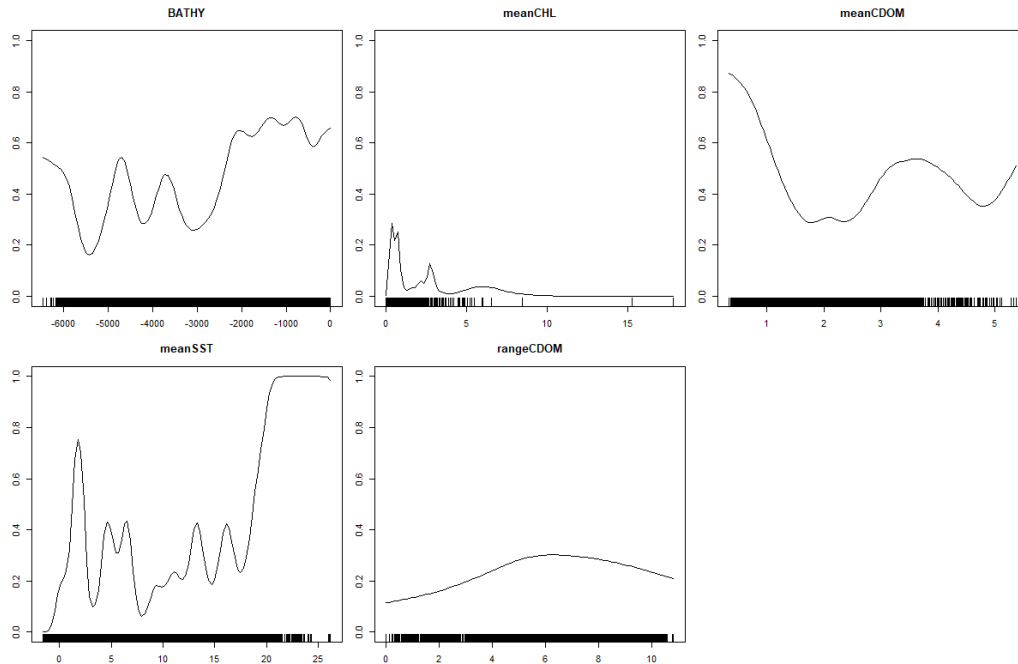
| BRT | model <- m.bf06.tc5.w2;
model <- gbm.step(data = mcal, gbm.x = c(7:12), gbm.y = 1, family = "bernoulli",
             tree.complexity = 5, bag.fraction = 0.6, site.weights = w2);

model evaluation via custom function |

Threshold	Threshold Value	Training Presences Predicted	Test Presences Predicted	Training OR	Test OR	Training MSE	Test MSE
MPT	0.029464444685	2314	747	99.96%	97.90%	0.146639	0.275099
MPT + E=5%	0.238379168344	2199	600	94.99&	78.64%		
MPT + E=10%	0.336609387138	2083	546	89.98%	71.56%		

Variable Importance
summary(model);

Variable	Relative Influence
meanSST	40.556030
BATHY	20.376001
meanCHL	19.414372
meanCDOM	8.381100
rangeCHL	6.965380
rangeCDOM	4.307115
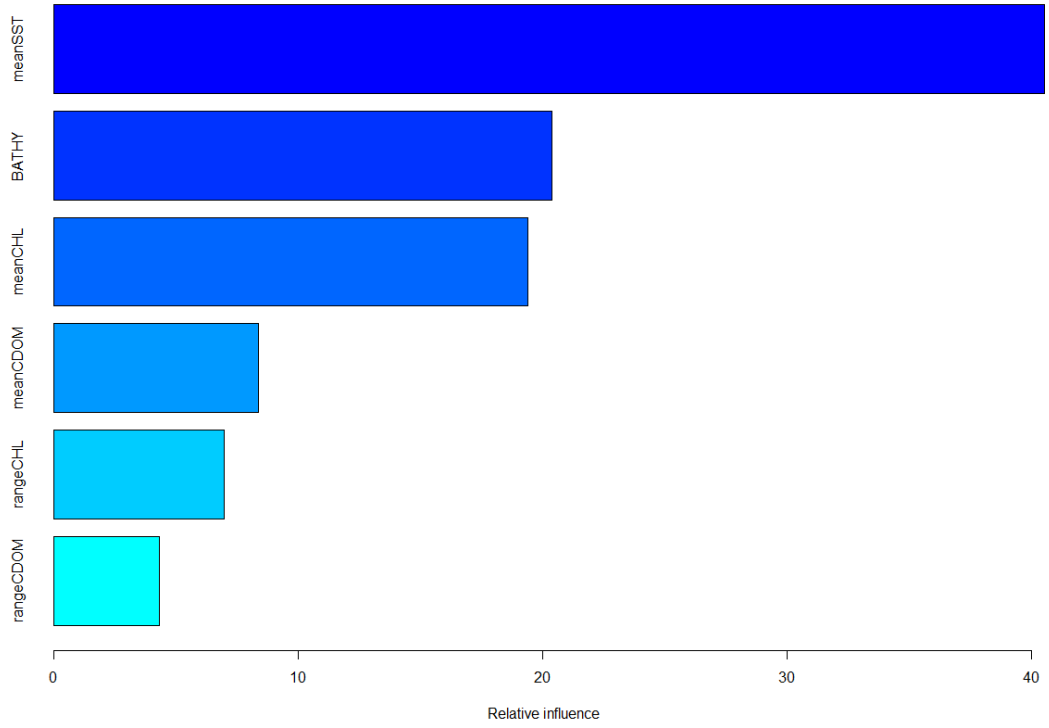
Supplemental Table 6. Time-averaged spatially rarefied and thinned final model calibration settings for each algorithm.

GLM	model <- ts.pair.w1.2;
	model <- glm(Presence ~ 1 + BATHY + meanCHL + meanCDOM + meanSST + rangeCHL +
	        meanCDOM:BATHY + meanCDOM:meanCHL + rangeCHL:meanCDOM +
	        rangeCHL:meanSST,
	        family = binomial, data = mcal, weights = w1);

summary(model);
Deviance Residuals:

Min	1Q	Median	3Q	Max
-1.8426	-0.3432	-0.2554	-0.1946	3.6426

Coefficients:

Variable	Estimate	Std. Error	z value	Pr(>|z|)
(Intercept)	-5.967e+00	4.556e-01	-13.098	< 2e-16 ***
BATHY	-4.433e-04	1.459e-04	-3.039	0.00237 **
meanCHL	5.504e+00	7.432e-01	7.406	1.30e-13 ***
meanCDOM	2.714e+00	2.299e-01	11.805	< 2e-16 ***
meanSST	6.790e-02	9.761e-03	6.956	3.49e-12 ***
rangeCHL	-2.606e-01	6.572e-02	-3.965	7.34e-05 ***
BATHY:meanCDOM	3.966e-04	7.479e-05	5.303	1.14e-07 ***
meanCHL:meanCDOM	-2.852e+00	2.922e-01	-9.760	< 2e-16 ***
meanCDOM:rangeCHL	7.407e-02	2.634e-02	2.813	0.00491 **
meanSST:rangeCHL	5.467e-03	2.281e-03	2.397	0.01654*

Signif. codes: 0 '***' 0.001 '**' 0.01 '*' 0.05 '.' 0.1 ' ' 1

(Dispersion parameter for binomial family taken to be 1)

Null deviance: 3594.3 on 7934 degrees of freedom
Residual deviance: 2948.1 on 7925 degrees of freedom
AIC: 1596.3

Number of Fisher Scoring iterations: 6

varImp(model); # variable importance derived using 'caret' package)

Variable	Overall
meanCDOM	11.804547
meanCHL:meanCDOM	9.759516
meanCHL	7.405665
meanSST	6.956424
BATHY:meanCDOM	5.303439
rangeCHL	3.964867
BATHY	3.038891
meanCDOM:rangeCHL	2.812589
meanSST:rangeCHL	2.396820

GAM	model <- m1.25k.w1;
	model <- gam(Presence ~ 1 + s(BATHY, k = 25) + s(meanCHL, k = 25)+ s(meanCDOM, k = 25)
	      + s(rangeCDOM, k = 25) + s(meanSST, k = 25),
	      family = binomial, data = mcal, select = TRUE,
	      weights = w1);

AIC(model); # 1099.472

summary(model);
Parametric coefficients:

	Estimate	Std. Error	z value	Pr(>|z|)
(Intercept)	-1.96591	0.08294	-23.7	<2e-16 ***

Approximate significance of smooth terms:

	edf	Ref.df	Chi.sq	p-value
BATHY	13.490	24	139.522	< 2e-16 ***
meanCHL	15.810	24	182.591	< 2e-16 ***
meanCDOM	5.220	24	27.42	5.9e-06 ***
rangeCDOM	2.367	24	3.603	0.179
meanSST	21.633	24	319.800	< 2e-16 ***

Signif. codes: 0 '***' 0.001 '**' 0.01 '*' 0.05 '.' 0.1 ' ' 1

R-sq.(adj) = 0.429   Deviance explained = 38.2%
UBRE = -0.70494 Scale est. = 1   n = 7935

variable response plot using 'response.plot2()' function
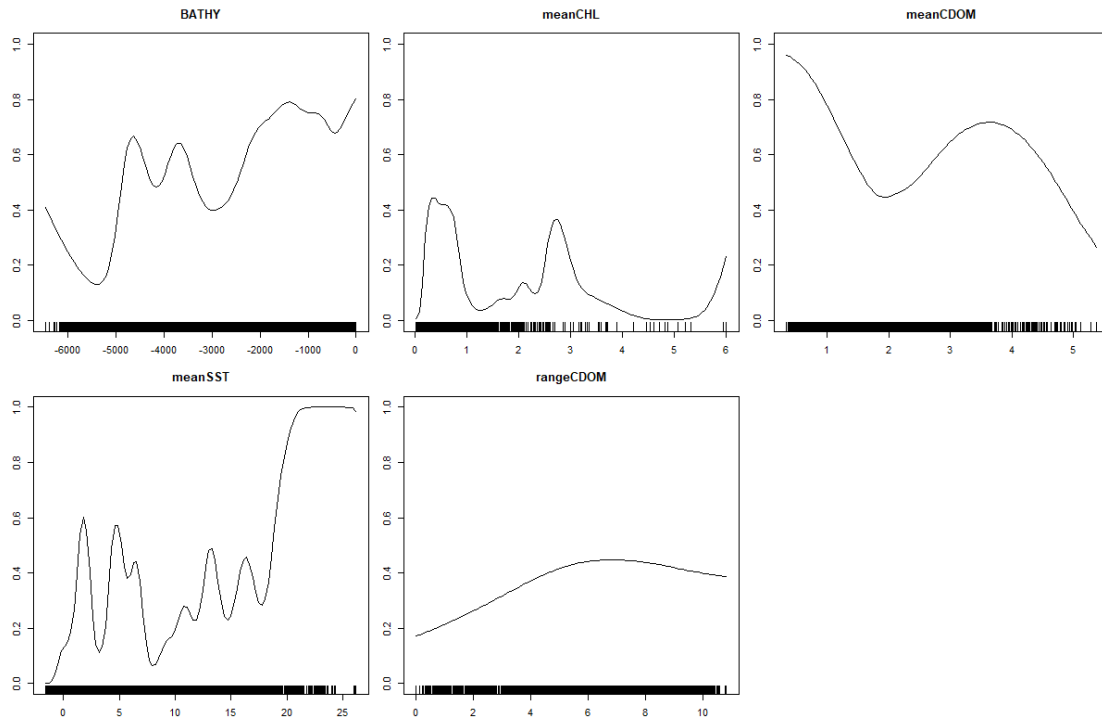
| BRT	model <- m.lr005.tc5.w2; model <- gbm.step(data = mcal, gbm.x = c(7:12), gbm.y = 1, family = "bernoulli", tree.complexity = 5, learning.rate = 0.005, site.weights = w2); m.lr005.tc5.or.w2; # model evaluation via custom function

Threshold	Threshold Value	Training Presences Predicted	Test Presences Predicted	Training OR	Test OR	Training MSE	Test MSE
MPT	0.03140610267	1608	510	99.94%	98.27%	0.169634	0.304359
MPT + E=5%	0.20169896205	1529	406	95.03%	78.23%		
MPT + E=10%	0.29559917425	1448	374	89.99%	72.06%		

Variable Importance
summary(model);
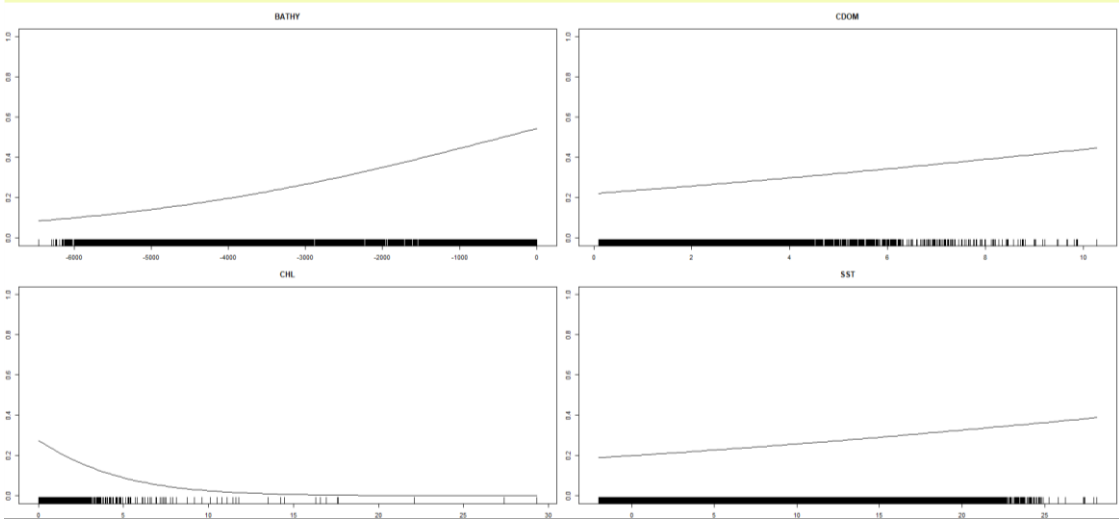
Variable	Relative Influence
meanSST	39.691589

BATHY	23.449343
meanCHL	21.117736
meanCDOM	6.999985
rangeCHL	5.515859
rangeCDOM	3.225488
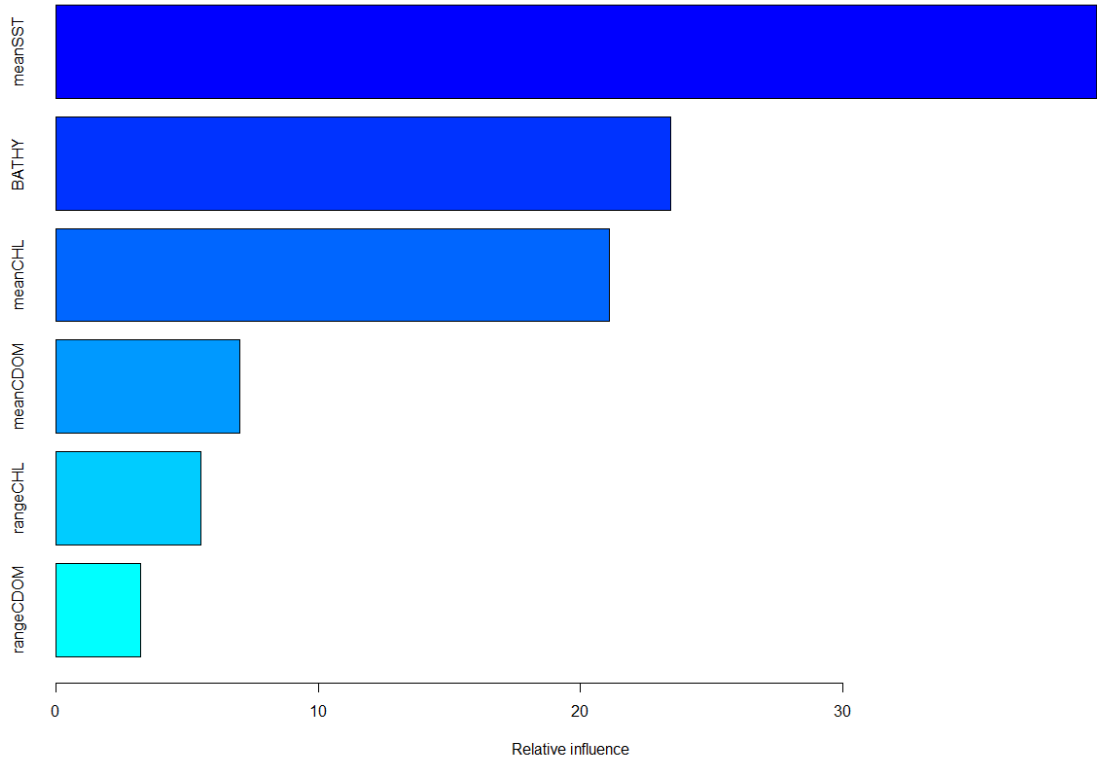
Supplemental Table 7. Time-specific spatially rarefied final model calibration settings for each algorithm.
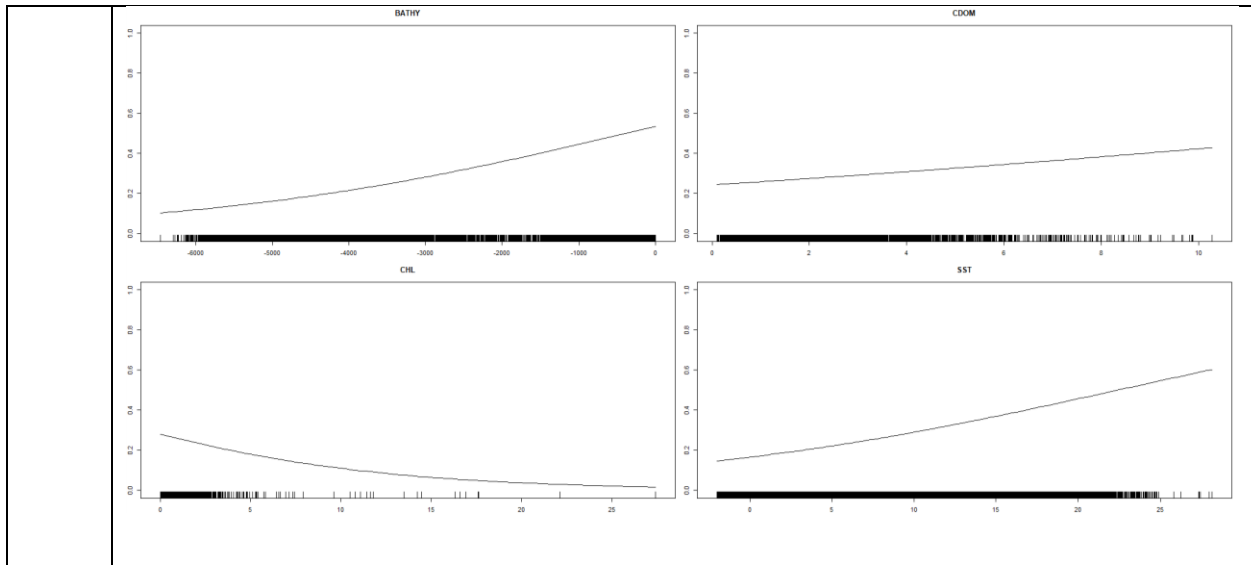

GLM	model <- ts.pair.w1.3;
	model <- glm(Presence ~ 1 + BATHY + CDOM:CHL + SST:CDOM + BATHY:SST,
	   family = binomial, data = mcal, weights = w1);
	
	summary(model);
	Deviance Residuals:

Deviance Residuals:

Min	1Q	Median	3Q	Max
-1.9471	-0.4543	-0.3739	0.8709	4.3458

Coefficients:

Variable	Estimate	Std. Error	z value	Pr(>|z|)
(Intercept)	-1.039e-01	5.981e-02	-1.737	0.0823 .
BATHY	3.373e-04	2.673e-05	12.621	< 2e-16 ***
CDOM:CHL	-1.520e-01	1.901e-02	-7.997	1.28e-15 ***
CDOM:SST	2.115e-02	1.830e-03	11.555	< 2e-16 ***
BATHY:SST	4.320e-06	2.042e-06	2.116	0.0344 *

Signif. codes: 0 '***' 0.001 '**' 0.01 '*' 0.05 '.' 0.1 ' ' 1

(Dispersion parameter for binomial family taken to be 1)

Null deviance: 7259.6 on 10218 degrees of freedom
Residual deviance: 6415.3 on 10214 degrees of freedom
AIC: 3728.8

Number of Fisher Scoring iterations: 5

varImp(model); # variable importance derived using the 'caret' package

Variable	Overall
BATHY	12.620922
CDOM:SST	11.555263
CDOM:CHL	7.996611
BATHY:SST	2.115645

GAM	model <- tsFull.1.25k.w1; model <- gam(Presence ~ 1 + s(CHL, k=25) + s(CDOM, k = 25) + s(SST, k=25) + s(BATHY, k=25),

	family = binomial , data = mcal, select = TRUE, weights = w1);
	AIC(model); # 2911.078
	
	summary(model);
	Parametric coefficients:
	              Estimate Std. Error z value Pr(>|z|)
	(Intercept) -1.46502 0.07003 -20.92 <2e-16 ***
	
	Approximate significance of smooth terms:
	
	Signif. codes: 0 '***' 0.001 '**' 0.01 '*' 0.05 '.' 0.1 ' ' 1
	
	R-sq.(adj) = 0.324 Deviance explained = 26.5%
	UBRE = -0.46391 Scale est. = 1 n = 10219

Approximate significance of smooth terms:

	edf	Ref.df	Chi.sq	p-value
s(CHL)	20.766	24	333.12	< 2e-16 ***
s(CDOM)	6.664	24	67.22	4.23e-14 ***
S(SST)	23.492	24	411.71	< 2e-16 ***
S(BATHY)	20.331	24	453.76	< 2e-16 ***

BRT

```
model <- m.bf07.tc4.w2;
model <- gbm.step(data = mcal, gbm.x = c(7:10),
            gbm.y = 1, family = "bernoulli", tree.complexity = 4, bag.fraction = 0.7,
            site.weights = w2); # lr default
```

model evaluation via custom function

Threshold	Threshold Value	Training Presences Predicted	Test Presences Predicted	Training OR	Test OR	Training MSE	Test MSE
MPT	0.01609685196	2821	967	99.96%	99.79%	0.198065	0.251652
MPT + E=5%	0.18039890121	2681	861	95%	88.85%		
MPT + E=10%	0.24789905927	2540	794	90.01%	81.94%		

Variable Importance
summary(model);

Variable	Relative Influence
BATHY	41.657
SST	33.599
CHL	15.604
CDOM	9.140

Relative influence

Supplemental Table 8. Time-specific spatially rarefied and thinned final model calibration settings for each algorithm.

GLM	model <- ts.pair.w1.2;
	model <- glm(Presence ~ 1 + SST + BATHY + CDOM:CHL + SST:CDOM +
	    BATHY:CHL + BATHY:CDOM + BATHY:SST, family = binomial, data = mcal,
	    weights = w1);
	
	Deviance Residuals:
	  Min 1Q Median 3Q Max
	-2.2351 -0.5002 -0.3798 0.8347 3.4838
	
	# Coefficients:

Variable	Estimate	Std. Error	z value	Pr(>|z|)
(Intercept)	-5.641e-01	1.004e-01	-5.617	1.94e-08 ***
SST	4.198e-02	1.108e-02	3.789	0.000152 ***
BATHY	2.433e-04	4.141e-05	5.875	4.23e-09 ***
CDOM:CHL	-1.010e-01	1.945e-02	-5.192	2.08e-07 ***
SST:CDOM	2.120e-02	3.030e-03	6.996	2.64e-12 ***
BATHY:CHL	-8.916e-05	4.014e-05	-2.221	0.026345 *
BATHY:CDOM	3.110e-05	1.253e-05	0.013065 *	0.013065 *
SST:BATHY	7.203e-06	3.000e-06	2.401	0.016333 *

Signif. codes: 0 '***' 0.001 '**' 0.01 '*' 0.05 '.' 0.1 ' ' 1

(Dispersion parameter for binomial family taken to be 1)

Null deviance: 6183.8 on 7808 degrees of freedom
Residual deviance: 5296.2 on 7801 degrees of freedom
AIC: 2993.4

Number of Fisher Scoring iterations: 5

Relative Variable Importance
varImp(model); # library(caret)

Variable	Overall
SST:CDOM	6.995575
BATHY	5.874933
CDOM:CHL	5.192034
SST	3.788529
BATHY:CDOM	2.481998
SST:BATHY	2.401386
BATHY:CHL	2.221090

| GAM | model <- tsFull.1.25k.w1;
model <- gam(Presence ~ 1 + s(CHL, k=25) + s(CDOM, k = 25) + s(SST, k=25) + s(BATHY, k=25),
           family = binomial , data = mcal, select = TRUE, weights = w1);
AIC(model); # 2423.718

summary(model);
Parametric coefficients:

Approximate significance of smooth terms: |

| GAM | model <- tsFull.1.25k.w1;
model <- gam(Presence ~ 1 + s(CHL, k=25) + s(CDOM, k = 25) + s(SST, k=25) + s(BATHY, k=25),
  family = binomial , data = mcal, select = TRUE, weights = w1);
AIC(model); # 2423.718 |

summary(model);
Parametric coefficients:

	Estimate	Std. Error	z value	Pr(>|z|)
(Intercept)	-1.27331	0.05174	-24.61	<2e-16 ***

 Signif. codes: 0 '***' 0.001 '**' 0.01 '*' 0.05 '.' 0.1 ' ' 1

Approximate significance of smooth terms:

	edf	Ref.df	Chi.sq	p-value
s(CHL)	19.88	24	252.94	< 2e-16 ***
s(CDOM)	12.30	24	52.83	4.93e-08 ***
S(SST)	13.46	24	364.91	< 2e-16 ***
S(BATHY)	20.14	24	403.23	< 2e-16 ***

Signif. codes: 0 '***' 0.001 '**' 0.01 '*' 0.05 '.' 0.1 ' ' 1

R-sq.(adj) = 0.336   Deviance explained = 28.1%
UBRE = -0.41329 Scale est. = 1   n = 7809

variable response plot using 'response.plot2()' function

BATHY CDOM

CHL SST
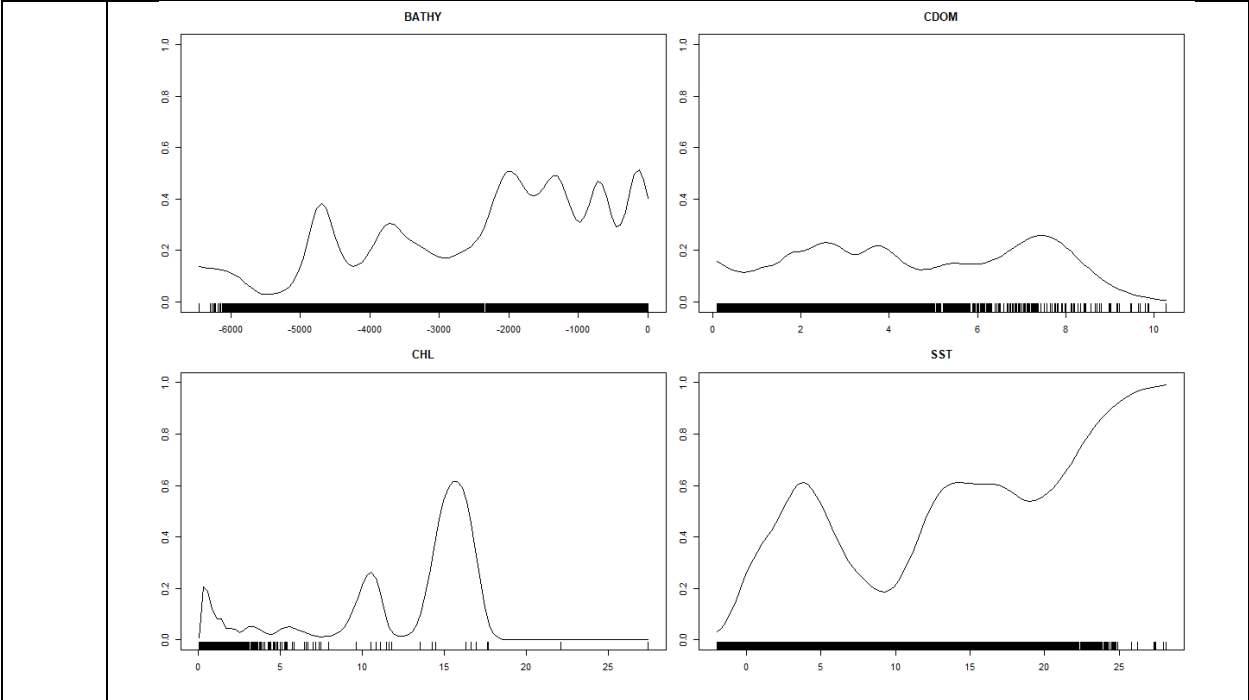
BRT	model <- m.tc4.w2;
	model <- gbm.step(data = mcal, gbm.x = c(7:10),
	            gbm.y = 1, family = "bernoulli",
	            tree.complexity = 4,
	            site.weights = w2); # default bf & lr

m.tc4.or.w2; # model evaluation via custom function

Threshold	Threshold Value	Training Presences Predicted	Test Presences Predicted	Training OR	Test OR	Training MSE	Test MSE
MPT	0.02627560590	2363	829	99.96%	99.64%	0.174213	0.222612
MPT + E=5%	0.18911294435	2246	759	95.01%	91.23%		
MPT + E=10%	0.29298187128	2128	689	90.02%	82.81%		

Variable Influence
summary(model);

Variable	Relative Influence
BATHY	41.865590
SST	35.750944
CHL	15.580212
CDOM	6.803255
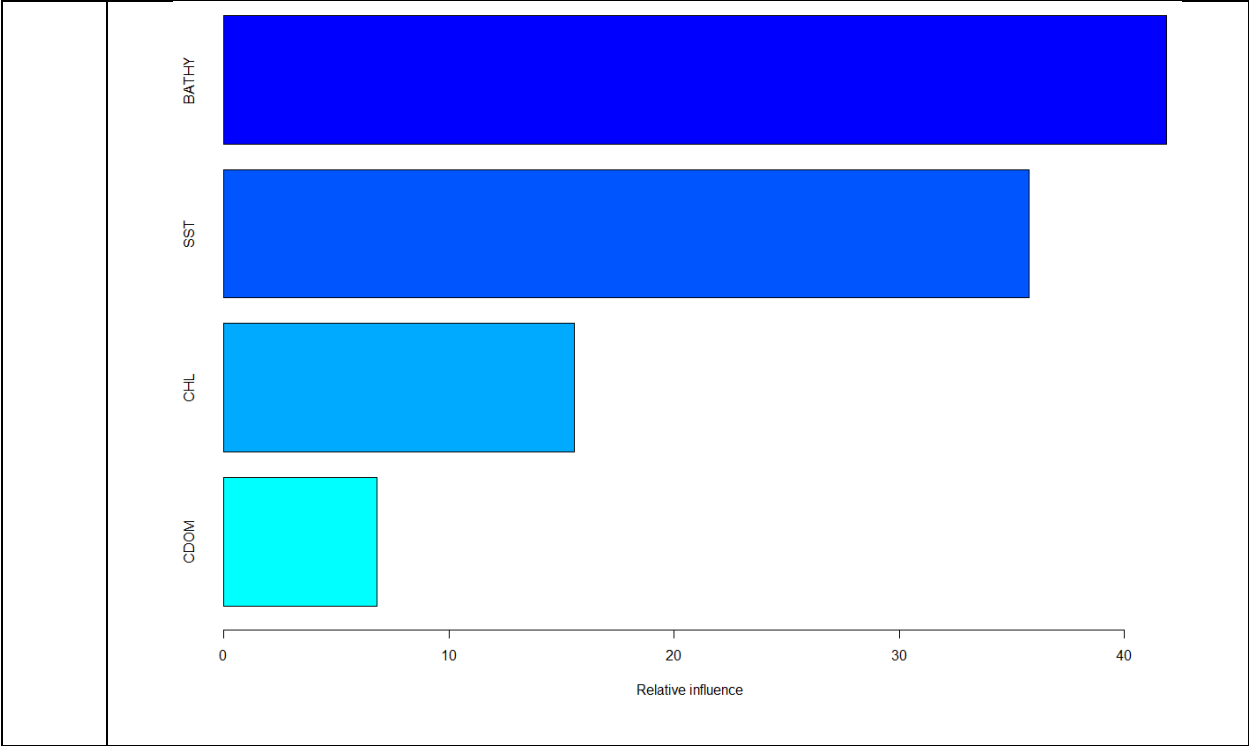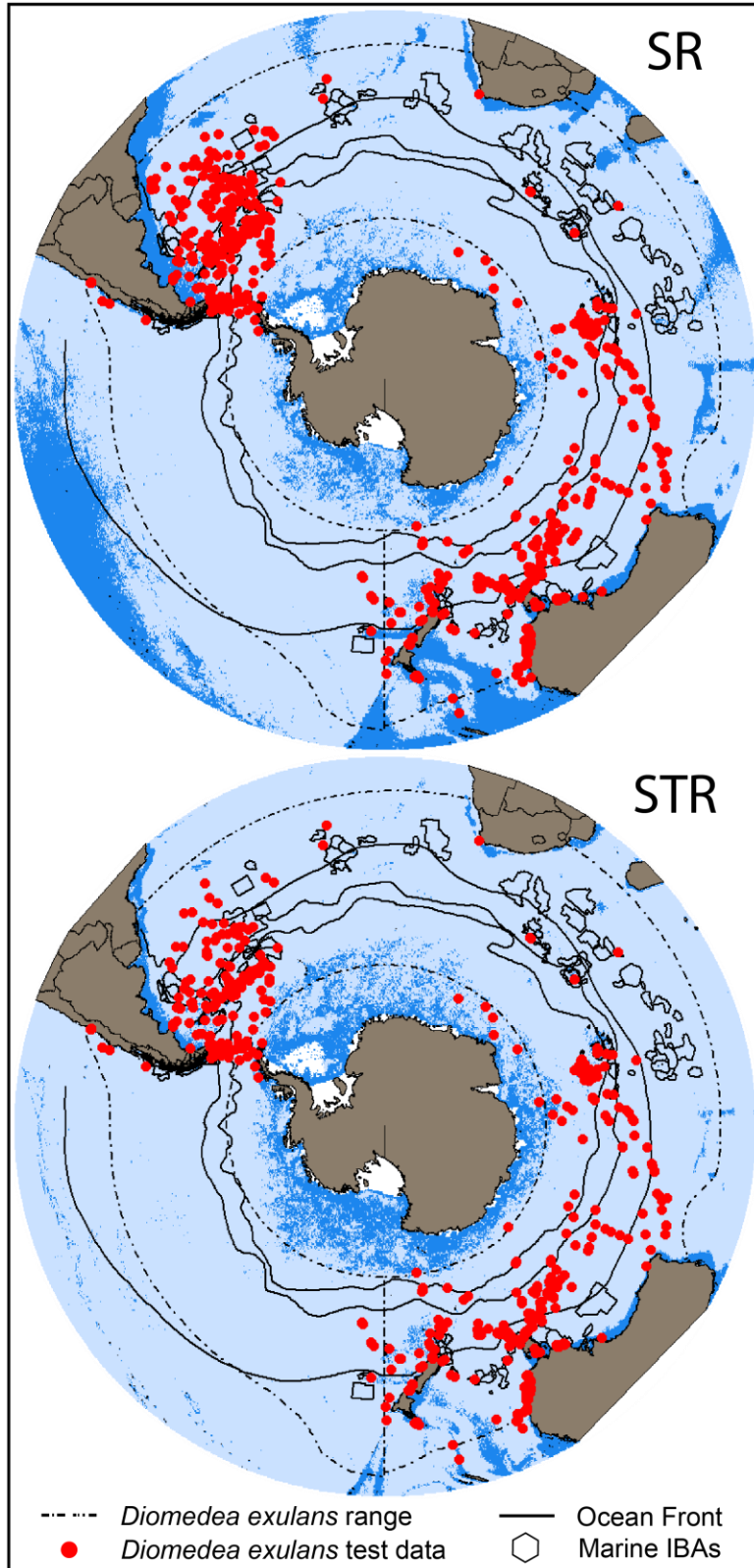
Supplemental Figure 9. Time-averaged spatially rarefied (SR; top) and spatially rarefied and thinned (STR; bottom) final GLM model predictions overlaid with *Diomedea exulans* range (dashed line; BirdLife International and NatureServe 2015), relevant marine IBAs (black polygons; BirdLife International 2016), and *D. exulans* test data (red points), and Subtropical (STF), Subantarctic (SAF) and Polar Fronts (PF; Orsi & Harris 2008).
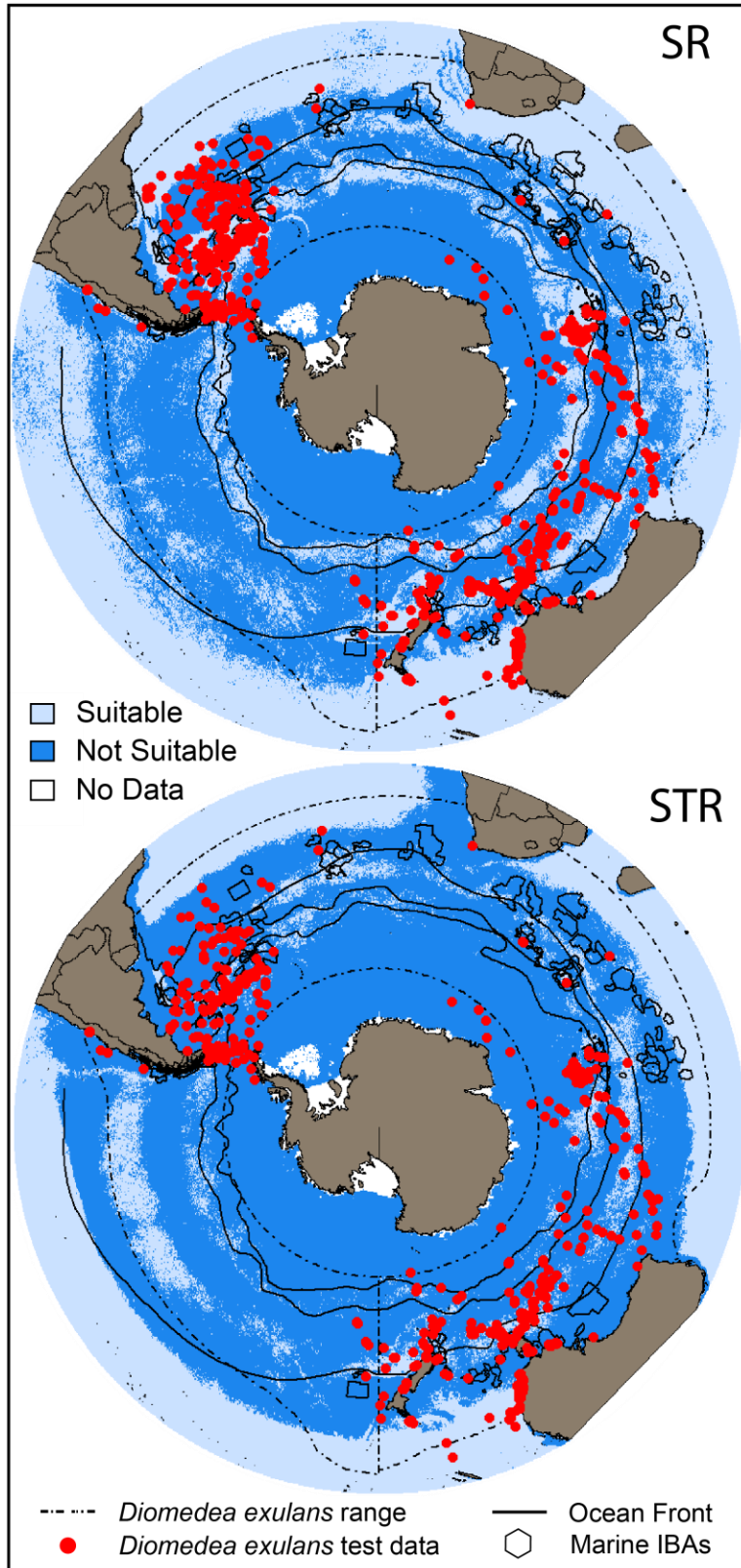
Supplemental Figure 10. Snapshot of time-averaged spatially rarefied (SR; top) and spatially rarefied and thinned (STR; bottom) final GAM model predictions overlaid with *Diomedea exulans* range (dashed line; BirdLife International and NatureServe 2015), relevant marine IBAs (black polygons; BirdLife International 2016), and *D. exulans* test data (red points), and Subtropical (STF), Subantarctic (SAF) and Polar Fronts (PF; Orsi & Harris 2008).
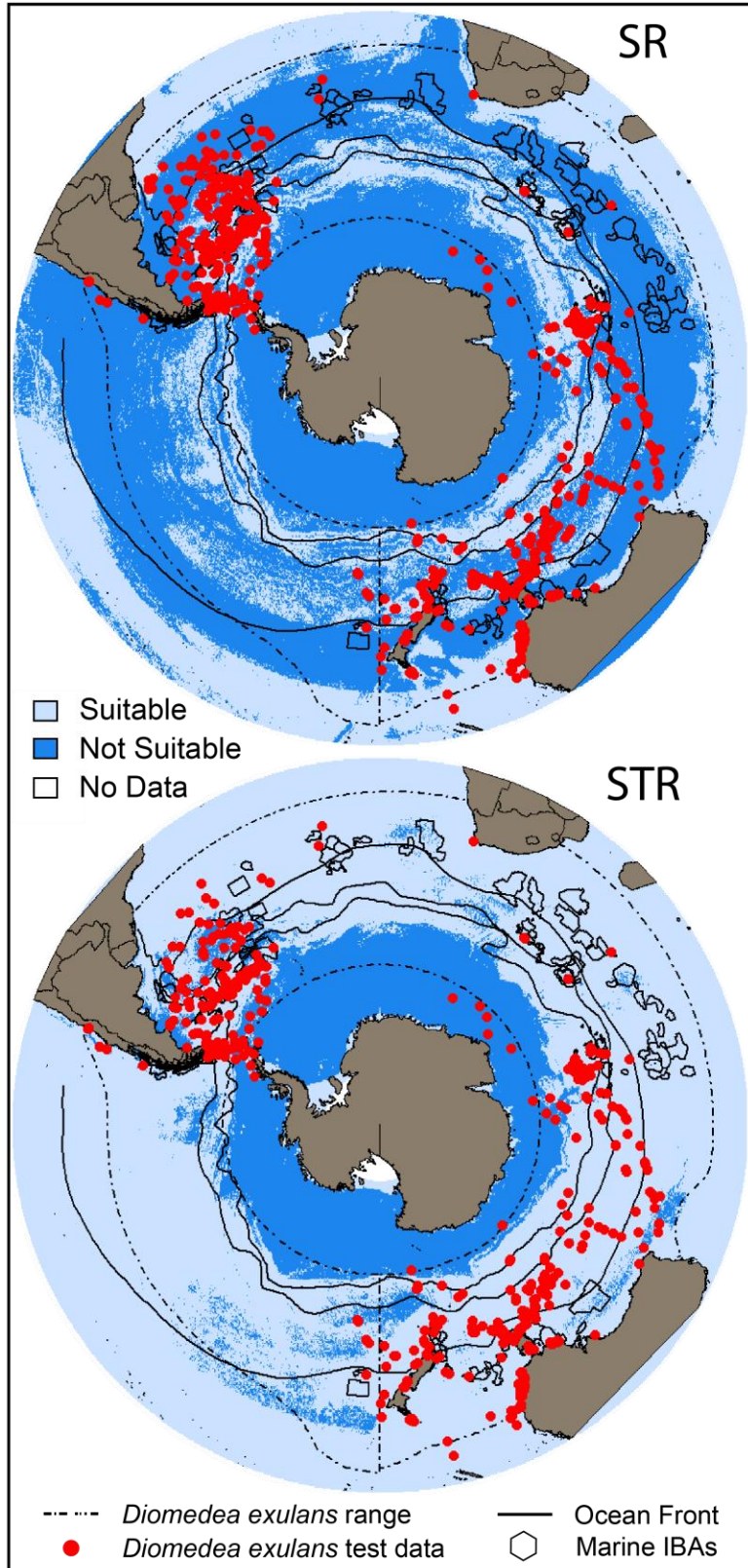
Supplemental Figure 11. Snapshot of time-averaged spatially rarefied (SR; top) and spatially rarefied and thinned (STR; bottom) final BRT model predictions overlaid with *Diomedea exulans* range (dashed line; BirdLife International and NatureServe 2015), relevant marine IBAs (black polygons; BirdLife International 2016), and *D. exulans* test data (red points), and Subtropical (STF), Subantarctic (SAF) and Polar Fronts (PF; Orsi & Harris 2008).
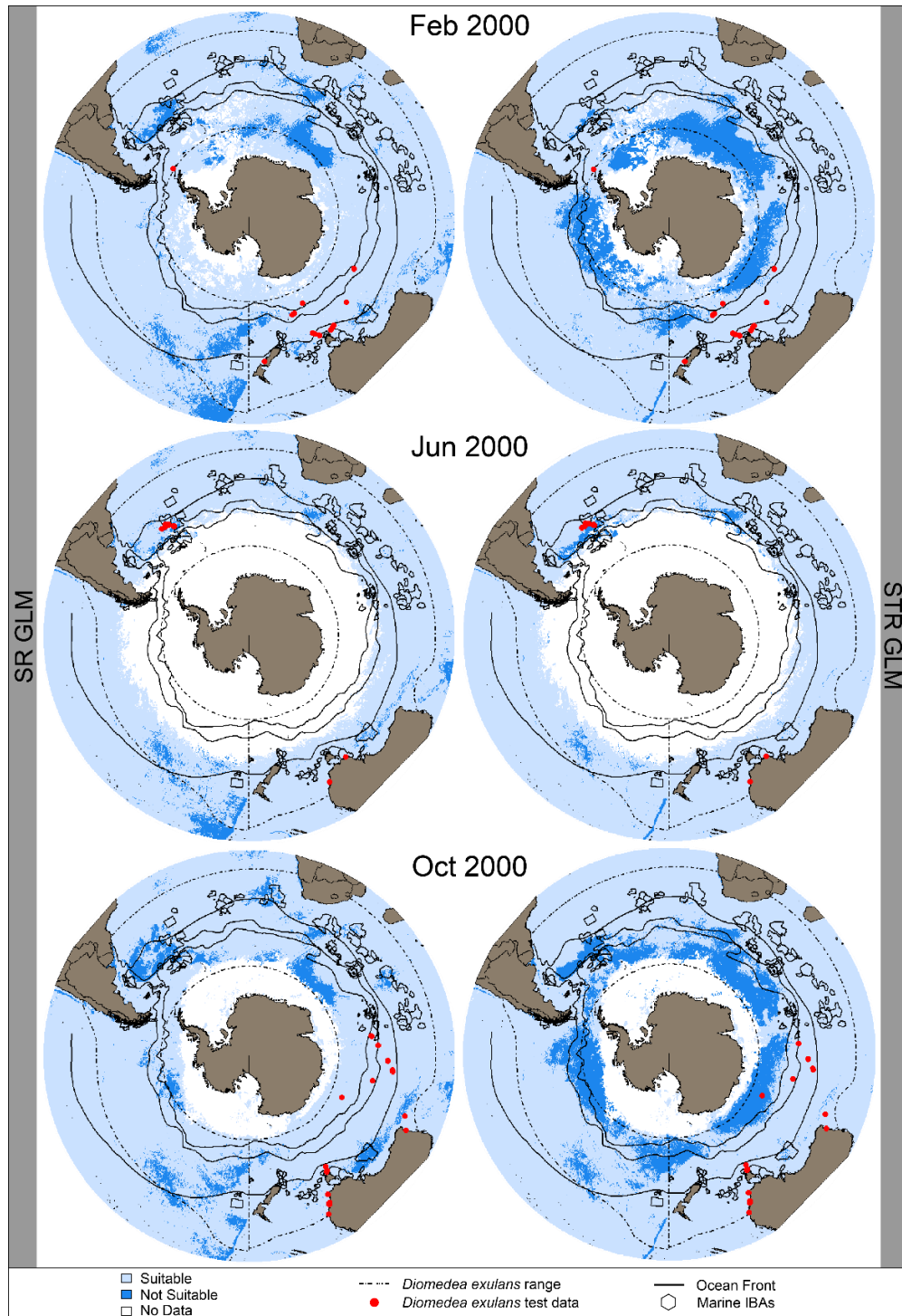
Supplemental Figure 12. Snapshot of time-specific spatially rarefied (SR; left) and spatially rarefied and thinned (STR; right) final GLM model predictions overlaid with *Diomedea exulans* range (dashed line; BirdLife International and NatureServe 2015), relevant marine IBAs (black polygons; BirdLife International 2016), and *D. exulans* test data (red points), and Subtropical (STF), Subantarctic (SAF) and Polar Fronts (PF; Orsi & Harris 2008). See dynamic prediction at doi.org/10.6084/m9.figshare.12612431.v1.
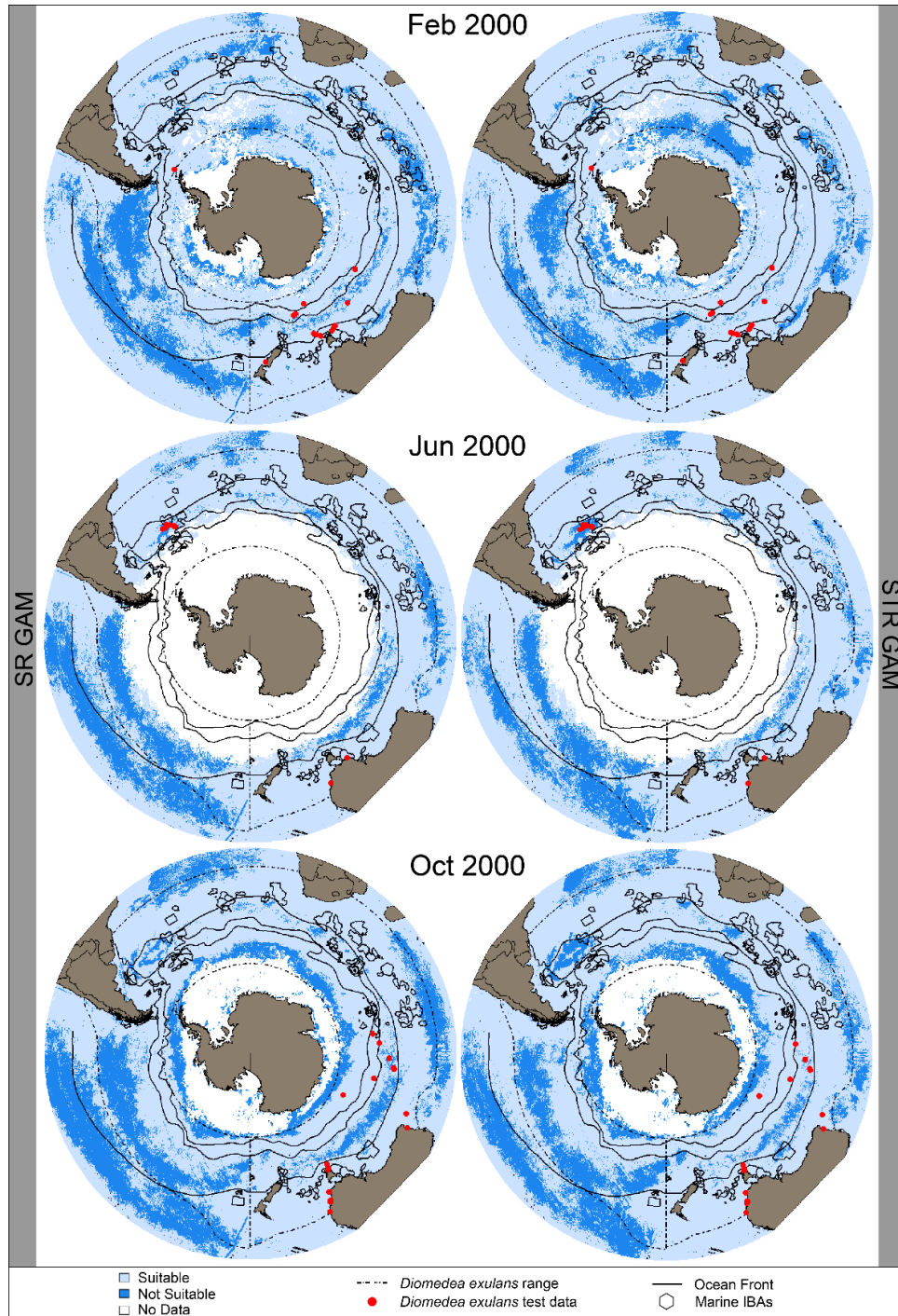
Supplemental Figure 13. Snapshot of time-specific spatially rarefied (SR; left) and spatially rarefied and thinned (STR; right) final GAM model predictions overlaid with *Diomedea exulans* range (dashed line; BirdLife International and NatureServe 2015), relevant marine IBAs (black polygons; BirdLife International 2016), and *D. exulans* test data (red points), and Subtropical (STF), Subantarctic (SAF) and Polar Fronts (PF; Orsi & Harris 2008). See dynamic prediction at doi.org/10.6084/m9.figshare.12612431.v1.
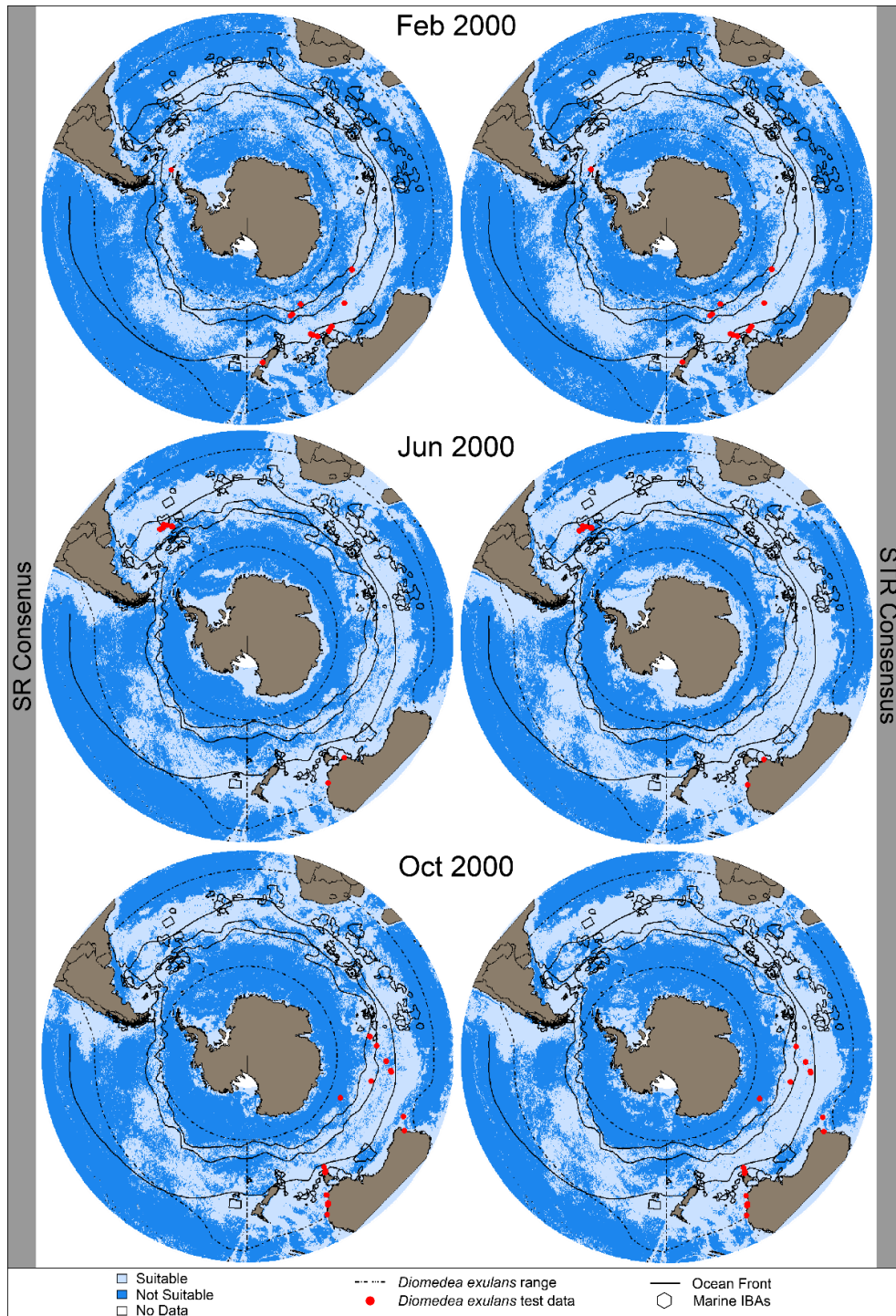
Supplemental Figure 14. Snapshot of time-specific spatially rarefied (SR; left) and spatially rarefied and thinned (STR; right) final BRT model predictions overlaid with *Diomedea exulans* range (dashed line; BirdLife International and NatureServe 2015), relevant marine IBAs (black polygons; BirdLife International 2016), and *D. exulans* test data (red points), and Subtropical (STF), Subantarctic (SAF) and Polar Fronts (PF; Orsi & Harris 2008). See dynamic prediction at doi.org/10.6084/m9.figshare.12612431.v1.

Supplemental Table 9. Performance statistics for spatially rarefied (SR) and spatially rarefied and thinned (STR) time-averaged consensus models.

	SR	STR
# *D. exulans* occurrences	761	517
# *D. exulans* occurrences: predicted present	488	409
# *D. exulans* occurrences: predicted absent	273	108
# *D. exulans* occurrences: NA	0	0
Omission Rate (OR)	0.3588 (35.88%)	0.2089 (20.89%)
Mean pROC value	1.1161	0.9954
pROC pValue	0.8	0.672

Supplemental Table 10. Summary of performance statistics for spatially rarefied (SR) and spatially rarefied and thinned (STR) time-specific consensus models.

	SR	STR
# *D. exulans* occurrences	969	832
# *D. exulans* occurrences: predicted present	945	787
# *D. exulans* occurrences: predicted absent	24	45
Omission rate: range	0–0.5	0–0.6923
Mean pROC range	0.8161–1.2248	0.7406–1.1785
pROC pValue range	0–0.762	0–1

Supplemental Table 11. Performance statistics for each time step for spatially rarefied (SR; blue) and spatially rarefied and thinned (STR; green) time-specific consensus models. Non-significant time steps are highlighted in peach; time steps for which no *Diomedea exulans* test data were present are gray.

Time	SR						STR					
	N Obs	N obs present	N obs absent	OR	mean pROC	pROC pVal	N Obs	N obs present	N obs absent	OR	mean pROC	pROC pVal
200002	17	17	0	0.000	1.1045	0.0000	17	17	0	0.000	1.1040	0.0000
200003	3	3	0	0.000	1.1041	0.0000	3	3	0	0.000	1.1028	0.0000
200004	5	5	0	0.000	1.1239	0.0000	5	5	0	0.000	1.1172	0.0000
200005	19	18	1	0.053	1.1241	0.0060	19	18	1	0.053	1.1037	0.0040
200006	13	8	5	0.385	0.9533	0.5680	13	4	9	0.692	0.7406	1.0000
200007	14	14	0	0.000	1.1608	0.0000	14	11	3	0.214	1.0099	0.3820
200008	1	1	0	0.000	1.1376	0.0000	1	1	0	0.000	1.1321	0.0000
200009	1	1	0	0.000	1.1388	0.0000	1	1	0	0.000	1.1366	0.0000
200010	25	25	0	0.000	1.1696	0.0000	21	20	1	0.048	1.1362	0.0020
200011	22	22	0	0.000	1.1717	0.0000	21	21	0	0.000	1.1643	0.0000
200012	4	4	0	0.000	1.1329	0.0000	4	4	0	0.000	1.1245	0.0000
200101	9	9	0	0.000	1.0955	0.0000	9	9	0	0.000	1.0900	0.0000
200102	19	18	1	0.053	1.0568	0.0460	19	18	1	0.053	1.0557	0.0320
200103	12	12	0	0.000	1.0837	0.0000	12	12	0	0.000	1.0913	0.0000
200104	0	NA	NA	NA	NA	NA	0	NA	NA	NA	NA	NA
200105	0	NA	NA	NA	NA	NA	0	NA	NA	NA	NA	NA
200106	0	NA	NA	NA	NA	NA	0	NA	NA	NA	NA	NA
200107	2	2	0	0.000	1.176	0.000	2	2	0	0.000	1.147	0.000
200108	1	1	0	0.000	1.125	0.000	1	1	0	0.000	1.136	0.000
200109	8	8	0	0.000	1.123	0.000	8	8	0	0.000	1.139	0.000
200110	4	4	0	0.000	1.157	0.000	4	4	0	0.000	1.159	0.000
200111	3	3	0	0.000	1.179	0.000	3	3	0	0.000	1.168	0.000
200112	3	3	0	0.000	1.147	0.000	3	3	0	0.000	1.135	0.000
200201	17	17	0	0.000	1.100	0.000	17	16	1	0.059	1.065	0.022
200202	2	1	1	0.500	0.816	0.762	2	2	0	0.000	1.095	0.000
200203	13	13	0	0.000	1.116	0.000	13	12	1	0.077	1.068	0.136
200204	2	2	0	0.000	1.166	0.000	2	2	0	0.000	1.143	0.000
200205	2	2	0	0.000	1.199	0.000	2	2	0	0.000	1.164	0.000
200206	1	1	0	0.000	1.225	0.000	1	1	0	0.000	1.170	0.000
200207	27	25	2	0.074	1.160	0.000	21	13	8	0.381	0.941	0.750
200208	38	37	1	0.026	1.147	0.000	21	17	4	0.190	1.037	0.320
200209	84	81	3	0.036	1.151	0.000	21	16	5	0.238	1.023	0.260
200210	27	25	2	0.074	1.139	0.000	21	19	2	0.095	1.110	0.012
200211	1	1	0	0.000	1.174	0.000	1	1	0	0.000	1.161	0.000
200212	2	2	0	0.000	1.143	0.000	2	2	0	0.000	1.129	0.000
200301	7	7	0	0.000	1.104	0.000	7	7	0	0.000	1.093	0.000

200302	2	2	0	0.000	1.096	0.000	2	2	0	0.000	1.086	0.000
200303	14	14	0	0.000	1.107	0.000	14	14	0	0.000	1.097	0.000
200304	0	NA	NA	NA	NA	NA	0	NA	NA	NA	NA	NA
200305	1	1	0	0.000	1.167	0.000	1	1	0	0.000	1.136	0.000
200306	1	1	0	0.000	1.190	0.000	1	1	0	0.000	1.143	0.000
200307	0	NA	NA	NA	NA	NA	0	NA	NA	NA	NA	NA
200308	2	2	0	0.000	1.126	0.000	2	2	0	0.000	1.133	0.000
200309	0	NA	NA	NA	NA	NA	0	NA	NA	NA	NA	NA
200310	1	1	0	0.000	1.153	0.000	1	1	0	0.000	1.154	0.000
200311	0	NA	NA	NA	NA	NA	0	NA	NA	NA	NA	NA
200312	37	37	0	0.000	1.152	0.000	21	21	0	0.000	1.133	0.000
200401	44	44	0	0.000	1.123	0.000	21	21	0	0.000	1.104	0.000
200402	7	6	1	0.143	1.031	0.148	7	7	0	0.000	1.097	0.000
200403	8	7	1	0.125	1.053	0.174	8	7	1	0.125	1.048	0.160
200404	1	1	0	0.000	1.155	0.000	1	1	0	0.000	1.138	0.000
200405	1	1	0	0.000	1.194	0.000	1	1	0	0.000	1.159	0.000
200406	0	NA	NA	NA	NA	NA	0	NA	NA	NA	NA	NA
200407	0	NA	NA	NA	NA	NA	0	NA	NA	NA	NA	NA
200408	4	4	0	0.000	1.155	0.000	4	4	0	0.000	1.145	0.000
200409	1	1	0	0.000	1.158	0.000	1	1	0	0.000	1.148	0.000
200410	2	2	0	0.000	1.181	0.000	2	2	0	0.000	1.167	0.000
200411	2	2	0	0.000	1.180	0.000	2	2	0	0.000	1.164	0.000
200412	4	4	0	0.000	1.137	0.000	4	4	0	0.000	1.125	0.000
200501	15	15	0	0.000	1.104	0.000	15	15	0	0.000	1.095	0.000
200502	6	6	0	0.000	1.097	0.000	6	6	0	0.000	1.091	0.000
200503	4	3	1	0.250	0.962	0.608	4	4	0	0.000	1.105	0.000
200504	1	1	0	0.000	1.130	0.000	1	1	0	0.000	1.127	0.000
200505	2	2	0	0.000	1.173	0.000	2	2	0	0.000	1.148	0.000
200506	8	8	0	0.000	1.206	0.000	8	8	0	0.000	1.159	0.000
200507	0	NA	NA	NA	NA	NA	0	NA	NA	NA	NA	NA
200508	3	3	0	0.000	1.168	0.000	3	3	0	0.000	1.153	0.000
200509	4	4	0	0.000	1.166	0.000	4	4	0	0.000	1.156	0.000
200510	1	1	0	0.000	1.189	0.000	1	1	0	0.000	1.174	0.000
200511	2	2	0	0.000	1.189	0.000	2	2	0	0.000	1.170	0.000
200512	12	12	0	0.000	1.135	0.000	12	12	0	0.000	1.120	0.000
200601	3	3	0	0.000	1.092	0.000	3	3	0	0.000	1.085	0.000
200602	5	5	0	0.000	1.089	0.000	5	5	0	0.000	1.084	0.000
200603	7	7	0	0.000	1.106	0.000	7	6	1	0.143	1.019	0.560
200604	2	2	0	0.000	1.138	0.000	2	2	0	0.000	1.126	0.000
200605	1	1	0	0.000	1.175	0.000	1	1	0	0.000	1.147	0.000
200606	1	1	0	0.000	1.200	0.000	1	1	0	0.000	1.156	0.000

200607	1	1	0	0.000	1.187	0.000	1	1	0	0.000	1.150	0.000
200608	2	2	0	0.000	1.157	0.000	2	2	0	0.000	1.144	0.000
200609	1	1	0	0.000	1.162	0.000	1	1	0	0.000	1.153	0.000
200610	4	4	0	0.000	1.180	0.000	4	4	0	0.000	1.169	0.000
200611	4	4	0	0.000	1.175	0.000	4	4	0	0.000	1.164	0.000
200612	2	2	0	0.000	1.129	0.000	2	2	0	0.000	1.120	0.000
200701	9	8	1	0.111	1.026	0.194	9	8	1	0.111	1.029	0.182
200702	3	3	0	0.000	1.087	0.000	3	2	1	0.333	0.917	0.686
200703	4	4	0	0.000	1.099	0.000	4	4	0	0.000	1.103	0.000
200704	2	2	0	0.000	1.127	0.000	2	2	0	0.000	1.123	0.000
200705	2	2	0	0.000	1.169	0.000	2	2	0	0.000	1.147	0.000
200706	3	3	0	0.000	1.197	0.000	3	3	0	0.000	1.152	0.000
200707	2	2	0	0.000	1.182	0.000	2	2	0	0.000	1.149	0.000
200708	3	3	0	0.000	1.154	0.000	3	3	0	0.000	1.152	0.000
200709	5	5	0	0.000	1.156	0.000	5	5	0	0.000	1.152	0.000
200710	5	5	0	0.000	1.174	0.000	5	5	0	0.000	1.164	0.000
200711	7	7	0	0.000	1.180	0.000	7	7	0	0.000	1.167	0.000
200712	7	7	0	0.000	1.146	0.000	7	7	0	0.000	1.132	0.000
200801	7	7	0	0.000	1.102	0.000	7	7	0	0.000	1.097	0.000
200802	3	3	0	0.000	1.089	0.000	3	3	0	0.000	1.091	0.000
200803	1	1	0	0.000	1.098	0.000	1	1	0	0.000	1.104	0.000
200804	0	NA	NA	NA	NA	NA	0	NA	NA	NA	NA	NA
200805	1	1	0	0.000	1.138	0.000	1	1	0	0.000	1.130	0.000
200806	2	2	0	0.000	1.170	0.000	2	2	0	0.000	1.133	0.000
200807	3	3	0	0.000	1.172	0.000	3	3	0	0.000	1.146	0.000
200808	1	1	0	0.000	1.148	0.000	1	1	0	0.000	1.150	0.000
200809	4	4	0	0.000	1.162	0.000	4	4	0	0.000	1.155	0.000
200810	9	9	0	0.000	1.184	0.000	9	9	0	0.000	1.166	0.000
200811	4	4	0	0.000	1.176	0.000	4	4	0	0.000	1.157	0.000
200812	3	3	0	0.000	1.144	0.000	3	3	0	0.000	1.123	0.000
200901	21	19	2	0.095	1.070	0.056	20	17	3	0.150	1.023	0.328
200902	1	1	0	0.000	1.105	0.000	1	1	0	0.000	1.091	0.000
200903	6	6	0	0.000	1.094	0.000	6	6	0	0.000	1.094	0.000
200904	1	1	0	0.000	1.098	0.000	1	1	0	0.000	1.110	0.000
200905	3	3	0	0.000	1.141	0.000	3	3	0	0.000	1.126	0.000
200906	0	NA	NA	NA	NA	NA	0	NA	NA	NA	NA	NA
200907	6	6	0	0.000	1.183	0.000	6	6	0	0.000	1.152	0.000
200908	1	1	0	0.000	1.155	0.000	1	1	0	0.000	1.152	0.000
200909	4	4	0	0.000	1.161	0.000	4	4	0	0.000	1.162	0.000
200910	4	4	0	0.000	1.174	0.000	4	4	0	0.000	1.175	0.000
200911	4	4	0	0.000	1.163	0.000	4	4	0	0.000	1.156	0.000

200912	4	4	0	0.000	1.136	0.000	4	4	0	0.000	1.120	0.000
201001	11	11	0	0.000	1.097	0.000	11	10	1	0.091	1.038	0.174
201002	8	8	0	0.000	1.100	0.000	8	8	0	0.000	1.093	0.000
201003	4	4	0	0.000	1.113	0.000	4	4	0	0.000	1.112	0.000
201004	3	2	1	0.333	0.940	0.714	3	2	1	0.333	0.944	0.688
201005	1	1	0	0.000	1.163	0.000	1	1	0	0.000	1.150	0.000
201006	1	1	0	0.000	1.199	0.000	1	1	0	0.000	1.154	0.000
201007	1	1	0	0.000	1.196	0.000	1	1	0	0.000	1.160	0.000
201008	2	2	0	0.000	1.172	0.000	2	2	0	0.000	1.160	0.000
201009	2	2	0	0.000	1.177	0.000	2	2	0	0.000	1.170	0.000
201010	6	6	0	0.000	1.190	0.000	6	6	0	0.000	1.178	0.000
201011	3	3	0	0.000	1.186	0.000	3	3	0	0.000	1.167	0.000
201012	1	1	0	0.000	1.149	0.000	1	1	0	0.000	1.130	0.000
201101	4	4	0	0.000	1.105	0.000	4	4	0	0.000	1.093	0.000
201102	3	3	0	0.000	1.105	0.000	3	3	0	0.000	1.094	0.000
201103	2	2	0	0.000	1.123	0.000	2	2	0	0.000	1.115	0.000
201104	4	4	0	0.000	1.137	0.000	4	4	0	0.000	1.132	0.000
201105	1	1	0	0.000	1.172	0.000	1	1	0	0.000	1.151	0.000
201106	2	2	0	0.000	1.210	0.000	2	2	0	0.000	1.164	0.000
201107	1	1	0	0.000	1.192	0.000	1	1	0	0.000	1.154	0.000
201108	0	NA	NA	NA	NA	NA	0	NA	NA	NA	NA	NA
201109	0	NA	NA	NA	NA	NA	0	NA	NA	NA	NA	NA
201110	1	1	0	0.000	1.171	0.000	1	1	0	0.000	1.168	0.000
201111	6	6	0	0.000	1.174	0.000	6	6	0	0.000	1.166	0.000
201112	7	7	0	0.000	1.152	0.000	7	7	0	0.000	1.136	0.000
201201	13	13	0	0.000	1.125	0.000	13	13	0	0.000	1.109	0.000
201202	3	3	0	0.000	1.119	0.000	3	3	0	0.000	1.104	0.000
201203	4	4	0	0.000	1.124	0.000	4	4	0	0.000	1.118	0.000
201204	5	5	0	0.000	1.137	0.000	5	5	0	0.000	1.133	0.000
201205	1	1	0	0.000	1.172	0.000	1	1	0	0.000	1.148	0.000
201206	2	2	0	0.000	1.199	0.000	2	2	0	0.000	1.153	0.000
201207	1	1	0	0.000	1.185	0.000	1	1	0	0.000	1.150	0.000
201208	1	1	0	0.000	1.160	0.000	1	1	0	0.000	1.146	0.000
201209	2	2	0	0.000	1.166	0.000	2	2	0	0.000	1.155	0.000
201210	10	10	0	0.000	1.181	0.000	10	10	0	0.000	1.172	0.000
201211	4	4	0	0.000	1.169	0.000	4	4	0	0.000	1.158	0.000
201212	8	8	0	0.000	1.140	0.000	8	8	0	0.000	1.124	0.000
201301	6	6	0	0.000	1.111	0.000	6	6	0	0.000	1.102	0.000
201302	3	3	0	0.000	1.095	0.000	3	3	0	0.000	1.101	0.000
201303	7	6	1	0.143	1.024	0.530	7	7	0	0.000	1.111	0.000
201304	0	NA	NA	NA	NA	NA	0	NA	NA	NA	NA	NA

201305	4	4	0	0.000	1.162	0.000	4	4	0	0.000	1.144	0.000
201306	2	2	0	0.000	1.197	0.000	2	2	0	0.000	1.151	0.000
201307	9	9	0	0.000	1.187	0.000	9	9	0	0.000	1.153	0.000
201308	4	4	0	0.000	1.153	0.000	4	4	0	0.000	1.146	0.000
201309	4	4	0	0.000	1.151	0.000	4	4	0	0.000	1.150	0.000
201310	3	3	0	0.000	1.162	0.000	3	3	0	0.000	1.162	0.000
201311	14	14	0	0.000	1.154	0.000	14	14	0	0.000	1.155	0.000
201312	9	9	0	0.000	1.124	0.000	9	9	0	0.000	1.121	0.000
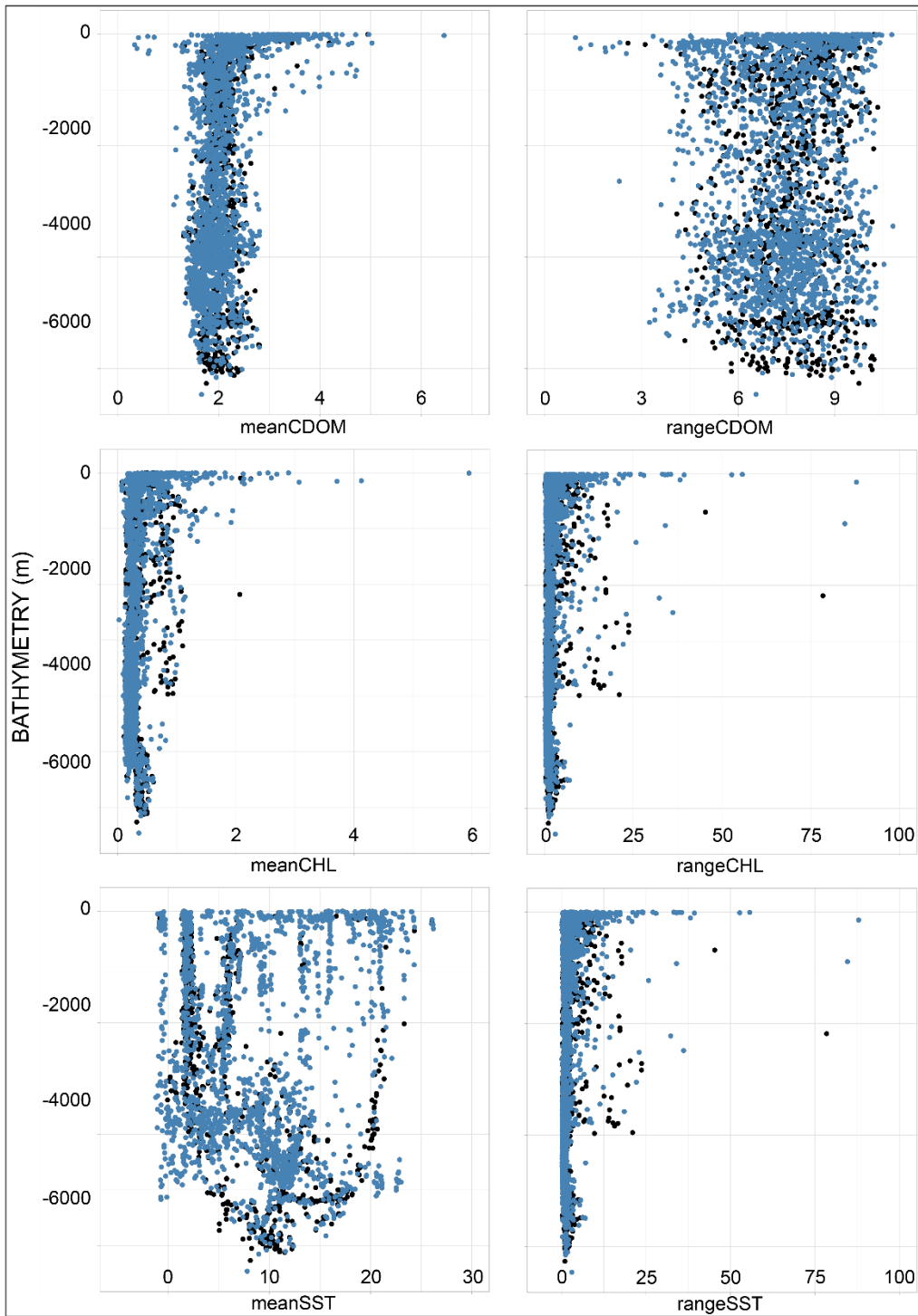
Supplemental Figure 15. Covariate space for spatially rarefied (black) and spatially rarefied and thinned (blue) time-averaged *Diomedea exulans* observation data. Visible black points denote unique covariate combinations lost during temporal rarefication.

REFERENCES

BirdLife International. 2016. Important Bird and Biodiversity Area (IBA) digital boundaries: December 2015 version. BirdLife International, Cambridge, UK and NatureServe, Arlington, USA.

BirdLife International and NatureServe. 2015. Bird species distribution maps of the world. BirdLife International, Cambridge, UK and NatureServe, Arlington, USA.

BirdLife International and NatureServe. 2020. Marine IBA e-Atlas. *Available at http://maps.birdlife.org/marineIBAs/default.html* (accessed 26 May 2020.

Orsi A, and Harris U. 2008. Locations of the various fronts in the Southern Ocean, Australian Antarctic Data Centre - CAASM Metadata (http://gcmd.nasa.gov).

Schloerke B, Crowley J, Cook D, Briatte F, Marbach M, Thoen E, Elberg A, and Larmarange J. 2018. GGally: Extension to 'ggplot2'. R package version 1.4.0. https://CRAN.R-project.org/package=GGally

Mischief managed.